AD



# WATERTOWN ARSENAL LABORATORIES

## ULTRASONIC ATTENUATION AND VELOCITY IN SAE 4150 STEEL

TECHNICAL REPORT NO. WAL TR 143/37



BY

EMMANUEL P. PAPADAKIS,
PAUL F. SULLIVAN
and
DONALD J. WALTMAN

DATE OF ISSUE - DECEMBER 1961

OMS CODE 5010.11.843005I
RESEARCH OF MATERIALS FOR HIGH TEMPERATURE USE
D/A PROJECT 5B93-32-004





WATERTOWN ARSENAL
WATERTOWN 72, MASS.

Ultrasonics

Steel, embrittlement - temper

# ULTRASONIC ATTENUATION AND VELOCITY IN SAE 4150 STEEL

Technical Report No. WAL-TR-143/37

By

Emmanuel P. Papadakis,
Paul F. Sullivan
and
Donald J. Waltman

Date of Issue - Dec[redacted]61

95

OMS Code 5010.11.8430051
Research of Materials for High Temperature Use
D/A Project 5B93-32-004

WATERTOWN ARSENAL
WATERTOWN 72, MASS.

370850

WATERTOWN ARSENAL LABORATORIES

TITLE

# ULTRASONIC ATTENUATION AND VELOCITY IN SAE 4150 STEEL


## ABSTRACT

Ultrasonic attenuation and velocity measurements have been made on SAE 4150 steel in the hot-rolled, austenitized-and-quenched, and tempered conditions to study temper embrittlement. It was found that the ultrasonic measurements did not show any correlation with the hardness or the notched-bar breaking energy of the steel. The attenuation from both elastic hysteresis and Rayleigh scattering decreased on quenching and also on tempering. The reduction of residual stresses lowered the elastic hysteresis. The decrease in Rayleigh scattering was caused partially on quenching and entirely on tempering by reductions in the elastic anisotropy of the contents of the prior austenite grain volume. The anisotropy was reduced by the change from pearlite to martensite first and by the removal of interstitial carbon second. Ultrasonic double refraction was observed during transverse wave measurements on the tempered specimens. Its most probable cause is a preferential orientation of the grains along the rolling direction. The alignment of 0.1% of the grains can be detected.





Emmanuel P. Papadakis
EMMANUEL P. PAPADAKIS
Physicist

Paul F. Sullivan
PAUL F. SULLIVAN
Physical Science Aid

Donald J. Waltman
DONALD J. WALTMAN
Student Trainee (Elec. Engr.)


APPROVED:

J. F. Sullivan
J. F. SULLIVAN
Director
Watertown Arsenal Laboratories

REPORT APPROVED
Date 19 Jan. 1962
WAL Board of Review
Chairman S.C.

CONTENTS

# INTRODUCTION

## Previous Work

At Brown University introductory work was done in 1953 by D. H. Evans and R. Truell on the ultrasonic attenuation of a temper-embrittled steel.[1] Samples of SAE 4150 steel were annealed at 1525 F for 3-1/2 hours and air cooled. Then they were austenitized at 1550 F for 2-1/2 hours and oil quenched. After that, pairs of samples were tempered at various temperatures, and one of each pair was water quenched while the other was furnace cooled. The latter one of each pair was considered embrittled while the former was toughened. Evans and Truell found interesting relationships between their samples, namely, that the attenuation of the tough samples went through a maximum when plotted against either breaking energy or hardness of the samples, while the attenuation of the brittle samples went through maxima on similar plots but at different values of the breaking energy and hardness. The attenuation could not be correlated with metallographic data. However, neither could the results be duplicated with samples taken from a new batch of SAE 4150 steel.

A more extensive investigation was carried out at Watertown Arsenal and was reported by Papadakis.[2] In that investigation, SAE 3140 steel as well as a few blocks of SAE 4150 steel were tested. The correlation between the attenuation and the hardness and breaking energy was found to be ambiguous at best. The attenuation did seem to depend on the microstructure, however, the SAE 3140 steel became bainite on quenching while the SAE 4150 steel became martensite. When the results of the attenuation measurements were mathematically normalized, according to theory, to correspond to the same ASTM grain size, the attenuation in bainite was found to be higher than the attenuation in martensite. Both structures lost attenuation proportional to the square of the frequency on tempering.

Several investigators have done experimental and theoretical work on the attenuation of ultrasonic waves in polycrystalline metals. Wegel and Walther[3] found a frequency-independent decrement yielding an attenuation proportional to the frequency for many metals in the 10-to-100 kilocycle region. This loss, termed elastic hysteresis, they found to be roughly proportional to the total amount of grain boundary area in a specimen. That is, the loss was smaller for larger grains. Kamigaki[4] on the other hand found that part of the attenuation in the 1-to-25 megacycle region, attributable in steel to elastic hysteresis, was independent of the grain size. The same author also found that the attenuation in pearlite was much higher than the attenuation in martensite of the same residual austenitic grain size, and that the martensite lost attenuation on tempering. Merkulov[5] found that the attenuation in pearlitic carbon steel was lower than the attenuation in pure iron, the ferritic grain size of which was equal to the austenitic grain size of the steel before its transformation. The attenuation decreased with increasing carbon content as the eutectoid composition was approached. Both authors attribute the attenuation, other than the elastic hysteresis, to Rayleigh scattering[6] of sound in the cases

in which the metallic grain size was smaller than the wavelength of the sound.

The scattering of sound by metal grains is dependent on the ratio of the wavelength of the sound to the grain diameter. Roth[7] and Mason and McSkimin[8] have established that the attenuation is inversely proportional to the grain diameter when the wavelength is smaller than the grain diameter. Both Roth and Merkulov[9] have observed this dependence experimentally. Merkulov's data and Mason and McSkimin's analysis both indicate that the attenuation in this region is independent of frequency, while Roth's data indicates that it is proportional to the frequency. Scattering formulas such as those derived in Morse[10] lead to attenuation independent of the frequency in the short wavelength region.

In the intermediate region, in which the wavelength is roughly the same as the grain diameter, the attenuation varies as the square of the frequency. One theory due to Huntington[11] ascribes the attenuation to stochastic phase scattering. Another due to Lifshits and Parkhomovskii[12,13] solves the equation of propagation of sound in the metal by making the differences in elasticity between grains into a perturbation upon the elasticity of the medium. Both theories predict the square-law dependence. Merkulov (see Reference 9) has observed that the square-law dependence occurs in iron while the wavelength is between 4 and 10 times the grain diameter, not equal to it. Mason and McSkimin (see Reference 8) predict that the Rayleigh scattering region should end when the wavelength becomes as small as three grain diameters. Presumably the transition to the square law should start near there.

In the low-frequency region in which the wavelength of the sound is much longer than the grain diameter, the attenuation arises from Rayleigh scattering. (See References 4, 6, 8, 9, 10, 12 and 13.) Other theoretical work has been done by Mason and McSkimin,[14] Bhatia,[15] Bhatia and Moore,[16] and Merkulov (see Reference 9). The work of Bhatia and Moore agrees with the work of Lifshits and Parkhomovskii (see References 12 and 13) in the Rayleigh scattering region. Merkulov bases his work on that of Lifshits and Parkhomovskii, and consequently agrees, also. Merkulov has shown that the Lifshits and Parkhomovskii theory gives better agreement with experiment both qualitatively and quantitatively. All the theories agree that the attenuation from Rayleigh scattering varies as the fourth power of the frequency, the third power of the grain diameter, a factor expressing the anisotropy of the elastic constants of a single grain, and a factor involving the velocities of the longitudinal and shear waves which carry off the scattered energy. The theory of Mason and McSkimin does not take into consideration the mode conversion at a grain boundary. Neither does the theory of Huntington (see Reference 11) mentioned in the preceding paragraph. Because of the theoretical completeness and the agreement with experiment exhibited by the theory of Lifshits and Parkhomovskii, we will adopt it to deal with Rayleigh scattering in the following work. The attenuation, $\alpha$, for grains of cubic crystalline structure is given as follows in nepers per centimeter:

Rayleigh Region: $\lambda > 2\pi D$:

Longitudinal Waves: $$a_\ell = \frac{8\pi^3\mu^2 T f^4}{375\rho^2 v_\ell^3}\left(\frac{2}{v_\ell^5} + \frac{3}{v_t^5}\right) \quad (1a)$$

Transverse Waves: $$a_t = \frac{2\pi^3\mu^2 T f^4}{125\rho^2 v_t^3}\left(\frac{2}{v_\ell^5} + \frac{3}{v_t^5}\right) \quad (1b)$$

Intermediate Region: $\lambda < 2\pi D$:

Longitudinal Waves: $$a_\ell = \frac{16\pi^2\mu^2 D f^2}{525 v_\ell^6 \rho^2} \quad (1c)$$

Transverse Waves: $$a_t = \frac{4\pi^2\mu^2 D f^2}{210\, v_t^6 \rho^2} \quad (1d)$$

Where: $f$ = frequency, megacycles per second

$\rho$ = density, grams per cubic centimeter

$T$ = average grain volume, cubic centimeters

$v_\ell$ = longitudinal wave velocity, centimeters per second

$v_t$ = transverse wave velocity, centimeters per second

$\mu$ = degree of elastic anisotropy of a grain, dynes per square centimeter

$= c_{11} - c_{12} - 2c_{44}$

where $c_{11}$, $c_{12}$, and $c_{44}$ are the elastic moduli of the cubic crystal grain.

The meaning of the elastic anisotropy is this: the compressibility without lateral expansion in one crystallographic direction, say the [100] direction, is different from the compressibility without lateral expansion in another crystallographic direction, say the [110] or the [111] direction. The same holds for the shear modulus without dilatation.

The application to steel is as follows. In the austenitic state at elevated temperatures, each steel grain is a face-centered-cubic crystallite. Upon quenching, the austenite transforms to various products

dependent on the rate of quenching. Slow quenching produces pearlite, a system of layers of iron (ferrite) and iron carbide within each grain. If the steel is of hypoeutectoid composition, iron (ferrite) grains and pearlite grains form separately. Fast quenching produces martensite, a system of small platelets of strained body-centered-tetragonal iron with interstitial carbon. The platelets form within the former austenitic grain at 24 different orientations with respect to the axes of the austenite. Intermediate quenching produces bainite. The lamellar structure of pearlite is considered to have a higher degree of elastic anisotropy than the platelet structure of martensite.

Kamigaki (see Reference 4) explains that the elastic modulus normal to the layers of a pearlite grain must be different from the elastic modulus tangential to the layers, while the elastic modulus of a grain containing many martensite platelets is quite isotropic with direction. He found experimentally that the attenuation caused by Rayleigh scattering in martensite was much smaller than that in pearlite of the same austenitic grain size before transormation. Papadakis[17] found experimentally that the attenuation in martensite was smaller than the attenuation in bainite. Both values were smaller than the attenuation found experimentally or predicted theoretically for body-centered-cubic iron (ferrite) by Merkulov (see Reference 9). It is considered that the partially randomized semi-lamellar structure of bainite is more anisotropic than the martensite but less anisotropic than the single crystal of ferrite. Concerning pearlite, Kamigaki (see Reference 4) disagrees with Merkulov (see Reference 5). Kamigaki finds that the attenuation in pearlite is higher than it should be in iron, while Merkulov finds that it is lower. This author feels the discrepancy lies in the fact that Kamigaki used the theory of Mason and McSkimin while Merkulov used the theory of Lifshits and Parkhomovskii.

The foregoing discussion serves to put the research contained in this report in its proper perspective. It has been shown that the grain size and the microstructure of the specimens can be expected to influence the attenuation strongly. The ultrasonic velocity does, also, as does the frequency, since both enter equation 1a through 1d in high powers.

## Purpose and Scope

The purpose of this report is to present the results of research aiming at the ultrasonic detection of temper embrittlement in SAE 4150 steel. A complete investigation, in the frequency range of 5 to 100 megacycles per second, has been carried out on a group of quenched and tempered specimens. The metal stock is the same for all specimens and was heat treated the same up to and including the quenching, so that the grain size and the microstructure are the same at each step before tempering.

The attenuation and velocity of both the longitudinal and transverse ultrasonic waves were measured on the tempered specimens, while the attenuation of the longitudinal waves was measured after various steps of the heat treatment. The specimens were tempered at different temperatures and cooled different ways to give a variety of hardnesses and breaking energies.

The quenching resulted in the formation of martensite and tempering precipitated the interstitial carbon as iron carbide, changing the internal strain and the microstructure. It is possible that both the elastic hysteresis and the Rayleigh scattering change. To investigate these changes, attenuation has been analyzed as a function of frequency. Also, it and its change on tempering have been correlated with the Rockwell C hardness and the Charpy impact data after tempering. The results of the investigation are compared with theory and with previous work. The correlation of ultrasonic attenuation and velocity with these parameters is in fulfillment of the purpose of the project.

## MATERIALS AND THEIR PREPARATION

The steel used was commercially available hot-rolled bar stock of SAE 4150 steel. It was treated according to the following schedule:

1. Machining of blocks 0.760 inch thick, 2 inches long, 1-1/2 inches wide, 200 millionths parallelism between top and bottom flat surfaces, 16 microinch top surface polish, Blanchard ground bottom.

2. Longitudinal wave attenuation measurements and some Rockwell C hardness tests and metallographic data.

3. Austenitizing of blocks, 1550 F in salt bath for one hour, and oil quench.

4. Machining of blocks 0.682 inch thick; same parallelism and surface specifications as in Step 1.

5. Longitudinal wave attenuation measurements, Rockwell C hardness measurements, and spectrographic analysis on all blocks. Metallographic data on some blocks.

6. Tempering of blocks:

   a. Four blocks heated to each temperature between 425 C and 725 C in steps of 25 C for one hour.

   b. Two of each group water quenched.

   c. The other two furnace cooled at no less than 17 C per hour.

7. Machining of blocks to 0.677 inch thickness; 8 microinch ground finish plus lap on both surfaces.

8. Longitudinal and transverse wave attenuation and velocity measurements and Rockwell C hardness measurements on all blocks. Metallographic data on some blocks.

9. Charpy impact tests on notched bars cut from each block.

10. Analysis of data: Attenuation versus (a) frequency, (b) hardness, (c) breaking energy, (d) theory. Velocity versus frequency. Small differences in transverse wave velocity caused by ultrasonic double refraction.

## TEST PROCEDURES

### General

All the chemical, metallographic, mechanical, and machine work on the specimens was done within the Watertown Arsenal Laboratories by standard methods used at this installation. The steel bar stock from which the specimens were made was purchased from commercial concerns.

### Ultrasonic Methods

Measurements of ultrasonic attenuation and velocity were made by the pulse-echo method described by Roderick and Truell[18] with an instrument built for the Watertown Arsenal Laboratories by Brown University. The instrument is similar to one described recently by Chick and others.[19] The specimens were cut so their parallel faces were much larger than the quartz transducers used. The length and breadth of the parallel faces was much larger than the ultrasonic path length between the faces. The rolling direction of the original bar stock was parallel to these two parallel plane faces. Circular quartz crystal disks one-half inch in diameter, with polished and gold-plated faces, were used as transducers. A single transducer was bonded to one of the parallel faces of the specimen to serve both as a transmitter and a receiver.

### Bonding

#### a. Longitudinal Waves

In previous experiments involving ultrasonic attenuation measurements made by bonding the transducer directly to the specimen (in contradistinction to measurements made in a water bath or by some similar method of indirect coupling), the repeatability of readings has been a severe problem. In this project, too, the same problem was encountered. Since it was necessary to obtain data which was extremely accurate, at least relatively, in order to confirm or refute previous work on this subject, some experimenting was done to determine a method of bonding which would give practically the same bond every time. Using the second method described below it was possible to repeat attenuation measurements to within 2% at 90 mc. At lower frequencies, because of a lower actual attenuation, the margin of repeatability is larger: 3% at 27 mc and 7% at 9 mc.

It was found that in setting up a bond between a gold-plated quartz transducer and one of the steel blocks used in this experiment, using glycerin as the bonding agent, the apparent attenuation passed through two minima. One of these minima occurred when the crystal was floated in a

very large amount of glycerin, almost the largest amount which could be used without getting glycerin on the top surface of the crystal. When the bonding method was adjusted so that this type of bond was produced, the attenuation readings went through a local minimum as a function of bond thickness. However, the amount of glycerin used proved to be very critical, a small difference in the amount used causing a drastic change in the apparent attenuation. Also, when the transducer was mounted in this way, it was very difficult to keep from getting glycerin on the top surface of the transducer. For these two reasons this method was abandoned.

The second local minimum occurred with very thin bonds when a very small amount of glycerin was used (just enough to keep the crystal from sticking) and the transducer was pressed down on the specimen. This method of bonding yielded apparent attenuations considerably lower than those obtained with the method of bonding described in the previous paragraph. Again the amount of glycerin used was extremely critical, more critical than in the previous method, and, in addition, the pressure applied was also critical. However, with this method, there was no tendency for the glycerin to flow over the top of the crystal, so solutions for the other problems were sought, using this bonding procedure.

To standardize the amount of glycerin used, a loop approximately 1-16" in diameter was made in a length of 30 gage wire and used to dip out the glycerin. A drop of glycerin was placed in the center of the top surface of each specimen with this wire and the transducer was placed on top of this drop and was slid, in a circular path, over the top surface of the specimen until the glycerin was spread so thin that the transducer just stuck when moved to the center of the specimen. These precautions insured a film of glycerin of closely repeatable thickness.

To standardize the pressure applied to the transducer, the original electrode (a 3/4-inch-long brass cylinder 1/2-inch in diameter) was weighted with a lead cap weighing approximately one pound. It was noticed, however, that the apparent attenuation obtained with this cap gradually decreased with time as the transducer slowly settled in the glycerin. It was assumed that a heavier cap on the electrode would eliminate this problem since it would cause the transducer to settle more rapidly to a stable position. Therefore a second cap was made, this one approximately 2-1/4 pounds in weight and more accurately balanced than the first. With this cap excellent results were obtained. Diagrams of both caps follow:

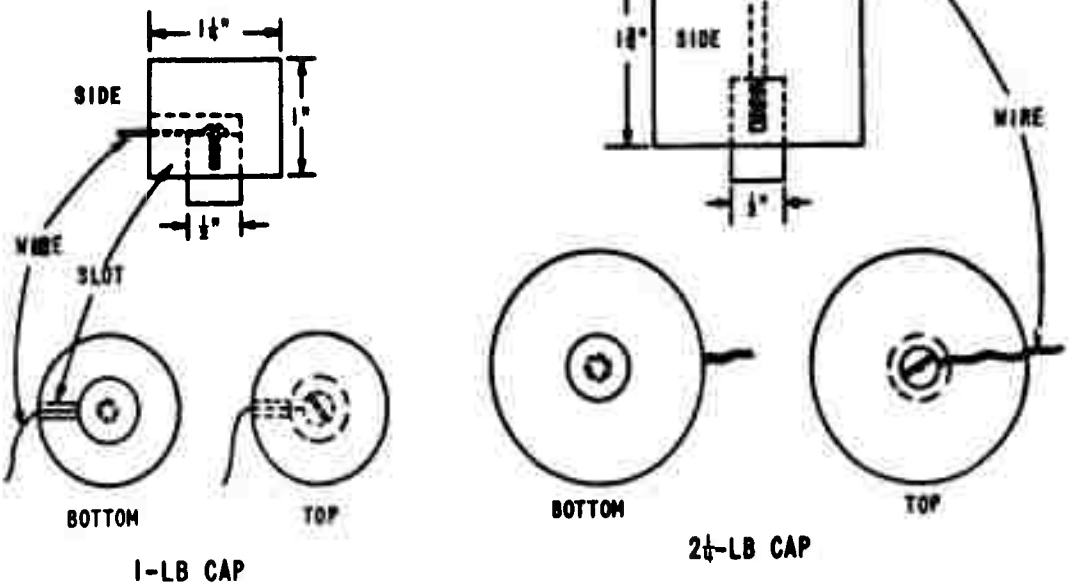


It is necessary to take great care in using this type of bonding in order to insure sufficient repeatability. Both the specimen and the transducer must be cleaned of all dust particles on the bonding surfaces (done best by wiping the surfaces with an artist's brush dampened with alcohol). Furthermore, there must be no water, alcohol, or air bubbles in the glycerin film, and care must be taken not to touch the film with the fingers. It is also imperative that the surface of the specimen be extremely smooth if plated crystals are to be used, for any roughness causes the plating to scrape off in fine dust particles which affect the readings adversely. In this project, rather than having the blocks refinished, the gold plating was scraped off one surface of the transducer, and the bare quartz was bonded to the specimens.

b. Transverse Waves

To provide the bond with shear elasticity necessary to transmit transverse waves from the Y-cut transducers into the specimens, phenyl salicylate (salol) was used. The specimens were first cleaned with acetone and then heated by means of an infrared heat lamp. A small amount of salol was placed in the center of the bonding surface of each specimen while it was still under the heat lamp. The melting point of the salol (41 - 43 C) was reached easily under the lamp and when a pool of molten salol had formed, an unplated Y-cut quartz crystal was centered on the top surface of each block. A light weight was placed on each transducer and the blocks were removed from under the heat lamp and allowed to cool. After the blocks had

cooled somewhat, a few crystals of salol were used to seed a single crystal from the pool, thus giving a good bond.

It was not possible to estimate the repeatability of the bond itself because ultrasonic double refraction caused a change in apparent attenuation of the order of ±50% even when there was no change in the amount of cancellation apparent from the shape of the envelope of the echoes. On some blocks the envelope of the echo train had visible nodes only when the crystal was polarized to within 10 degrees of a line drawn at a 45 degree angle to the rolling direction in the steel. The crystal could be turned through 70 degrees, causing a continuous change in the amount of cancellation and, hence, in the apparent attenuation without producing any noticeable change in the shape of the envelope. Since there was no marking on the transducers to indicate the direction of polarization, there were no means for orienting the crystals the same way on each block. It is suggested that, when making transverse wave attenuation measurements, only transducers with the direction of polarization marked on them be used, or that the orientation of the crystal be adjusted for complete cancellation at nodes, the attenuation be read from peak to peak and a proper correction for interference be applied.

Type of Measurements Taken and Range of Frequencies

Before austenitizing the specimens, only longitudinal wave attenuation measurements in the range from 5 mc to 15 mc were made. This range was expanded to 75 mc in the measurements made on the austenitized blocks. After the blocks had been tempered, because the extremely low attenuation at low frequencies was entirely absorbed by the errors, measurements below 9 mc were found to be of no value; however the range of longitudinal wave attenuation measurements was further extended to 100 mc and more complete coverage of this range was made. In addition, longitudinal wave velocity measurements at 18 mc and 54 mc, along with transverse wave attenuation measurements from 7 mc to 90 mc and velocity measurements at 7 mc, 18 mc, 21 mc, and 54 mc, were made. Finally, measurements of the fractional difference between the velocities of transverse waves polarized parallel to and perpendicular to the rolling direction in the steel were also made in the range from 7 mc to 35 mc.

Corrections

a. Diffraction Losses

Corrections for diffraction losses in the ultrasonic field of the crystal transducer were necessary. Seki, Granato, and Truell[20] computed these losses as a function of penetration distance for waves from a circular transducer. From the formula given by Papadakis[21] for two specific echoes number j and k, the correction is given by

$$\alpha_{Td} = \frac{db(k) - db(j)}{2\,(k - j)\,L}\,c \qquad (2)$$

in decibels per microsecond, where

db(j,k) = decibel drop at echoes j and k respectively

c = velocity of sound in block

L = thickness of block

The decibel drop is given versus S which is the distance the wave has traveled in the specimen in units of $a^2/\lambda$ or $a^2f/c$, where

a = crystal radius

$\lambda$ = wavelength

f = frequency;

so the distances corresponding to echoes j and k are

$$S_j = \frac{2jLc}{a^2f} \tag{3a}$$

$$S_k = \frac{2kLc}{a^2f} \tag{3b}$$

and db(j) is $db(S_j)$ and can be found from the table in References 20 and 21.

Wherever it was possible, the exponential curve was matched at the top of the first echo and at the echo nearest the third peak.

b. Changes in the Equipment

It was also necessary to compensate for any changes in the equipment such as those produced by aging and by replacement of parts. For this purpose, longitudinal wave attenuation measurements were made on blocks 401 and 441 through 445 at all frequencies within a period of two days at the end of the experiment. At each frequency the attenuation values obtained for 441 through 445 (which were chosen because they formed a tight-knit attenuation group) were averaged. This average value was subtracted from the average of the original post-tempering data on these blocks to give a set of correction figures. The corrections were added to the original post-tempering data to bring them to the level of the second set of post-tempering attenuation data which were taken after the changes in the equipment. At each frequency an average was also taken of five attenuation readings on block 401, which had not been tempered. This average was then subtracted from the data on block 401 which was taken at the time of the attenuation measurements on the austenitized blocks, the difference being

the amount of attenuation change which could be credited to the equipment changes in the period between the taking of the two sets of data. This difference, added to the previous correction figure, gave the proper correction for equipment changes to be applied to the post-tempering data. Application of this correction not only made the data consistent from one stage of the project to another, but it also made the post-tempering data more accurate absolutely, since the equipment had been calibrated immediately previous to the pre-tempering data but not immediately before the post-tempering data. A period of several months had elapsed in the interim.

c. Interpolation for Velocity

In making velocity measurements, it was necessary to correct for the nonlinearity of the time delay dial. This was accomplished by using a crystal-controlled oscillator which produced marker pulses at ten-microsecond intervals. The dial readings were then converted to the true value by interpolation between the markers. The true time interval to a given echo is given by

$$t = t_1 + (t' - t_1') \frac{10}{t_2' - t_1'} \tag{4}$$

where

$t$ = true time to the echo

$t'$ = dial reading at the echo

$t_1$ = true time to the marker immediately preceding the echo (ten times the marker number)

$t_1'$ = dial reading at the marker immediately preceding the echo

$t_2'$ = dial reading at the marker immediately following the echo

Errors

a. Errors in Attenuation

Errors in attenuation arise from both the measurement and the corrections. The maximum error is calculated as follows.

Let

$a$ = attenuation

$a'$ = measured attenuation

$a_{Te}$ = equipment correction

$a_{Td}$ = diffraction correction

Since

$$a = a' - a_{Te} - a_{Td},$$

then

$$\Delta a = \Delta a' + \Delta a_{Te} + \Delta a_{Td}.$$

Now $a'$ is a function of the dial reading, the coupling, and the conversion graph; so $\Delta a'$ is the sum of the errors in each of these, or

$$\Delta a' = \Delta a_D + \Delta a_C + \Delta a_G.$$

Now

| | |
|---|---|
| $\Delta D \approx 0.005$ | from observation, where D is the attenuation dial reading. |
| $\therefore \Delta a_D \approx \frac{da}{dD} (\Delta D) \approx 0.002$ | from graph of $a$ versus D |
| $\Delta a_C \approx 0.005$ | from average repeatability |
| $\Delta a_G \approx 0.002$ | from error in graph of $a$ versus D |
| $\therefore \Delta a' \approx 0.009$ | maximum error in $a'$. |

Now

$$a_{Te} = a_1' - a_{Td} - (a_2' - a_{Td}) = a_1' - a_2'$$

where

$a_1'$ = measured attenuation of 401, post-tempering data

$a_2'$ = measured attenuation of 401, pre-tempering data.

Therefore,

$$\Delta a_{Te} = \Delta a_1' + \Delta a_2' = 2\Delta a' \approx 0.018.$$

Now

$$a_{Td} = \frac{db(Sn) - db(S_1)}{2(n-1)L}\, c$$

$$\Delta db(S_n) \cong 0.005$$

$$S_1 = (2L/a^2)\lambda = 2Lc/a^2 f$$

$$\Delta S_1 = \left\{\frac{\Delta L}{L} + \frac{\Delta c}{c} + 2\frac{\Delta a}{a} + \frac{\Delta f}{f}\right\} S_1.$$

Supposing one percent error in each quantity,

$$\Delta S_1 \cong S_1\ (0.01 + 0.01 + 0.02 + 0.01)$$

$$\cong 0.05\ S_1.$$

At 35 megacycles,

$$\Delta S_1 \cong 0.05\ (0.143) \cong 0.007.$$

Now

$$\Delta db(S_1) = \Delta db\ (\text{intrinsic})^* + \Delta db\ (\text{rounding})$$

$$\cong 1.5\ \ \Delta S_1{}^* + 0.005$$

$$\cong 0.011 + 0.005$$

$$\cong 0.016.$$

So

$$\Delta[db(S_n) - db(S_1)] = \Delta db(S_n) + \Delta db(S_1)$$

$$= \Delta(\Delta db) \qquad \cong 0.005 + 0.016$$

$$\cong 0.021.$$

We find

$$\Delta a_{Td} = a_{Td}\left[\frac{\Delta(\Delta db)}{\Delta db} + \frac{\Delta c}{c} + \frac{\Delta L}{L}\right]$$

*From slope of db versus S.

$$\simeq 0.04 \left[\frac{0.02}{0.83} + 0.01 + 0.01\right]$$

$$\simeq 0.04\ (0.02 + 0.01 + 0.01)$$

$$\simeq 0.04\ (0.04)$$

$$\simeq 0.002$$

$$\therefore \Delta\alpha = \Delta\alpha' + \Delta\alpha_{Te} + \Delta\alpha_{Td}$$

$$\simeq 0.009 + 0.018 + 0.002$$

$$\simeq 0.029 \simeq 0.03$$

$$\frac{\Delta\alpha}{\alpha} \simeq \frac{0.03}{0.12} = 0.25 = 25\% \text{ at } 35 \text{ mcps.}$$

A maximum error of 25 percent is possible in the post-tempering longitudinal wave attenuation data at 35 megacycles; however, this error varies greatly with frequency. At 10 megacycles, because the attenuation is much lower, the error is close to 90 percent of the final attenuation; and at 90 megacycles the error decreases to 8 percent. This decrease in percent error with an increase in frequency probably accounts for the fact that the higher frequency attenuation points correspond more closely to the lines on the graphs in Figure 3.

It is important to note that the bulk of the error calculated immediately above is due to the equipment change correction. In the pre-tempering data, because of the absence of this correction, the error is smaller and, since the pre-tempering attenuation is larger, the percent error is smaller still. It also should be noted that in transverse wave attenuation measurements there is the additional error caused by misorientation of the crystal. Because the error varies so much with these different parameters, the maximum error at each frequency for each set of measurements is given in the tables (I, IV, VIII, and X) where the results of the measurements are found.

b. Errors in Velocity

Errors in the velocity calculations arise from errors in the measurement of the thickness of the blocks and errors in the measurement and averaging of the time delay between echoes. Since the time was an average of several values, the statistical limit of error, rather than the maximum error, was calculated for the velocity measurements. There is one chance in 500 that the true value of the velocity will differ from the mean value (listed in Tables XI and XII) by an amount more than this error. The statistical limit of error was calculated as follows:

Let

$v$ = velocity of sound in the block

$d$ = thickness of the block

$t$ = time between echoes,

then

$$v = \frac{2d}{t}$$

and

$$\Delta v = \sqrt{\left(\frac{\Delta d}{d}\right)^2 + \left(\frac{\Delta t}{t}\right)^2}\, v.$$

But

$$d = d_m + d_z$$

where

$d_m$ = measured thickness of the block

$d_z$ = micrometer zero correction

so

$$\Delta d = \Delta d_m + \Delta d_z.$$

Now

$\Delta d_m \tilde{=} 0.0002$ from observation

$\Delta d_z \tilde{=} 0.0001$ micrometer least count

$\therefore \Delta_d \tilde{=} 0.0003$

$d \tilde{=} 0.677$

$$\therefore \left(\frac{\Delta d}{d}\right)^2 \tilde{=} 20.3 \times 10^{-8}.$$

The error in the time factor is given by

$$\Delta t = \Delta t_m + \Delta t_a$$

where

$\Delta t_m$ = error in measurement of t

$\Delta t_a$ = error in averaging t over several echoes.

Now

$$\Delta t_m \cong 0.02 \quad \text{from observation}$$

and

$$\Delta t_a = \sqrt{\frac{4}{n-1}} \frac{\sum_{j=1}^{j=n-1} |t_j - \bar{t}|}{n-1}$$

where

$t_j$ = time between the $j^{th}$ and $(j+1)^{th}$ echoes

$$\bar{t} = \frac{\sum_{j=1}^{j=n-1} t_j}{n-1}$$

n = number of echoes used.

At 18 megacycles, for transverse waves,

$$\bar{t} \cong 10.71$$

$$n = 10$$

$$\sum_{j=1}^{j=n-1} |t_j - \bar{t}| \cong 0.32$$

or

$$\Delta t \cong 0.067.$$

Now

$$t \cong 10.7$$

$$\therefore \left(\frac{\Delta t}{t}\right)^2 \cong 39.5 \times 10^{-6}.$$

Therefore

$$\frac{\Delta v}{v} = \sqrt{\left(\frac{\Delta d}{d}\right)^2 + \left(\frac{\Delta t}{t}\right)^2}$$

$$\cong \sqrt{39.7 \times 10^{-6}}$$

$$\cong 6.3 \times 10^{-3} \cong 0.6\%$$

$$v \cong 0.127$$

$$\therefore \Delta v = 8 \times 10^{-4} \quad \text{in}/\mu\text{sec}.$$

The error in velocity increases rapidly as the frequency gets higher and fewer echoes are available from which measurements may be made; hence, the error for each set of measurements is listed on the table (XI or XII) where the results of those measurements occur.

## RESULTS AND DISCUSSION

### Presentation of Tables and Graphs

The first group of tables in Appendix A (Tables I - III) gives results of the work on the as-received hot-rolled specimens. Table I gives attenuation versus frequency. The maximum error in the attenuation is listed at the head of the table. Table II presents the metallographic information on a group of thirteen specimens. Table III is a list of the Rockwell C hardnesses of ten of the specimens. All specimens were virtually identical, as they should have been since they were cut from the same piece of bar stock. The specimens had a grain size from ASTM 5 to ASTM 6. Their microstructure was fine, medium, and coarse pearlite with at most a trace of ferrite. All had stringers and showed various degrees of banding. The average of the hardness readings taken at four points on each block ranged from 22.4 to 23.1 among the blocks. In attenuation all the blocks were nearly indistinguishable.

The second group of tables (Tables IV - VI) represents the work on the specimens after they were austenitized and quenched. Table IV gives attenuation versus frequency. The maximum error in the attenuation is listed at the head of the table. Table V presents the metallographic information on a group of four specimens. Table VI is a list of the Rockwell C hardnesses of all the specimens. Again the specimens were nearly identical. They were almost 100% martensite with 2 or 3% bainite, a trace of carbide, and many stringers. Their residual austenitic grain size (measured after tempering) had been refined to between ASTM 8 and ASTM 9. The attenuation did not differ significantly from block to block. A computation of the skewness in the attenuation readings at 75 megacycles per second indicated[22] that there was a 90% chance that these attenuation values were not normally distributed about their mean value. The large value of this probability indicates that the combination of errors and intrinsic specimen properties which contributed to the attenuation did bias the attenuation in one direction very strongly. For instance, the presence of some specimens in which the grain size grew too large or in which the quench was too slow would skew the attenuation readings toward large values because both these conditions produce specimens with excessive attenuation relative to the group to which they are supposed to belong. Hence the 90% probability for skewness indicated that there could have been several of these improper specimens produced by the austenitizing and quenching.

The third group of tables (Tables VII - XVII) represents the work on the specimens after they were tempered. Table VII lists the tempering temperatures and the cooling conditions of the various blocks. Table VIII gives the attenuation of longitudinal waves versus frequency. The maximum error in the attenuation is listed at the head of the table. Table IX is the attenuation lost on tempering. This table contains the differences between the attenuation values in Table IV and those in Table VIII. Table X gives the attenuation of transverse waves versus frequency. The values in this table are in error by large amounts because the envelope of the interference pattern caused by ultrasonic double refraction tended to obscure the true heights of the echoes on the oscilloscope. Ultrasonic double refraction will be treated at length in a subsequent section.

The velocity of longitudinal waves appears in Table XI while the velocity of transverse waves appears in Table XII. The errors in the velocities appear at the heads of the tables. The errors cover any trends which seem to appear in the velocity measurements. The velocity data was taken on one water-quenched specimen and one furnace-cooled specimen in the low, middle, and high portions of the tempering temperature range. That is, six specimens were measured for their ultrasonic velocities. Table XIII lists the transverse wave interference parameters associated with the ultrasonic double refraction observed in the tempered specimens. The computed fractional differences between the velocities of transverse waves polarized parallel to the rolling direction of the steel and perpendicular to it are also listed in this table. One will note that the variation in velocity detectable by the interference pattern is much smaller than the error in the velocity measurements made by the pulse-echo method alone.

The Rockwell C hardnesses of the tempered specimens are listed in Table XIV. These values are an average of four readings taken on the top surface of each specimen. The breaking energies of notched Charpy impact specimens (cut from the tempered specimens after all ultrasonic measurements were completed) are given in Table XV. The breaking energies and the hardnesses correlate strongly with the tempering conditions, as they should. The metallographic analysis of several blocks spanning the tempering temperature range is presented in Table XVI, and the spectrographic analysis of the chemical constituents of all the blocks is reported in Table XVII. All the blocks were essentially the same. The ASTM grain size varied between 8 and 9 with a few blocks showing some grains of ASTM 7 or 10. The microstructure was 100% tempered martensite in all the blocks. All were fine acicular martensite except some tempered at the highest temperatures. These few showed carbides resolvable at 1000X. There was more grain boundary segregation in the furnace-cooled specimens than in the water-quenched ones.

Using the hysteresis and Rayleigh scattering terms, the attenuation is expressed as

$$\alpha = a_1 f + a_4 f^4 \qquad (5)$$

where $\alpha$ is the attenuation, $f$ is the frequency, and $a_1$ and $a_4$ are coefficients. It is valid to use the Rayleigh scattering term in this experiment because the wavelength of the ultrasonic waves is always much larger than the grain diameter in the specimens. At 100 megacycles per second the wavelength of the sound in steel is 0.0023 inches for longitudinal waves while the grain diameter in a specimen of ASTM grain size 10 is about 0.00046 inches. The ratio is five to one. According to the theory of Lifshits and Parkhomovskii (see References 12 and 13), the Rayleigh-type scattering is valid for wavelengths greater than $2\pi D$ or about 6D. Thus Rayleigh scattering is approximately valid over the entire range of frequencies treated in this experiment. Equation 2 was fitted to the data for all the blocks at each stage of heat treatment by a machine computation using a least-squares method.[23] The program was written for the Royal-McBee LGP 30 using equal weights for all the data.

The coefficients $a_1$ and $a_4$ appear in Table XVIII. In the case of the hot-rolled stock, $a_1$ varies from $1.65 \times 10^{-2}$ to $2.46 \times 10^{-2}$ and $a_4$ varies from $2.89 \times 10^{-5}$ to $3.66 \times 10^{-5}$ with the units of frequency being megacycles per second, and the coefficients referring to longitudinal waves. Similarly, in the case of the austenitized and quenched stock above 15 megacycles per second, $a_1$ varies from $3.72 \times 10^{-3}$ to $8.69 \times 10^{-3}$ and $a_4$ varies from $5.77 \times 10^{-8}$ to $7.80 \times 10^{-8}$. The austenitizing and quenching to martensite lowered the elastic hysteresis by a factor of 3 and lowered the Rayleigh scattering by a factor of 500. The metallographic data from Table II and Table V indicate that the grain size was refined from ASTM 5-6 to ASTM 8-9. Since an increase of one ASTM unit represents a decrease in the grain diameter by a factor of $2^{\frac{1}{2}}$, an increase of three ASTM units decreases the grain

diameter by a factor of $2^{3/2}$, or 2.828. The attenuation is proportional to the cube of the grain diameter, so the decrease in the attenuation caused by the refining of the grain size goes as $(2.828)^3$ or 22.6. Since the real decrease is by a factor of 500, the extra factor of 500/22.6 or 22.1 must come from a decrease in the anisotropy of the elastic constants of the single grains on the change from pearlite in the hot-rolled specimens to martensite in the specimens after their austenitizing and quenching.

In the case of the specimens after tempering, $a_1$ varies from $2.16 \times 10^{-3}$ to $5.70 \times 10^{-3}$ and $a_4$ varies from $1.57 \times 10^{-8}$ to $2.50 \times 10^{-8}$ for the longitudinal waves above 15 megacycles per second. For the shear waves, $a_1$ varies from $2.33 \times 10^{-3}$ to $11.07 \times 10^{-3}$ while $a_4$ varies from $0.71 \times 10^{-8}$ to $10.07 \times 10^{-8}$. As mentioned earlier, the shear wave measurements are inaccurate because of the ultrasonic double refraction interference pattern. The values of $a_1$ for longitudinal waves decreased to about 3/4 of their former value and the values of $a_4$ decreased to about 1/3 of their former value upon tempering. Apparently the removal of interstitial carbon from the martensite upon tempering decreases the anisotropy of the elastic constants of the martensite platelets and hence of the whole grain. The ratio of $a_4$ for transverse waves to $a_4$ for longitudinal waves in the tempered specimens appears in Table XIX for thirty-six specimens. In all but two cases, the ratio lies between 2.20 and 4.70. According to Equations 1(a) and 1(b), the ratio should be

$$\frac{a_t}{a_\ell} = \frac{3}{4}\left(\frac{v_\ell}{v_t}\right)^2 \qquad (6)$$

for attenuation in decibels per microsecond. Using the values $v_\ell = 0.232$ and $v_t = 0.127$ inches per microsecond, the ratio becomes

$$\frac{a_t}{a_\ell} = 2.50.$$

The agreement here is fairly good despite the errors. A computation of the skewness (see Reference 22) in the distribution of $a_t/a_\ell$ indicates an almost certain biasing of this ratio toward values larger than the mean. The longitudinal wave attenuation is skewed, too, but not nearly as badly as the ratio. It is evident that the ratio cannot be skewed by natural causes other than changes in the velocity. The one percent errors in the velocity readings certainly do not afford the opportunity for the extreme skewness in the ratio, so one must conclude that the skewness in the ratio arises from an error. It is probable that the error is introduced by the interference envelope of the ultrasonic double refraction in the transverse waves.

Table XX gives the ultrasonic double refraction fractional velocity change as a function of frequency and branch number. Branch zero (0) is the only one independent of frequency.

Appendix B contains the graphs of the data and other figures. Figure 1 is a set of photomicrographs of the specimens at various stages in their heat treatment. Figure 2 is a set of oscilloscope photographs showing the rectified echoes and the exponential matching curve. Some of the photographs illustrate the exponential decay of the longitudinal waves and others show the double refraction interference pattern of the transverse waves. Figure 3 contains plots of attenuation versus frequency for four specimens which are typical. The data from Table I, Table IV, Table VIII and Table X are plotted together for easy comparison. The drop in longitudinal wave attenuation at each stage of heat treatment is clearly seen. The fact that the transverse wave attenuation was larger than the longitudinal wave attenuation is also clearly visible. The attenuation values smaller than 0.01 decibels per microsecond can be disregarded since the maximum error in those values is larger than the value itself. The diffraction corrections are about 0.03 or 0.04 for most frequencies, so any unknown systematic error in these corrections would tend to invalidate the attenuation values at the lower frequencies. In the computation of the coefficients in Table XIX, the frequencies below 15 megacycles per second were disregarded because at those frequencies the attenuation was smaller than its maximum error. The differences in attenuation before and after tempering are plotted in Figure 4 for the four typical specimens of Figure 3. All the blocks behaved identically. The slope of the best line of all the plots through the points on log-log paper is around 2.4 and the intercept of the line is about 0.5 decibels per microsecond at 50 megacycles per second.

Wegel and Walther had noticed (see Reference 3) that the elastic hysteresis decreased as the grain diameter increased. Since Rayleigh scattering increases with increasing grain diameter, a spread in the grain diameter should show up as a correlation between $a_1$ and $a_4$, the elastic hysteresis and Rayleigh scattering coefficients of Equation 2. Figure 5 is a scatter diagram of $a_4$ versus $a_1$. There is plenty of scatter and no correlation among either the water-quenched specimens or the furnace-cooled specimens.

The next group of figures (Figures 6 - 11) concerns the hardness of the specimens. Figure 6 is a plot of Rockwell C hardness versus tempering temperature. The hardness decreased linearly with the tempering temperature up to 675 C. Above that temperature, the hardness decreased more rapidly. The furnace-cooled specimens followed a different linear function than did the water-quenched specimens. The hardness of the furnace-cooled specimens was lower than the hardness of the water-quenched specimens, and decreased more rapidly with increasing temperature. Figures 7, 8 and 9 are scatter diagrams of the attenuation of longitudinal waves after tempering, the attenuation of longitudinal waves lost on tempering, and the attenuation of transverse waves after tempering, respectively, versus Rockwell C hardness. Figures 10 and 11 are respectively the elastic hysteresis coefficient $a_1$ and the Rayleigh scattering coefficient $a_4$ for longitudinal waves versus Rockwell C hardness. There is no correlation or functional relationship present in Figures 7 through 11.

Figure 12 is a plot of the breaking energy of Type 1 Charpy bars versus tempering temperature. The energy increases with tempering temperature as expected. The curve for the bars broken at -60 F lies below the curve for the bars broken at 74 F. The lower curve does not begin to rise as soon as the upper one does. There is no evidence for embrittlement at the higher tempering temperatures. The bars cut from the furnace-cooled blocks do not differ in breaking energy from the bars cut from the blocks water-quenched after tempering. Figures 13, 14 and 15 are scatter diagrams of the attenuation of longitudinal waves after tempering, the attenuation of longitudinal waves lost on tempering, and the attenuation of transverse waves after tempering, respectively, versus breaking energy. Figures 16 and 17 are respectively the elastic hysteresis coefficient $a_1$ and the Rayleigh scattering coefficient $a_4$ for longitudinal waves versus breaking energy. There is no correlation or functional dependence of the ultrasonic quantities on the breaking energy.

Figure 18 is the hardness versus the breaking energy. The water-quenched specimens follow a different curve from the furnace-cooled ones.

In Figure 19 the attenuation of longitudinal waves in block 417 after tempering is compared with the theory of Lifshits and Parkhomovskii (see References 12 and 13) as expressed in Equations 1a and 1c. Similarly the attenuation of transverse waves in block 417 after tempering is compared with the theory in Figure 20 using Equations 1b and 1c. The theoretical curves of attenuation versus frequency were constructed by connecting a point well within the region in which the dependence of the attenuation on the frequency is f4 and a point well within the region in which the dependence of the attenuation on frequency is f2. The slope of the curve at the first point is 4 and at the second point is 2 on a log-log paper. The curves were computed for several grain sizes in the region of interest. The elastic moduli of iron listed in the American Institute of Physics Handbook were used in computing $\mu 2$, and the velocities measured in this experiment were also used. The experimentally found attenuation was then superimposed upon the set of theoretical curves. The lines representing the contributions of $a_1$ and $a_4$ of Equation 2 were added also.

## Correlation of Acoustic Quantities With Hardness and Breaking Energy

A correlation between the ultrasonic velocity and the other quantities was not attempted because errors in the velocity measurements exceeded the variation in the measurements themselves. Attenuation after tempering, attenuation lost on tempering, and the coefficients in Equation 2 corresponding to the attenuation of longitudinal waves after tempering were plotted against the Rockwell C hardness of the blocks in Figures 7 through 11. No correlation or functional relationship could be found between any of these acoustic quantities and the hardness. The same acoustic quantities were plotted against the breaking energies of Type 1 Charpy bars cut from the blocks. The plots appear in Figures 13 through 17. Again, no correlation or functional relationship could be found between any of these acoustic quantities and the breaking energy. Since Figures 6, 12 and 18 indicate

that the heat treatment proceeded correctly, it must be concluded that the ultrasonic methods used in this experiment are incapable of testing for the changes brought about in the mechanical properties through tempering. Failure to temper a specimen could be detected since there would be no change in the attenuation of this block measured before and after "tempering", while other tempered specimens would show a change.

Type of Attenuation Lost on Heat Treatment

The graphs in Figure 3 indicate that the total attenuation of longitudinal waves in the blocks decreased at each stage of the heat treatment. Both the elastic hysteresis and the Rayleigh scattering decreased each time according to Table XVIII. Part of the large decrease in the Rayleigh scattering upon austenitizing and quenching to martensite arose from the refining of the austenitic grain size, and part came from the decrease in the anisotropy of the elastic moduli of the grains on their transformation from pearlite in the hot-rolled stock to martensite in the quenched stock. It is possible that part of the decrease was caused by a change in the grain size distribution attendant upon the austenitizing of the specimens. The elastic hysteresis decreased markedly on austenitizing and quenching as mentioned earlier. The elastic hysteresis decreased to about three-fourths of its previous value on tempering, and the Rayleigh scattering decreased to about one-third of its former value.

Since the grain size and distribution remained unchanged on tempering the decrease in attenuation from Rayleigh scattering must be caused by a decrease in the anisotropy of the elastic constants of the grains. The grains are composed of martensite platelets, so the anisotropy of the grains is a space average of the anisotropy of the platelets taking into consideration their orientations with respect to the axes of the crystallite of austenite from which they were formed. Apparently the anisotropy of the elastic constants of the martensite platelets is reduced on tempering when the body-centered-tetragonal iron with interstitial carbon changes to body-centered-cubic iron.

Tempering effects this change by precipitating the carbon as iron carbide ($Fe_3C$) in submicroscopic globules which interrupt the iron lattice at various spots. The decrease in the anisotropy attending the change from tetragonal to cubic structure outweighs any effect of the presence of the iron carbide spheroids. The attenuation lost on tempering as plotted on log-log paper in Figure 4 shows a slope of about 2.4 indicating a functional dependence on frequency of $f^{2.4}$. The slope of 2.4 is the slope of the best straight line drawn by eye through the points. The true function is a sum of two terms, one for the elastic hysteresis and the other for the Rayleigh scattering. The straight line is an approximation to this function, or

$$\Delta\alpha \cong Af^{2.4} \cong b_1 f + b_4 f^4. \qquad (7)$$

The slope of 2.4 intermediate between unity and four indicates that both terms contribute amounts to $\Delta\alpha$ of the same order of magnitude. The coefficients for changes in attenuation are called b here to distinguish them from the coefficients a in the total attenuation. One should notice that the formula $\Delta\alpha \approx Af^{2.4}$ could equally well be used to approximate a function containing a term in the square of the frequency. Probably a better fit could be obtained if the following function were used:

$$\Delta\alpha \approx Af^{2.4} \approx b_1 f + b_2 f^2 + b_4 f^4 \qquad (8)$$

There is some reason to believe that a term in $f^2$ might not be unreasonable in the attenuation. Wegel and Walther (see Reference 3) found variations in the exponent of the frequency in their elastic hysteresis experiments. Steel drill rod had an attenuation proportional to $f^{0.87}$ while polycrystalline nickel had an attenuation proportional to $f^{1.54}$ in the region around 10,000 cycles per second. This means that the elastic hysteresis, as given by $a_1 f$, is in conformity with the theory of hysteresis, but not borne out perfectly by experiment.

Double Refraction

When transverse wave attenuation measurements were being made on the tempered blocks, it was noticed that the envelope of the echo train, rather than approximating an exponential curve, showed several depressions at regular intervals. On some blocks these depressions almost completely obliterated certain echoes. It was found that the amount of cancellation was greatly dependent on the orientation of the transducer, being greatest when the polarization direction of the transducer was approximately 45 degrees out of alignment with the rolling direction in the specimens.

This phenomenon is very similar to that observed in germanium[24] and silicon[25, 26] single crystals. The transverse wave emitted by the transducer splits into two transverse waves polarized perpendicular to each other, which travel at different velocities. These waves, because of the difference in their velocities, return to the transducer out of phase causing interference and cancellation in the received echo train. This occurs in single crystals when the polarization direction of the transducer is misaligned with the two orthogonal directions in which transverse particle movement is possible in the crystal. In polycrystalline solids this phenomenon will also occur, as is evidenced by this experiment, when there is an axis along which the individual crystals tend to become oriented.

In our experiment, a y-cut transducer was bonded to each specimen with phenyl salicilate, and when the polarization of the transducer happened to be approximately 45 degrees out of alignment with the rolling direction in the steel, the cancellation due to interference became almost complete at some echoes (see Figure 2). In such cases the echo numbers at which the nodes occurred were noted and the fractional differences in velocity were

calculated from the m = 0 through m = 4 branches of the equation (see Reference 24)

$$\frac{\Delta v}{v} = \frac{1}{2ft_T} = \frac{(2m+1)t_A + (-1)^m(2t_o - t_A)}{4ft_o t_A} \qquad (9)$$

where

$f$ = frequency,

$t_o$ = round trip time in the specimen,

$t_A$ = travel time to the first apparent node, and

$t_T$ = travel time to the first true node.

Higher branches were excluded since they would have yielded a difference in velocity well above the minimum difference observable by the pulse-echo method. In the experimental work, no such difference was actually observed.

Since this project did not involve the determination of $\Delta v/v$, the data on this phenomenon are incidental to the other measurements. When interference patterns occurred, the nodes were recorded; but when there was no interference pattern, no attempt to produce one was made. As a result the data are incomplete.

The possibility that the observed differences in velocity were due to preferential orientation of the grains in the steel due to rolling was explored. If $\Delta v/v$ is due to crystal orientation, it is frequency-independent, and as can be seen from Table XX it must be calculated from the m = 0 branch of the formulas in Reference 24. On other branches, $\Delta v/v$ is not independent of frequency. Calculation on the 0-branch yields a difference in velocity in the range from 0.02% to 0.13%.

When a transverse ultrasonic wave is propagated through a single crystal in a given direction, there are only two directions (perpendicular both to each other and to the direction of propagation) in which particle movement is permitted. Transverse waves vibrating in these two directions may have different velocities, as can be seen from the following table. Here the $C_{ij}$ are the elastic moduli of the crystallites and $\rho$ is their density.

| Direction of Propagation | Direction of Particle Movement | Velocity Formula | Velocity In Steel (in./μsec) |
|---|---|---|---|
| [100] | [010] | $\sqrt{\frac{C_{44}}{\rho}}$ | 0.152 |
| | [001] | $\sqrt{\frac{C_{44}}{\rho}}$ | 0.152 |
| [110] | [001] | $\sqrt{\frac{C_{44}}{\rho}}$ | 0.152 |
| | [1$\bar{1}$0] | $\sqrt{\frac{C_{11}-C_{12}}{2\rho}}$ | 0.098 |
| [111] | any direction in the [111] plane | $\sqrt{\frac{C_{11}-C_{12}+C_{44}}{3\rho}}$ | 0.116 |

It can be seen from this table that only when the direction of propagation is [110] is there a difference between the velocity of propagation for the two modes of vibration.

A difference in the velocity of transverse waves of different polarizations also results when the wave enters a single crystal at a small angle to one of the directions of propagation. This difference (see Reference 25) is given by

$$\frac{\Delta v}{v} = \frac{|K_1|\theta^2}{2C_{44}}\left[K_2^2 - \sin^2 2\phi\,(2K_2 - 1)\right]^{\frac{1}{2}} \qquad (10)$$

for the case where the direction of propagation is nearly [100], where

$$K_1 = C_{11} - C_{12} - 2C_{44},\quad K_2 = \frac{C_{11} + C_{12}}{C_{11} - C_{44}}$$

and $\phi$ and $\theta$ are as in the diagram below

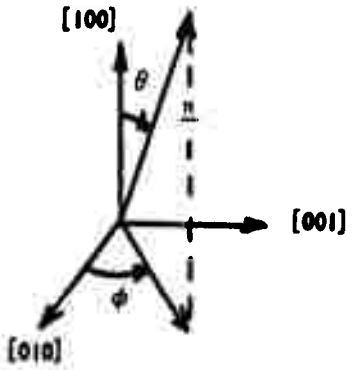


n is the normal to the wave front.

It is obvious that differences in the velocities of the different modes of transverse waves arising from either of the above causes will cancel out in a polycrystalline solid composed of randomly oriented crystals; for every crystal oriented in such a way that it passes one mode a certain amount faster than the other mode there will be another crystal so oriented that it passes the second mode faster than the first by the same amount. For this reason a polycrystalline solid with a preferential orientation of crystals can be considered as being composed of a few crystals oriented in the most preferential way imbedded in a matrix of randomly oriented crystals. The characteristics of the preferentially oriented crystals are then superimposed on the characteristics of the matrix.

In the matrix there is no difference in the velocity of transverse waves of different modes, and the matrix as a whole will pass a transverse wave polarized in any direction in exactly the same way. The wave passing through the matrix is, then, in effect, vibrating in the same direction as the original wave emitted by the transducer. When this wave impinges on the group of preferentially oriented crystals, it splits up into the two distinct quasi-transverse waves which this group of crystals will pass. One mode of vibration is passed at a faster rate and arrives back at the transducer sooner than the other, and the interference resulting from the phase difference between the two waves causes the cancellation observed in the echo pattern.

Since the specimens used in this project were blocks of hot-rolled steel, there was originally a general alignment of the [110] axes of the individual crystals with the rolling direction. Austenitizing and tempering removed some of this preferential orientation, but it seems that there is still some preferred orientation in the blocks. Since there is no reason for the crystals to be aligned in any other direction, it is assumed that the preferred orientation, if there is any, is a residue of the original orientation due to rolling. Therefore, the polycrystal will be treated as if it were a matrix of randomly oriented crystals with a few crystals oriented with their [110] axes parallel to the rolling direction superimposed on this matrix.

The direction of wave propagation in this experiment is known to have been perpendicular to the rolling direction of the specimen but it is not known what the relation between the rolling plane and the direction of propagation was. If the direction of wave propagation were perpendicular to the rolling plane, however, it seems that there would be no difference between the velocities of the waves of different modes; for the [001] direction of the crystals tends to align itself perpendicular to the rolling plane. The direction of wave propagation would then be along the [001] direction in the crystals. Since a difference in velocity arises from the first cause we discussed only when the wave is propagated along the [110] direction, there would be no difference in the velocity of the two modes of vibration due to this cause. Differences in velocity due to the second

cause (entrance of the wave at a small angle to the crystal axes) are also precluded since the crystals show no preference for one direction of rotation about their [110] axes over the other - for every crystal slanted one way there is another one slanted in such a way that $\theta$ (see diagram above) is the same for both crystals and the $\phi$ of one is the complement of the $\phi$ of the other, resulting in mutual negation.

If the angle between the rolling plane and the direction of wave propagation is approximately 35 degrees, the wave is propagated along the long diagonal of the crystal, the [111] direction, and there are not two distinct modes of vibration, for particle movement with equal wave velocity is possible in any direction in the [111] plane. Thus there can be no difference in velocity due to either of the above causes.

If the direction of propagation of the ultrasonic wave is parallel to the rolling plane, we have the ideal case for a difference in velocity due to the first cause discussed above. Now the wave is propagated along the $[1\bar{1}0]$ direction and splits up into a component with particle movement along the [001] direction (perpendicular to the rolling direction) and a slower component with particle movement along the $[1\bar{1}0]$ direction (parallel to the rolling direction). In order to have a crystal oriented in such a way as to counteract the effect of this perfectly oriented crystal, the counteracting crystal would have to be rotated 90 degrees about its $[1\bar{1}0]$ axis from the position most easily occupied.

A velocity difference, caused by the angle at which the sound wave enters the crystal, is very unlikely in this case too, for the effect of a crystal skewed by an angle $\alpha$ about its [110] axis and an angle $\beta$ about its [001] axis is cancelled by the effect of another crystal skewed by $-\beta$ about its [110] axis and $-\alpha$ about its [001] axis. Since rotation by any amount about one axis is just as probable as rotation by the same amount about the other axis, no velocity difference will arise due to this cause.

From the discussion above, it is obvious that the most probable source of the observed velocity difference between different modes of transverse waves, if due to crystal orientation, is an orientation of crystals in such a way as to create the same effect as would be created by a certain number of crystals having their [110] axes aligned with the rolling direction and their $[1\bar{1}0]$ axes aligned with the direction of propagation of the ultrasonic wave, superimposed on a matrix of randomly oriented crystals. Calculation of the percent of crystals oriented in the above way, necessary to produce the observed velocity difference, was undertaken in the following way.

Superimpose on the polycrystal a set of axes such that the x axis corresponds to the direction of rolling and the y axis is perpendicular to both the x axis and the direction in which the ultrasonic wave is propagated through the polycrystal.

Let

$v$ = average velocity of sound in the polycrystal,

$v_x$ = velocity of transverse waves in the oriented crystals when the particle motion is along the x-axis in the specimen

$v_y$ = velocity of transverse waves in the oriented crystals when the particle motion is along the y-axis in the specimen,

$L$ = thickness of the polycrystal along the direction of propagation,

$k$ = fraction of the crystals oriented in the most preferential way,

$t_x$ = travel time of transverse waves polarized along the x-axis for a path length L, and

$t_y$ = travel time of transverse waves polarized along the y-axis for a path length L.

Since the path length in the oriented crystals is proportional to the fraction of oriented crystals, the two equations for the travel time become

$$t_x = \frac{L(1-k)}{v} + \frac{Lk}{v_x} \tag{11a}$$

$$t_y = \frac{L(1-k)}{v} + \frac{Lk}{v_y} \tag{11b}$$

The difference between these is

$$t_x - t_y = \frac{Lk(v_y - v_x)}{v_x v_y} . \tag{12}$$

To estimate the value of k necessary to produce the differences in travel time observed, one can use the data in Table XIII and the two velocities listed above for propagation of transverse waves in the [110] direction. Thus, $v_y = 0.152$ in./$\mu$sec. and $v_x = 0.098$ in./$\mu$sec. Typically, $n_1 = 6$ at 18 mcps. Thus the wave travels a distance of 12L for half a wavelength path difference for interference on the branch m = 0 or 24L for one wavelength (equivalently, one cycle) path difference. The time difference $(t_y - t_x)$ thus corresponds to 1/24 of a cycle at 18 mcps.

The length L is about 0.65 inch so the result on solving the above equation for k is

$$k = 0.00098 \cong 0.001$$

Thus the alignment of 0.1% of the crystallites would suffice to produce the interference patterns observed. It seems that the method of ultrasonic double refraction can be used to detect preferential alignment of crystallites in rolled metal stock when less than 0.1% of the crystallites are aligned.

X-ray diffraction traces of the first four peaks of the martensite [110], [200], [211], and [220] were recorded on two perpendicular faces (one of which was perpendicular to the rolling direction) of four of the specimens showing the double refraction, but the results indicated only that if there were any preferential orientation of the crystals in the steel, it was less than the 2% minimum orientation which could be detected by the X-ray method. Thus the X-ray measurements do not contradict the ultrasonic double refraction measurements.

There is a second possible cause of the ultrasonic double refraction in this steel. Nonmetallic stringers parallel to the direction of rolling occupy 2% of the volume. These stringers are analogous to the elongated damaged regions produced by neutron bombardment of silicon (see Reference 25). Only about 0.1% of the silicon volume was damaged, however. Since the stringers are present uniformly in all the specimens, they should affect the ultrasonic double refraction equally in all specimens. Since the double refraction was pronounced in some specimens and absent in others, it is concluded that stringers do not play a role in the double refraction.

## CONCLUSIONS AND RECOMMENDATIONS

1. Both the elastic hysteresis and the Rayleigh scattering are reduced by the austenitizing and quenching process and by tempering. It is probable that the reduction in the elastic hysteresis loss is caused by the stress reduction brought about by the heat treatment. The reduction in the Rayleigh scattering arises from the changes of the grain size, the ultrasonic velocity (slight change), and the anisotropy of the elastic constants of the grains. In particular, grains of martensite are more elastically isotropic than grains of pearlite. The martensite platelets themselves are too small to contribute appreciably to the Rayleigh scattering since the scattering is proportional to the cube of the diameter of the scattering center. The prior austenite grain volume is the scattering volume, but its anisotropy is reduced by its division into many platelets of martensite. Since the platelets form in 24 directions with respect to the crystal axes of the austenite and not at random, the prior austenite grain volume does not lose all its anisotropy on its transformation to martensite (see References 4, 5 and 17). The grains also become more elastically isotropic on tempering when the interstitial carbon straining the lattice is removed.

2. There is no significant correlation between the ultrasonic data and the hardness or breaking energy of the specimens. In particular, the raw data on longitudinal wave attenuation (equivalent to the corrected data of Table VIII since the correction is the same for all blocks at a particular frequency) show no correlation with the strength parameters. Since the longitudinal wave attenuation measurements are the only ones practical to make on a production line, it is not possible to develop an industrial-scale ultrasonic test for hardness or breaking energy when the variations in these quantities arise from temper-embrittlement. The correlations found in References 1 and 2 were not confirmed. Variations arising from improper quenching could be detected very readily, however, because the pearlite produced in a slow quench has a greater elastic anisotropy than does martensite, and hence has higher Rayleigh scattering and higher attenuation for the same grain size (see References 4, 5 and 17). More work should be done on this.

3. Preferential orientation of metal grains can be detected with great accuracy by the method of ultrasonic double refraction using transverse ultrasonic waves. According to calculations, using known ultrasonic velocities in single crystallites and measured velocity differences in the steel, it is possible to detect a case of preferential orientation involving less than 0.1% of the grains in the specimen. This accuracy is an order of magnitude better than that obtained by the currently used X-ray methods. More research and development work should be done on the application of ultrasonic double refraction to the problems of the preferential orientation of grains in metals. In principle it is possible to make ultrasonic pole figures analogous to the X-ray pole figures used currently.

Studies on rolled, swaged, drawn, or forged metal would yield different ultrasonic double refraction patterns. For instance, swaged iron has the [110] direction of its crystallites aligned preferentially along the swaging axis and the $[1\bar{1}0]$ directions distributed randomly in a plane perpendicular to the swaging axis. Ultrasonic waves propagating normal to the swaging axis will experience equal double refraction at any azimuthal angle about the swaging axis. On the other hand, rolled iron has the [110] direction of its crystallites aligned preferentially along the rolling direction and their $[1\bar{1}0]$ directions aligned parallel to the rolling plane. The fractional velocity changes leading to the ultrasonic double refraction will be a function of the azimuthal angle about the rolling direction when the ultrasonic waves are propagated in a direction perpendicular to the rolling direction.

Propagation normal to the rolling plane will be along the [100] direction in the aligned crystallites, and no velocity difference will be observed because there is four-fold symmetry. Propagation perpendicular to the rolling direction and at an azimuthal angle of about 55 degrees from the normal to the rolling plane will be along the [111] direction in the aligned crystallites, and again there will be no velocity difference because of the three-fold symmetry. Propagation perpendicular to the rolling direction and in the rolling plane will be along the $[1\bar{1}0]$ direction in the aligned

crystallites, so there will be a velocity difference in this case because of the two-fold symmetry. The case of propagation along a [1$\bar{1}$0] direction was treated earlier in the text, and it was found that preferential orientation of 0.1% of the crystallites could be detected easily this way. On some blocks the double refraction effect could not be found even though the transducers were rotated to many positions. Either there was no preferential orientation of the crystallites or the direction of propagation happened to be near the [100] or the [111] directions in the oriented crystallites. If the latter is the case, then there is evidence here for the feasibility of ultrasonic pole patterns. The possibility of a contribution by stringers should not be disregarded in the case of other specimens when further work is done.

## ACKNOWLEDGMENTS

The authors wish to acknowledge the generous help and advice given by Dr. Everett L. Reed and Mr. Stanley M. Lopata.

## APPENDIX A

## TABLE I

## ATTENUATION $\alpha$ VERSUS FREQUENCY f

## AS-RECEIVED BLOCKS

Longitudinal Waves
Attenuation in decibels per microsecond

| f, mcps | 5 | 7 | 9 | 10 | 12 | 15 |
|---|---|---|---|---|---|---|
| Error in $\alpha$ | 0.031 | 0.029 | 0.06 | 0.06 | 0.06 | 0.06 |
| Block | | | | | | |
| 401 | 0.206 | 0.303 | 0.41 | 0.55 | 0.88 | 2.04 |
| 402 | 0.208 | 0.298 | 0.41 | 0.59 | 0.90 | 2.08 |
| 403 | 0.203 | 0.303 | 0.38 | 0.50 | 0.77 | 1.94 |
| 404 | 0.196 | 0.285 | 0.37 | 0.49 | 0.75 | 1.85 |
| 405 | 0.217 | 0.296 | 0.37 | 0.49 | 0.77 | 1.88 |
| 406 | 0.197 | 0.296 | 0.35 | 0.49 | 0.70 | 1.83 |
| 407 | 0.181 | 0.294 | 0.37 | 0.53 | 0.77 | 2.04 |
| 408 | 0.204 | 0.291 | 0.37 | 0.49 | 0.73 | 1.88 |
| 409 | 0.210 | 0.276 | 0.35 | 0.49 | 0.73 | 1.88 |
| 410 | 0.206 | 0.294 | 0.38 | 0.57 | 0.88 | 2.17 |
| 411 | 0.217 | 0.291 | 0.33 | 0.50 | 0.72 | 1.85 |
| 412 | 0.203 | 0.305 | 0.37 | 0.55 | 0.86 | 2.01 |
| 413 | 0.210 | 0.285 | 0.33 | 0.50 | 0.77 | 1.91 |
| 414 | 0.214 | 0.318 | 0.37 | 0.55 | 0.86 | 2.11 |
| 415 | 0.187 | 0.309 | 0.37 | 0.55 | 0.79 | 1.88 |
| 416 | 0.221 | 0.280 | 0.33 | 0.49 | 0.72 | 1.83 |
| 417 | 0.210 | 0.289 | 0.35 | 0.50 | 0.73 | 1.88 |
| 418 | 0.185 | 0.285 | 0.33 | 0.52 | 0.77 | 1.91 |
| 419 | 0.181 | 0.289 | 0.38 | 0.57 | 0.88 | 2.01 |
| 420 | 0.212 | 0.284 | 0.38 | 0.57 | 0.90 | 2.04 |
| 421 | 0.206 | 0.285 | 0.35 | 0.52 | 0.77 | 1.88 |
| 422 | 0.214 | 0.303 | 0.37 | 0.52 | 0.81 | 1.91 |
| 423 | 0.192 | 0.294 | 0.33 | 0.49 | 0.75 | 1.85 |
| 424 | 0.190 | 0.285 | 0.33 | 0.49 | 0.72 | 1.83 |
| 425 | 0.210 | 0.287 | 0.33 | 0.49 | 0.73 | 1.83 |
| 426 | 0.212 | 0.287 | 0.38 | 0.57 | 0.88 | 2.11 |
| 427 | 0.219 | 0.278 | 0.37 | 0.53 | 0.79 | 1.94 |
| 428 | 0.204 | 0.280 | 0.37 | 0.53 | 0.81 | 1.88 |
| 429 | 0.203 | 0.266 | 0.35 | 0.49 | 0.73 | 1.83 |
| 430 | 0.214 | 0.264 | 0.33 | 0.49 | 0.72 | 1.80 |
| 431 | 0.201 | 0.262 | 0.37 | 0.53 | 0.77 | 2.01 |
| 432 | 0.206 | 0.262 | 0.37 | 0.53 | 0.77 | 2.04 |
| 433 | 0.201 | 0.260 | 0.37 | 0.53 | 0.79 | 2.01 |
| 434 | 0.208 | 0.262 | 0.35 | 0.50 | 0.75 | 1.97 |

(continued)

TABLE I (continued)

| f, mcps | 5 | 7 | 9 | 10 | 12 | 15 |
|---|---|---|---|---|---|---|
| Error in a | 0.031 | 0.029 | 0.06 | 0.06 | 0.06 | 0.06 |
| Block | | | | | | |
| 435 | 0.192 | 0.258 | 0.35 | 0.49 | 0.73 | 1.88 |
| 436 | 0.201 | 0.268 | 0.37 | 0.50 | 0.75 | 1.88 |
| 437 | 0.212 | 0.270 | 0.37 | 0.50 | 0.77 | 1.91 |
| 438 | 0.223 | 0.280 | 0.39 | 0.59 | 0.88 | 2.17 |
| 439 | 0.223 | 0.293 | 0.39 | 0.57 | 0.86 | 2.14 |
| 440 | 0.212 | 0.289 | 0.39 | 0.57 | 0.88 | 2.20 |
| 441 | 0.219 | 0.272 | 0.39 | 0.59 | 0.90 | 2.20 |
| 442 | 0.196 | 0.252 | 0.33 | 0.49 | 0.70 | 1.85 |
| 443 | 0.199 | 0.248 | 0.35 | 0.52 | 0.77 | 2.01 |
| 444 | 0.221 | 0.233 | 0.38 | 0.55 | 0.84 | 2.08 |
| 445 | 0.203 | 0.256 | 0.39 | 0.59 | 0.88 | 2.08 |
| 446 | 0.214 | 0.278 | 0.38 | 0.53 | 0.84 | 2.08 |
| 447 | 0.201 | 0.241 | 0.35 | 0.50 | 0.77 | 1.97 |
| 448 | 0.187 | 0.270 | 0.35 | 0.49 | 0.75 | 1.94 |
| 449 | 0.210 | 0.256 | 0.35 | 0.49 | 0.73 | 1.88 |
| 450 | 0.185 | 0.262 | 0.37 | 0.52 | 0.81 | 2.04 |
| 451 | 0.216 | 0.266 | 0.37 | 0.50 | 0.77 | 2.04 |
| 452 | 0.208 | 0.254 | 0.37 | 0.55 | 0.81 | 1.94 |
| 453 | 0.204 | 0.266 | 0.37 | 0.52 | 0.77 | 1.97 |
| 454 | 0.201 | 0.287 | 0.38 | 0.53 | 0.84 | 2.08 |
| 455 | 0.176 | 0.282 | 0.35 | 0.49 | 0.73 | 1.83 |

TABLE II

METALLOGRAPHIC DATA

AS-RECEIVED BLOCKS

| Block | Austenitic Grain Size ASTM | Pearlite | Ferrite | Banding | Stringers |
|---|---|---|---|---|---|
| 401 | 5-6 | fine-coarse | no | moderate | yes |
| 403 | 5 | fine-coarse | no | slight | yes |
| 407 | 5-6 | fine-coarse | trace | pronounced | yes |
| 413 | 5-6 | fine-coarse | trace | slight | yes |
| 417 | 5-6 | fine-coarse | no | pronounced | yes |
| 419 | 5-6 | fine-medium | trace | slight | yes |
| 425 | 5-6 | fine-medium | trace | moderate | yes |
| 431 | 5-6 | fine-coarse | trace | pronounced | yes |
| 433 | 5 | fine-coarse | no | slight | yes |
| 437 | 5-6 | fine-coarse | trace | slight | yes |
| 443 | 5-6 | fine-medium | trace | pronounced | yes |
| 449 | 5-6 | fine-coarse | no | pronounced | yes |
| 455 | 5-6 | fine-coarse | trace | pronounced | yes |

TABLE III

ROCKWELL C HARDNESS

AS-RECEIVED BLOCKS

| Block | Hardness, Average of Four Points |
|---|---|
| 401 | 22.4 |
| 407 | 22.7 |
| 413 | 22.7 |
| 419 | 23.0 |
| 425 | 22.6 |
| 431 | 22.8 |
| 437 | 22.8 |
| 443 | 23.1 |
| 449 | 23.1 |
| 455 | 23.0 |

## TABLE IV

## ATTENUATION α VERSUS FREQUENCY f

## AUSTENITIZED BLOCKS

Longitudinal Waves
Attenuation in decibels per microsecond

| f, mcps | 5 | 6 | 7 | 10 | 12 | 15 | 18 | 20 | 27 | 35 | 40 | 45 | 60 | 75 |
|---|---|---|---|---|---|---|---|---|---|---|---|---|---|---|
| Error in α | 0.032 | 0.025 | 0.021 | 0.018 | 0.021 | 0.020 | 0.018 | 0.015 | 0.013 | 0.02 | 0.05 | 0.06 | 0.05 | 0.06 |
| Block | | | | | | | | | | | | | | |
| 401 | 0.011 | 0* | 0* | 0.014 | 0.007 | 0.044 | 0.042 | 0.056 | 0.19 | 0.26 | 0.37 | 0.48 | 1.09 | 2.19 |
| 402 | 0.015 | 0 | 0 | 0.006 | 0.000* | 0.041 | 0.048 | 0.062 | 0.19 | 0.29 | 0.46 | 0.64 | 1.39 | 2.60 |
| 403 | 0.000* | 0 | 0 | 0.014 | 0.000 | 0.039 | 0.040 | 0.052 | 0.19 | 0.26 | 0.40 | 0.54 | 1.20 | 2.52 |
| 404 | 0.015 | 0 | 0 | 0.018 | 0.002 | 0.038 | 0.046 | 0.056 | 0.19 | 0.26 | 0.37 | 0.51 | 1.15 | 2.28 |
| 405 | 0.004 | 0 | 0 | 0.016 | 0.000 | 0.043 | 0.042 | 0.050 | 0.18 | 0.25 | 0.37 | 0.49 | 1.15 | 2.31 |
| 406 | 0.000 | 0 | 0 | 0.010 | 0.000 | 0.036 | 0.040 | 0.052 | 0.20 | 0.27 | 0.40 | 0.55 | 1.34 | 2.52 |
| 407 | 0.013 | 0 | 0 | 0.010 | 0.006 | 0.044 | 0.050 | 0.054 | 0.20 | 0.27 | 0.40 | 0.58 | 1.37 | 2.78 |
| 408 | 0.004 | 0 | 0 | 0.019 | 0.002 | 0.044 | 0.048 | 0.052 | 0.19 | 0.25 | 0.37 | 0.57 | 1.22 | 2.56 |
| 409 | 0.000 | 0 | 0 | 0.016 | 0.002 | 0.038 | 0.032 | 0.050 | 0.18 | 0.25 | 0.38 | 0.57 | 1.29 | 2.64 |
| 410 | 0.000 | 0 | 0 | 0.018 | 0.000 | 0.038 | 0.046 | 0.064 | 0.20 | 0.30 | 0.46 | 0.67 | 1.53 | 2.90 |
| 411 | 0.010 | 0 | 0 | 0.019 | 0.004 | 0.041 | 0.048 | 0.050 | 0.17 | 0.25 | 0.35 | 0.48 | 1.18 | 2.35 |
| 412 | 0.015 | 0 | 0 | 0.020 | 0.009 | 0.051 | 0.061 | 0.060 | 0.19 | 0.27 | 0.40 | 0.58 | 1.39 | 2.69 |
| 413 | 0.004 | 0 | 0 | 0.019 | 0.006 | 0.032 | 0.048 | 0.050 | 0.18 | 0.26 | 0.40 | 0.54 | 1.29 | 2.64 |
| 414 | 0.006 | 0 | 0 | 0.018 | 0.007 | 0.041 | 0.058 | 0.069 | 0.22 | 0.33 | 0.49 | 0.72 | 1.48 | 2.86 |
| 415 | 0.000 | 0 | 0 | 0.024 | 0.007 | 0.041 | 0.048 | 0.062 | 0.20 | 0.27 | 0.43 | 0.60 | 1.29 | 2.69 |
| 416 | 0.008 | 0 | 0 | 0.018 | 0.006 | 0.041 | 0.050 | 0.048 | 0.19 | 0.25 | 0.37 | 0.52 | 1.20 | 2.42 |
| 417 | 0.010 | 0 | 0 | 0.018 | 0.009 | 0.046 | 0.063 | 0.054 | 0.18 | 0.24 | 0.37 | 0.52 | 1.22 | 2.42 |
| 418 | 0.020 | 0 | 0.072 | 0.089 | 0.071 | 0.169 | 0.277 | 0.206 | 0.24 | 0.32 | 0.44 | 0.60 | 1.39 | 2.52 |
| 419 | 0.000 | 0 | 0 | 0.012 | 0.007 | 0.036 | 0.054 | 0.054 | 0.19 | 0.27 | 0.42 | 0.57 | 1.29 | 2.56 |
| 420 | 0.002 | 0 | 0 | 0.019 | 0.006 | 0.036 | 0.046 | 0.048 | 0.19 | 0.29 | 0.43 | 0.60 | 1.39 | 2.64 |
| 421 | 0.006 | 0 | 0 | 0.024 | 0.009 | 0.049 | 0.058 | 0.045 | 0.17 | 0.25 | 0.38 | 0.55 | 1.03 | 2.31 |
| 422 | 0.008 | 0 | 0 | 0.024 | 0.002 | 0.038 | 0.048 | 0.041 | 0.18 | 0.25 | 0.35 | 0.52 | 1.07 | 2.42 |
| 423 | 0.015 | 0 | 0 | 0.024 | 0.009 | 0.036 | 0.040 | 0.043 | 0.20 | 0.24 | 0.32 | 0.49 | 1.01 | 2.25 |
| 424 | 0.002 | 0 | 0 | 0.018 | 0.000 | 0.036 | 0.039 | 0.040 | 0.18 | 0.23 | 0.32 | 0.48 | 1.03 | 2.35 |
| 425 | 0.010 | 0 | 0 | 0.014 | 0.000 | 0.030 | 0.039 | 0.036 | 0.17 | 0.24 | 0.35 | 0.48 | 0.98 | 2.31 |
| 426 | 0.000 | 0 | 0 | 0.012 | 0.002 | 0.034 | 0.048 | 0.046 | 0.17 | 0.29 | 0.37 | 0.55 | 1.18 | 2.38 |
| 427 | 0.006 | 0 | 0 | 0.012 | 0.000 | 0.032 | 0.046 | 0.041 | 0.17 | 0.24 | 0.35 | 0.51 | 1.15 | 2.31 |
| 428 | 0.010 | 0 | 0 | 0.023 | 0.000 | 0.039 | 0.052 | 0.048 | 0.16 | 0.24 | 0.33 | 0.49 | 1.13 | 2.31 |
| 429 | 0.008 | 0 | 0 | 0.016 | 0.000 | 0.032 | 0.044 | 0.046 | 0.18 | 0.26 | 0.35 | 0.55 | 1.27 | 2.42 |
| 430 | 0.008 | 0 | 0 | 0.026 | 0.000 | 0.039 | 0.054 | 0.043 | 0.17 | 0.25 | 0.32 | 0.51 | 1.07 | 2.35 |
| 431 | 0.000 | 0 | 0 | 0.024 | 0.009 | 0.048 | 0.048 | 0.050 | 0.16 | 0.23 | 0.31 | 0.49 | 1.15 | 2.25 |
| 432 | 0.000 | 0 | 0 | 0.016 | 0.007 | 0.036 | 0.046 | 0.052 | 0.18 | 0.25 | 0.37 | 0.54 | 1.15 | 2.52 |
| 433 | 0.000 | 0 | 0 | 0.021 | 0.007 | 0.041 | 0.046 | 0.050 | 0.17 | 0.23 | 0.35 | 0.49 | 1.13 | 2.45 |
| 434 | 0.008 | 0 | 0 | 0.019 | 0.007 | 0.039 | 0.046 | 0.048 | 0.17 | 0.24 | 0.33 | 0.52 | 1.15 | 2.42 |
| 435 | 0.006 | 0 | 0 | 0.019 | 0.004 | 0.039 | 0.042 | 0.048 | 0.19 | 0.26 | 0.37 | 0.55 | 1.22 | 2.52 |
| 436 | 0.004 | 0 | 0 | 0.012 | 0.000 | 0.034 | 0.042 | 0.048 | 0.25 | 0.40 | 0.58 | 0.86 | 1.43 | 2.90 |
| 437 | 0.000 | 0 | 0 | 0.014 | 0.000 | 0.034 | 0.040 | 0.038 | 0.18 | 0.25 | 0.37 | 0.52 | 1.13 | 2.52 |
| 438 | 0.000 | 0 | 0 | 0.012 | 0.000 | 0.036 | 0.042 | 0.048 | 0.23 | 0.35 | 0.52 | 0.67 | 1.53 | 2.82 |
| 439 | 0.000 | 0 | 0 | 0.010 | 0.000 | 0.036 | 0.046 | 0.052 | 0.24 | 0.35 | 0.47 | 0.68 | 1.51 | 2.86 |
| 440 | 0.004 | 0 | 0 | 0.012 | 0.004 | 0.034 | 0.044 | 0.056 | 0.18 | 0.27 | 0.37 | 0.54 | 1.18 | 2.52 |
| 441 | 0.000 | 0 | 0 | 0.010 | 0.000 | 0.039 | 0.040 | 0.045 | 0.22 | 0.35 | 0.50 | 0.67 | 1.37 | 2.74 |
| 442 | 0.002 | 0 | 0 | 0.014 | 0.000 | 0.034 | 0.039 | 0.046 | 0.17 | 0.25 | 0.38 | 0.52 | 1.11 | 2.25 |
| 443 | 0.022 | 0 | 0 | 0.024 | 0.004 | 0.041 | 0.050 | 0.041 | 0.18 | 0.24 | 0.35 | 0.51 | 1.05 | 2.19 |
| 444 | 0.008 | 0 | 0 | 0.006 | 0.002 | 0.032 | 0.035 | 0.040 | 0.21 | 0.31 | 0.44 | 0.64 | 1.34 | 2.74 |
| 445 | 0.008 | 0 | 0 | 0.010 | 0.000 | 0.032 | 0.040 | 0.045 | 0.18 | 0.27 | 0.37 | 0.52 | 1.22 | 2.45 |
| 446 | 0.020 | 0 | 0 | 0.014 | 0.000 | 0.044 | 0.044 | 0.043 | 0.18 | 0.25 | 0.33 | 0.51 | 1.05 | 2.42 |
| 447 | 0.013 | 0 | 0 | 0.016 | 0.000 | 0.038 | 0.044 | 0.041 | 0.18 | 0.25 | 0.38 | 0.51 | 1.18 | 2.31 |
| 448 | 0.013 | 0 | 0 | 0.014 | 0.004 | 0.036 | 0.044 | 0.040 | 0.19 | 0.25 | 0.38 | 0.51 | 1.15 | 2.42 |
| 449 | 0.018 | 0 | 0 | 0.019 | 0.000 | 0.041 | 0.042 | 0.041 | 0.18 | 0.23 | 0.35 | 0.49 | 1.09 | 2.25 |
| 450 | 0.002 | 0 | 0 | 0.019 | 0.000 | 0.038 | 0.046 | 0.041 | 0.19 | 0.25 | 0.44 | 0.52 | 1.24 | 2.52 |
| 451 | 0.011 | 0 | 0 | 0.019 | 0.004 | 0.044 | 0.046 | 0.041 | 0.17 | 0.22 | 0.33 | 0.49 | 1.07 | 2.28 |
| 452 | 0.011 | 0 | 0 | 0.016 | 0.000 | 0.039 | 0.042 | 0.041 | 0.16 | 0.23 | 0.33 | 0.49 | 1.15 | 2.28 |
| 453 | 0.010 | 0 | 0 | 0.028 | 0.007 | 0.070 | 0.072 | 0.088 | 0.24 | 0.35 | 0.55 | 0.67 | 1.56 | 2.82 |
| 454 | 0.151 | 0 | 0 | - | 0.117 | - | - | - | - | 0.71 | 0.71 | 0.88 | 1.82 | 4.08 |
| 455 | 0.131 | 0 | 0.43 | 0.296 | - | 0.366 | 0.387 | 0.653 | - | - | - | - | - | - |

*The attenuation minus the diffraction correction was negative, therefore it was set equal to zero.

TABLE V

METALLOGRAPHIC DATA

AUSTENITIZED BLOCKS

| Block | Martensite | Bainite | Carbide | Stringers |
|---|---|---|---|---|
| 410 | 98% | 2% | trace | many |
| 425 | 97% | 3% | trace | many |
| 436 | 100% | 0 | fine throughout | many |
| 443 | 97% | 3% | fine throughout | many |

TABLE VI

ROCKWELL C HARDNESS

AUSTENITIZED BLOCKS

AVERAGE OF FOUR POINTS

| Block | Hardness | Block | Hardness | Block | Hardness |
|---|---|---|---|---|---|
| 401 | 63.3 | 421 | 60.4 | 441 | 60.2 |
| 402 | 59.9 | 422 | 60.4 | 442 | 60.2 |
| 403 | 60.5 | 423 | 60.2 | 443 | 60.1 |
| 404 | 60.7 | 424 | 60.4 | 444 | 60.2 |
| 405 | 60.0 | 425 | 60.6 | 445 | 60.4 |
| 406 | 60.1 | 426 | 60.7 | 446 | 60.4 |
| 407 | 59.5 | 427 | 60.8 | 447 | 60.3 |
| 408 | 59.6 | 428 | 60.6 | 448 | 60.7 |
| 409 | 60.3 | 429 | 60.3 | 449 | 60.7 |
| 410 | 59.9 | 430 | 60.7 | 450 | 60.6 |
| 411 | 60.2 | 431 | 60.5 | 451 | 60.4 |
| 412 | 60.2 | 432 | 60.6 | 452 | 60.4 |
| 413 | 60.3 | 433 | 60.5 | 453 | 42.6 |
| 414 | 59.8 | 434 | 60.4 | 454 | 43.2 |
| 415 | 60.3 | 435 | 60.2 | 455 | 45.5 |
| 416 | 60.2 | 436 | 60.4 | | |
| 417 | 60.3 | 437 | 60.5 | | |
| 418 | 60.6 | 438 | 60.5 | | |
| 419 | 60.3 | 439 | 60.4 | | |
| 420 | 60.5 | 440 | 60.4 | | |

TABLE VII

TEMPERING CONDITIONS

ONE HOUR TEMPER

| Tempering Temperature, Deg Cent | Cooling | |
|---|---|---|
| | Water Quenched | Furnace Cooled |
| | Blocks | Blocks |
| 425 | 402, 403 | 404, 405 |
| 450 | 406, 407 | 408, 409 |
| 475 | 410, 411 | 412, 413 |
| 500 | 414, 415 | 416, 417 |
| 525 | 418, 419 | 420, 421 |
| 550 | 422, 423 | 424, 425 |
| 575 | 426, 427 | 428, 429 |
| 600 | 430, 431 | 432, 433 |
| 625 | 434, 435 | 436, 437 |
| 650 | 438, 439 | 440, 441 |
| 675 | 442, 443 | 444, 445 |
| 700 | 446, 447 | 448, 449 |
| 725 | 450, 451 | 452 |

## TABLE VIII

## ATTENUATION a VERSUS FREQUENCY f

## TEMPERED BLOCKS

Longitudinal Waves

Attenuation in decibels per microsecond

| f, mcps | | | 9 | 10 | 12 | 15 | 18 | 20 | 21 | 27 | 30 | 35 | 45 | 60 | 75 | 90 | 100 |
|---|---|---|---|---|---|---|---|---|---|---|---|---|---|---|---|---|---|
| Error in a | | | 0.016 | 0.016 | 0.020 | 0.020 | 0.018 | 0.014 | 0.018 | 0.022 | 0.022 | 0.024 | 0.10 | 0.10 | 0.11 | 0.14 | 0.21 |
| Block | Temp.* | Quench** | | | | | | | | | | | | | | | |
| 401 | - | - | - | - | - | - | - | - | - | - | - | - | - | - | - | - | - |
| 402 | 425 | Wa | | 0.008 | 0 | 0.013 | 0.015 | 0.018 | 0.012 | 0.028 | 0.094 | 0.161 | 0.25 | 0.54 | 1.51 | 2.18 | 2.63 |
| 403 | 425 | Wa | | 0.001 | 0 | 0.011 | 0.004 | 0.007 | 0.014 | 0 | 0.075 | 0.148 | 0.21 | 0.47 | 1.31 | 1.92 | 2.53 |
| 404 | 425 | Fu | | 0.014 | 0 | 0.008 | 0.005 | 0.007 | 0.002 | 0 | 0.041 | 0.126 | 0.19 | 0.40 | 1.36 | 1.73 | 2.15 |
| 405 | 425 | Fu | | 0.005 | 0 | 0.008 | 0.002 | 0.011 | 0.004 | 0.008 | 0.073 | 0.117 | 0.17 | 0.44 | 1.26 | 1.75 | 2.27 |
| 406 | 450 | Wa | | 0.005 | 0 | 0.009 | 0.004 | 0.013 | 0.025 | 0.023 | 0.123 | 0.122 | 0.19 | 0.44 | 1.43 | 1.86 | 2.53 |
| 407 | 450 | Wa | | 0.005 | 0 | 0.009 | 0.005 | 0.007 | 0.001 | 0.014 | 0.062 | 0.120 | 0.23 | 0.47 | 1.41 | 1.78 | 2.27 |
| 408 | 450 | Fu | | 0.005 | 0 | 0.008 | 0.002 | 0.007 | 0.010 | 0.018 | 0.049 | 0.122 | 0.25 | 0.45 | 1.43 | 1.78 | 2.19 |
| 409 | 450 | Fu | | 0.014 | 0 | 0.009 | 0.002 | 0.003 | 0.019 | 0.025 | 0.077 | 0.122 | 0.19 | 0.44 | 1.31 | 1.89 | 2.63 |
| 410 | 475 | Wa | | 0 | 0 | 0.004 | 0.004 | 0.005 | 0.012 | 0.021 | 0.079 | 0.153 | 0.20 | 0.50 | 1.48 | 2.02 | 2.78 |
| 411 | 475 | Wa | 0 | 0.006 | 0.002 | 0.005 | 0 | 0.007 | 0.015 | 0.030 | 0.103 | 0.19 | 0.19 | 0.48 | 1.12 | 1.75 | 2.23 |
| 412 | 475 | Fu | 0 | 0.014 | 0 | 0.013 | 0.011 | 0.013 | 0.004 | 0.004 | 0.020 | 0.115 | 0.21 | 0.40 | 1.26 | 1.75 | 2.12 |
| 413 | 475 | Fu | 0 | 0.003 | 0.007 | 0.008 | 0 | 0.005 | 0.019 | 0.036 | 0.103 | 0.145 | 0.20 | 0.47 | 1.19 | 1.92 | 2.49 |
| 414 | 500 | Wa | 0 | 0.017 | 0.005 | 0.006 | 0.007 | 0.019 | 0.020 | 0.049 | 0.114 | 0.168 | 0.23 | 0.54 | 1.46 | 1.95 | 2.68 |
| 415 | 500 | Wa | 0 | 0.010 | 0 | 0.008 | 0.009 | 0.009 | 0.012 | 0.018 | 0.062 | 0.129 | 0.19 | 0.50 | 1.22 | 1.75 | 2.08 |
| 416 | 500 | Fu | 0 | 0.014 | 0 | 0.009 | 0.004 | 0.007 | 0.024 | 0.046 | 0.115 | 0.120 | 0.18 | 0.35 | 1.14 | 1.73 | 2.32 |
| 417 | 500 | Fu | 0 | 0.025 | 0.007 | 0.013 | 0.009 | 0.007 | 0.019 | 0.023 | 0.103 | 0.124 | 0.17 | 0.47 | 1.22 | 1.78 | 2.19 |
| 418 | 525 | Wa | 0.061 | 0.185 | 0.082 | 0.214 | 0.143 | 0.163 | 0.083 | 0.072 | 0.129 | 0.131 | 0.18 | 0.42 | 1.28 | 1.62 | 2.05 |
| 419 | 525 | Wa | 0 | 0.014 | 0 | 0.014 | 0.001 | 0.005 | 0.019 | 0.021 | 0.053 | 0.124 | 0.15 | 0.35 | 1.31 | 1.81 | 2.19 |
| 420 | 525 | Fu | 0 | 0.010 | 0 | 0.013 | 0.015 | 0.011 | 0.015 | 0.034 | 0.068 | 0.119 | 0.19 | 0.45 | 1.24 | 1.92 | 2.27 |
| 421 | 525 | Fu | 0.001 | 0.010 | 0 | 0.006 | 0.009 | 0.003 | 0.012 | 0.047 | 0.105 | 0.091 | 0.15 | 0.37 | 1.09 | 1.54 | 2.15 |
| 422 | 550 | Wa | 0 | 0.019 | 0.002 | 0.006 | 0.007 | 0.009 | 0.014 | 0.049 | 0.073 | 0.109 | 0.15 | 0.34 | 1.09 | 1.57 | 2.19 |
| 423 | 550 | Wa | 0 | 0.017 | 0.003 | 0.008 | 0.009 | 0.007 | 0.006 | 0.002 | 0.041 | 0.091 | 0.14 | 0.34 | 1.24 | 1.47 | 2.12 |
| 424 | 550 | Fu | 0.001 | 0.025 | 0.005 | 0.003 | 0.009 | 0 | 0.015 | 0.030 | 0.087 | 0.103 | 0.14 | 0.42 | 1.17 | 1.49 | 2.19 |
| 425 | 550 | Fu | 0 | 0.021 | 0 | 0.004 | 0.005 | 0.001 | 0.002 | 0.010 | 0.051 | 0.080 | 0.13 | 0.38 | 1.07 | 1.44 | 2.08 |
| 426 | 575 | Wa | 0 | 0.017 | 0.003 | 0.004 | 0.009 | 0.005 | 0.017 | 0.047 | 0.105 | 0.101 | 0.17 | 0.34 | 1.14 | 1.64 | 2.12 |
| 427 | 575 | Wa | 0 | 0.027 | 0.002 | 0.014 | 0.017 | 0.009 | 0.012 | 0.014 | 0.035 | 0.103 | 0.15 | 0.40 | 1.22 | 1.49 | 1.82 |
| 428 | 575 | Fu | 0 | 0.025 | 0.011 | 0.003 | 0.002 | 0 | 0.024 | 0.038 | 0.109 | 0.093 | 0.17 | 0.40 | 1.14 | 1.64 | 2.15 |
| 429 | 575 | Fu | 0 | 0.010 | 0 | 0.003 | 0.002 | 0.001 | 0.001 | 0.026 | 0.069 | 0.103 | 0.15 | 0.35 | 1.28 | 1.57 | 2.08 |
| 430 | 600 | Wa | 0 | 0.017 | 0.007 | 0.011 | 0.015 | 0.011 | 0.012 | 0.004 | 0.026 | 0.103 | 0.18 | 0.44 | 1.14 | 1.59 | 1.98 |
| 431 | 600 | Wa | 0 | 0.014 | 0.007 | 0.008 | 0.005 | 0.011 | 0.010 | 0.014 | 0.039 | 0.101 | 0.13 | 0.34 | 0.94 | 1.62 | 2.08 |
| 432 | 600 | Fu | 0 | 0.016 | 0 | 0.006 | 0.007 | 0.003 | 0.013 | 0.025 | 0.041 | 0.091 | 0.18 | 0.40 | 1.31 | 1.62 | 2.08 |
| 433 | 600 | Fu | 0 | 0.014 | 0 | 0.003 | 0.002 | 0.001 | 0.008 | 0.008 | 0.041 | 0.087 | 0.15 | 0.35 | 1.07 | 1.54 | 2.01 |
| 434 | 625 | Wa | 0 | 0.014 | 0.005 | 0.011 | 0.007 | 0.011 | 0.022 | 0.038 | 0.105 | 0.119 | 0.18 | 0.44 | 1.19 | 1.64 | 2.05 |
| 435 | 625 | Wa | 0 | 0.019 | 0.003 | 0.006 | 0.009 | 0.003 | 0.017 | 0.038 | 0.089 | 0.107 | 0.14 | 0.38 | 1.14 | 1.59 | 2.12 |
| 436 | 625 | Fu | 0 | 0.012 | 0.007 | 0 | 0.009 | 0 | 0.015 | 0.028 | 0.053 | 0.111 | 0.15 | 0.37 | 1.05 | 1.59 | 2.27 |

*Tempering temperature in degrees centigrade

**Quenching method: Wa = Water, Fu = Furnace

(continued)

TABLE VIII (continued)

| f, mcps | | | 9 | 10 | 12 | 15 | 18 | 20 | 21 | 27 | 30 | 35 | 45 | 60 | 75 | 90 | 100 |
|---|---|---|---|---|---|---|---|---|---|---|---|---|---|---|---|---|---|
| Error in α | | | 0.016 | 0.016 | 0.020 | 0.020 | 0.018 | 0.014 | 0.018 | 0.022 | 0.022 | 0.024 | 0.10 | 0.10 | 0.11 | 0.14 | 0.21 |
| Block | Temp.* | Quench** | | | | | | | | | | | | | | | |
| 437 | 625 | Fu | 0 | 0.012 | 0 | 0.004 | 0.004 | 0 | 0.012 | 0.019 | 0.066 | 0.097 | 0.14 | 0.40 | 1.22 | 1.59 | 2.05 |
| 438 | 650 | Wa | 0 | 0.014 | 0 | 0.004 | 0.004 | 0.005 | 0.006 | 0.040 | 0.068 | 0.126 | 0.12 | 0.45 | 1.31 | 1.70 | 2.27 |
| 439 | 650 | Wa | 0 | 0.025 | 0.002 | 0.006 | 0.005 | 0.007 | 0.018 | 0.046 | 0.085 | 0.111 | 0.17 | 0.45 | 1.26 | 1.70 | 2.27 |
| 440 | 650 | Fu | 0 | 0.021 | 0 | 0.004 | 0.004 | 0.001 | 0.025 | 0.049 | 0.114 | 0.120 | 0.15 | 0.38 | 1.14 | 1.64 | 2.15 |
| 441 | 650 | Fu | 0 | 0.021 | 0 | 0.001 | 0.007 | 0.003 | 0.013 | 0.049 | 0.136 | 0.101 | 0.17 | 0.45 | 1.14 | 1.67 | 2.37 |
| 442 | 675 | Wa | 0 | 0.010 | 0 | 0.004 | 0.017 | 0.011 | 0 | 0.042 | 0.069 | 0.101 | 0.17 | 0.35 | 1.05 | 1.64 | 2.32 |
| 443 | 675 | Wa | 0 | 0.014 | 0.005 | 0.003 | 0.004 | 0.011 | 0.006 | 0.025 | 0.049 | 0.113 | 0.14 | 0.45 | 1.09 | 1.64 | 2.15 |
| 444 | 675 | Fu | 0 | 0.014 | 0 | 0.006 | 0.015 | 0.018 | 0.020 | 0.046 | 0.119 | 0.111 | 0.13 | 0.42 | 1.33 | 1.67 | 2.23 |
| 445 | 675 | Fu | 0 | 0.014 | 0 | 0.001 | 0.009 | 0.007 | 0.012 | 0.046 | 0.083 | 0.109 | 0.14 | 0.40 | 1.22 | 1.64 | 2.19 |
| 446 | 700 | Wa | 0 | 0.017 | 0 | 0.011 | 0.013 | 0.011 | 0.012 | 0.012 | 0.013 | 0.109 | 0.13 | 0.40 | 1.26 | 1.52 | 2.15 |
| 447 | 700 | Wa | 0 | 0.027 | 0.003 | 0.009 | 0.025 | 0.014 | 0.050 | 0.062 | 0.214 | 0.170 | 0.23 | 0.58 | 1.07 | 1.84 | 2.27 |
| 448 | 700 | Fu | 0 | 0.012 | 0.002 | 0.006 | 0.009 | 0.005 | 0.012 | 0.006 | 0.069 | 0.107 | 0.17 | 0.44 | 1.00 | 1.73 | 2.12 |
| 449 | 700 | Fu | 0 | 0.027 | 0.007 | 0.006 | 0.005 | 0.001 | 0.025 | 0.025 | 0.130 | 0.105 | 0.15 | 0.47 | 1.12 | 1.59 | 2.15 |
| 450 | 725 | Wa | 0.003 | 0.023 | 0.002 | 0.018 | 0.018 | 0.016 | 0.043 | 0.023 | 0.160 | 0.147 | 0.18 | 0.40 | 1.46 | 1.62 | 2.32 |
| 451 | 725 | Wa | 0.001 | 0.027 | 0.007 | 0.030 | 0.038 | 0.032 | 0.044 | 0.078 | 0.172 | 0.190 | 0.19 | 0.54 | 1.51 | 1.95 | 2.53 |
| 452 | 725 | Fu | 0 | 0.019 | 0.009 | 0.006 | 0.015 | 0.013 | 0.037 | 0.066 | 0.146 | 0.133 | 0.18 | 0.45 | 1.33 | 2.05 | 2.63 |
| 453 | - | - | 0 | 0.019 | 0 | 0.011 | 0.011 | 0.011 | 0.022 | 0.066 | 0.146 | 0.119 | 0.18 | 0.44 | 1.12 | 1.86 | 2.41 |

*Tempering temperature in degrees centigrade

**Quenching method: Wa = Water, Fu = Furnace

TABLE IX

ATTENUATION Δ α LOST ON TEMPERING

Longitudinal Waves

Attenuation in Decibels Per Microsecond

| f, mcps | | | 10 | 12 | 15 | 18 | 20 | 27 | 35 | 45 | 60 | 75 |
|---|---|---|---|---|---|---|---|---|---|---|---|---|
| Block | Temp.* | Quench** | | | | | | | | | | |
| 401 | - | - | - | - | - | - | - | - | - | - | - | - |
| 402 | 425 | Wa | 0 | 0 | 0.028 | 0.033 | 0.044 | 0.16 | 0.13 | 0.39 | 0.85 | 1.09 |
| 403 | 425 | Wa | 0.013 | 0 | 0.028 | 0.036 | 0.045 | 0.19 | 0.11 | 0.33 | 0.73 | 1.21 |
| 404 | 425 | Fu | 0.004 | 0.002 | 0.030 | 0.041 | 0.049 | 0.19 | 0.13 | 0.32 | 0.75 | 0.92 |
| 405 | 425 | Fu | 0.011 | 0 | 0.035 | 0.040 | 0.039 | 0.17 | 0.13 | 0.32 | 0.71 | 1.05 |
| 406 | 450 | Wa | 0.005 | 0 | 0.034 | 0.036 | 0.039 | 0.18 | 0.15 | 0.36 | 0.90 | 1.09 |
| 407 | 450 | Wa | 0.004 | 0.006 | 0.035 | 0.045 | 0.047 | 0.19 | 0.15 | 0.35 | 0.90 | 1.37 |
| 408 | 450 | Fu | 0.014 | 0.002 | 0.036 | 0.046 | 0.045 | 0.17 | 0.13 | 0.32 | 0.77 | 1.13 |
| 409 | 450 | Fu | 0.002 | 0.002 | 0.029 | 0.030 | 0.047 | 0.16 | 0.13 | 0.38 | 0.85 | 1.33 |
| 410 | 475 | Wa | 0.018 | 0 | 0.034 | 0.042 | 0.059 | 0.18 | 0.15 | 0.47 | 1.03 | 1.42 |
| 411 | 475 | Wa | 0.013 | 0.002 | 0.035 | 0.048 | 0.043 | 0.14 | 0.15 | 0.29 | 0.70 | 1.23 |
| 412 | 475 | Fu | 0.015 | 0.009 | 0.038 | 0.050 | 0.047 | 0.19 | 0.15 | 0.37 | 0.99 | 1.43 |
| 413 | 475 | Fu | 0.016 | 0 | 0.024 | 0.048 | 0.045 | 0.14 | 0.12 | 0.34 | 0.82 | 1.45 |
| 414 | 500 | Wa | 0.001 | 0.002 | 0.035 | 0.051 | 0.050 | 0.17 | 0.16 | 0.49 | 0.94 | 1.40 |
| 415 | 500 | Wa | 0.014 | 0.007 | 0.033 | 0.039 | 0.053 | 0.18 | 0.14 | 0.41 | 0.79 | 1.47 |
| 416 | 500 | Fu | 0.004 | 0.006 | 0.032 | 0.046 | 0.041 | 0.14 | 0.13 | 0.34 | 0.85 | 1.28 |
| 417 | 500 | Fu | 0 | 0.002 | 0.033 | 0.054 | 0.047 | 0.16 | 0.12 | 0.35 | 0.75 | 1.20 |
| 418 | 525 | Wa | 0 | 0 | 0 | 0.034 | 0.043 | 0.14 | 0.19 | 0.42 | 0.97 | 1.24 |
| 419 | 525 | Wa | 0 | 0.007 | 0.022 | 0.053 | 0.049 | 0.17 | 0.15 | 0.42 | 0.94 | 1.25 |
| 420 | 525 | Fu | 0.009 | 0.006 | 0.023 | 0.031 | 0.037 | 0.16 | 0.17 | 0.41 | 0.94 | 1.40 |
| 421 | 525 | Fu | 0.014 | 0.009 | 0.043 | 0.049 | 0.042 | 0.12 | 0.16 | 0.40 | 0.66 | 1.22 |
| 422 | 550 | Wa | 0.005 | 0 | 0.032 | 0.041 | 0.032 | 0.13 | 0.14 | 0.37 | 0.73 | 1.33 |
| 423 | 550 | Wa | 0.007 | 0.006 | 0.026 | 0.031 | 0.036 | 0.20 | 0.15 | 0.35 | 0.67 | 1.01 |
| 424 | 550 | Fu | 0 | 0 | 0.033 | 0.030 | 0.040 | 0.15 | 0.13 | 0.34 | 0.61 | 1.18 |
| 425 | 550 | Fu | 0 | 0 | 0.026 | 0.034 | 0.035 | 0.16 | 0.16 | 0.35 | 0.60 | 1.24 |
| 426 | 575 | Wa | 0 | 0 | 0.030 | 0.039 | 0.041 | 0.12 | 0.19 | 0.38 | 0.84 | 1.24 |
| 427 | 575 | Wa | 0 | 0 | 0.018 | 0.029 | 0.032 | 0.16 | 0.14 | 0.36 | 0.75 | 1.09 |
| 428 | 575 | Fu | 0 | 0 | 0.033 | 0.050 | 0.048 | 0.12 | 0.15 | 0.32 | 0.73 | 1.17 |
| 429 | 575 | Fu | 0.006 | 0 | 0.029 | 0.042 | 0.045 | 0.15 | 0.16 | 0.40 | 0.92 | 1.14 |
| 430 | 600 | Wa | 0.009 | 0 | 0.028 | 0.039 | 0.032 | 0.17 | 0.15 | 0.33 | 0.63 | 1.21 |
| 431 | 600 | Wa | 0.010 | 0.002 | 0.040 | 0.043 | 0.039 | 0.15 | 0.13 | 0.36 | 0.81 | 1.31 |
| 432 | 600 | Fu | 0 | 0.007 | 0.030 | 0.039 | 0.049 | 0.16 | 0.16 | 0.36 | 0.75 | 1.21 |
| 433 | 600 | Fu | 0.007 | 0.007 | 0.038 | 0.044 | 0.049 | 0.16 | 0.14 | 0.34 | 0.78 | 1.38 |
| 434 | 625 | Wa | 0.005 | 0.002 | 0.028 | 0.039 | 0.037 | 0.13 | 0.12 | 0.34 | 0.71 | 1.23 |
| 435 | 625 | Wa | 0 | 0.001 | 0.033 | 0.033 | 0.045 | 0.15 | 0.15 | 0.41 | 0.84 | 1.38 |
| 436 | 625 | Fu | 0 | 0 | 0.034 | 0.035 | 0.048 | 0.22 | 0.29 | 0.71 | 1.06 | 1.85 |
| 437 | 625 | Fu | 0.002 | 0 | 0.030 | 0.036 | 0.038 | 0.16 | 0.15 | 0.38 | 0.73 | 1.30 |
| 438 | 650 | Wa | 0 | 0 | 0.032 | 0.038 | 0.043 | 0.19 | 0.22 | 0.55 | 1.08 | 1.51 |
| 439 | 650 | Wa | 0 | 0 | 0.030 | 0.041 | 0.046 | 0.19 | 0.24 | 0.51 | 1.06 | 1.60 |
| 440 | 650 | Fu | 0 | 0.004 | 0.030 | 0.040 | 0.055 | 0.13 | 0.15 | 0.39 | 0.80 | 1.38 |
| 441 | 650 | Fu | 0 | 0 | 0.038 | 0.033 | 0.042 | 0.17 | 0.25 | 0.50 | 0.92 | 1.60 |
| 442 | 675 | Wq | 0.004 | 0 | 0.030 | 0.022 | 0.035 | 0.13 | 0.15 | 0.35 | 0.76 | 1.20 |
| 443 | 675 | Wa | 0.010 | 0 | 0.038 | 0.046 | 0.030 | 0.16 | 0.13 | 0.37 | 0.60 | 1.10 |
| 444 | 675 | Fu | 0 | 0.002 | 0.026 | 0.030 | 0.022 | 0.16 | 0.20 | 0.51 | 0.92 | 1.41 |
| 445 | 675 | Fu | 0 | 0 | 0.031 | 0.031 | 0.039 | 0.13 | 0.16 | 0.38 | 0.82 | 1.23 |
| 446 | 700 | Wa | 0 | 0 | 0.033 | 0.031 | 0.032 | 0.17 | 0.14 | 0.38 | 0.65 | 1.16 |
| 447 | 700 | Wa | 0 | 0 | 0.029 | 0.019 | 0.027 | 0.12 | 0.08 | 0.28 | 0.60 | 1.24 |
| 448 | 700 | Fu | 0.002 | 0.002 | 0.030 | 0.035 | 0.035 | 0.18 | 0.14 | 0.34 | 0.71 | 1.42 |
| 449 | 700 | Fu | 0 | 0 | 0.025 | 0.037 | 0.040 | 0.16 | 0.13 | 0.34 | 0.62 | 1.13 |
| 450 | 725 | Wa | 0 | 0 | 0.020 | 0.028 | 0.025 | 0.17 | 0.10 | 0.34 | 0.84 | 1.06 |
| 451 | 725 | Wa | 0 | 0 | 0.014 | 0.008 | 0.009 | 0.09 | 0.03 | 0.30 | 0.53 | 0.77 |
| 452 | 725 | Fu | 0 | 0 | 0.033 | 0.027 | 0.028 | 0.09 | 0.10 | 0.31 | 0.70 | 0.95 |
| 453 | - | - | 0.009 | 0.007 | 0.059 | 0.061 | 0.077 | 0.17 | 0.23 | 0.49 | 1.12 | 1.70 |

*Tempering temperature in degrees Centigrade

**Quenching method: Wa = Water, Fu = Furnace

TABLE X

ATTENUATION a VERSUS FREQUENCY f

TEMPERED BLOCKS

Transverse Waves

Attenuation in Decibels Per Microsecond

| f, mcps | | | 7 | 10 | 18 | 21 | 30 | 35 | 54 | 63 | 90 |
|---|---|---|---|---|---|---|---|---|---|---|---|
| Error in a | | | 0.034 | 0.027 | 0.047 | 0.045 | 0.06 | 0.06 | 0.06 | 0.06 | 0.06 |
| Block | Temp.* | Quench** | | | | | | | | | |
| 401 | - | - | 0.073 | - | 0.157 | 0.239 | - | 0.52 | - | - | - |
| 402 | 425 | Wa | 0.018 | 0.055 | 0.086 | 0.198 | - | 0.32 | 1.73 | - | - |
| 403 | 425 | Wa | 0.025 | 0.036 | 0.073 | - | 0.34 | - | 1.04 | - | - |
| 404 | 425 | Fu | 0.010 | 0.069 | 0.065 | 0.233 | 0.32 | 0.32 | 1.10 | - | - |
| 405 | 425 | Fu | 0.022 | 0.044 | 0.086 | 0.124 | 0.28 | 0.27 | 0.76 | 1.78 | - |
| 406 | 450 | Wa | 0.018 | 0.037 | 0.067 | 0.102 | 0.31 | 0.32 | 0.53 | - | - |
| 407 | 450 | Wa | 0.028 | 0.050 | 0.075 | 0.146 | 0.35 | 0.33 | 0.32 | 1.83 | - |
| 408 | 450 | Fu | 0.046 | 0.018 | 0.073 | 0.118 | 0.24 | 0.20 | 0.97 | 1.57 | 1.85 |
| 409 | 450 | Fu | 0.037 | 0.052 | 0.138 | 0.188 | 0.27 | 0.28 | 0.96 | 1.42 | - |
| 410 | 475 | Wa | 0.028 | 0.162 | 0.111 | 0.106 | 0.34 | 0.33 | - | 1.75 | 0.82 |
| 411 | 475 | Wa | 0.040 | 0.037 | 0.083 | 0.172 | 0.24 | 0.32 | 1.14 | - | - |
| 412 | 475 | Fu | 0.030 | 0.046 | 0.075 | 0.156 | 0.28 | 0.29 | 1.02 | 1.40 | - |
| 413 | 475 | Fu | 0.014 | 0.040 | 0.086 | 0.126 | 0.35 | 0.26 | 1.21 | 1.42 | - |
| 414 | 500 | Wa | 0.014 | 0.022 | 0.079 | 0.198 | 0.35 | 0.32 | 1.10 | 0.81 | 6.25 |
| 415 | 500 | Wa | 0.015 | 0.052 | 0.094 | 0.120 | 0.35 | 0.25 | 1.84 | 1.49 | 2.31 |
| 416 | 500 | Fu | 0.009 | 0.032 | 0.083 | 0.237 | 0.39 | 0.33 | 1.10 | 1.40 | 1.22 |
| 417 | 500 | Fu | 0.012 | 0.050 | 0.071 | 0.148 | 0.29 | 0.27 | 1.21 | 1.12 | 5.60 |
| 418 | 525 | Wa | 0.038 | 0.077 | 0.131 | 0.132 | 0.32 | 0.21 | 0.94 | 0.57 | - |
| 419 | 525 | Wa | 0.016 | 0.117 | 0.067 | 0.114 | 0.25 | 0.27 | 0.87 | 1.69 | 2.02 |
| 420 | 525 | Fu | 0.022 | 0.018 | 0.081 | 0.141 | 0.31 | 0.40 | 1.23 | 1.94 | 1.63 |
| 421 | 525 | Fu | 0.026 | 0.016 | 0.060 | 0.102 | 0.31 | 0.25 | 0.65 | 1.28 | 1.93 |
| 422 | 550 | Wa | 0.022 | 0.016 | 0.090 | 0.134 | 0.35 | 0.28 | 0.97 | 1.75 | 1.96 |
| 423 | 550 | Wa | 0.018 | 0.071 | 0.086 | 0.084 | 0.27 | 0.25 | 1.04 | 1.28 | - |
| 424 | 550 | Fu | 0.018 | 0.028 | 0.079 | 0.124 | 0.31 | 0.22 | 1.31 | 1.44 | 1.51 |
| 425 | 550 | Fu | 0.018 | 0.022 | 0.056 | 0.196 | 0.29 | 0.31 | 1.04 | - | 1.58 |
| 426 | 575 | Wa | 0.012 | 0.052 | 0.090 | 0.100 | 0.32 | 0.27 | 1.08 | 1.75 | - |
| 427 | 575 | Wa | 0.020 | 0.017 | 0.119 | 0.116 | 0.28 | 0.21 | 0.92 | 1.28 | 2.34 |
| 428 | 575 | Fu | 0.009 | 0.024 | 0.069 | 0.132 | 0.33 | 0.25 | 1.36 | 1.38 | 2.16 |
| 429 | 575 | Fu | 0.020 | 0.020 | 0.077 | 0.106 | 0.28 | 0.26 | 1.06 | 1.36 | - |
| 430 | 600 | Wa | 0.007 | 0.036 | 0.103 | 0.241 | 0.39 | 0.33 | - | - | 2.31 |
| 431 | 600 | Wa | 0.025 | 0.065 | 0.077 | 0.112 | - | 0.31 | 0.94 | 1.42 | 1.88 |
| 432 | 600 | Fu | 0.023 | 0.014 | 0.066 | 0.141 | 0.34 | - | 1.10 | 1.67 | 1.11 |
| 433 | 600 | Fu | 0.022 | 0.016 | 0.052 | 0.134 | 0.33 | 0.34 | 0.92 | 1.49 | 1.51 |
| 434 | 625 | Wa | 0.051 | 0.012 | 0.065 | 0.130 | 0.35 | 0.26 | 1.08 | 1.49 | - |
| 435 | 625 | Wa | 0.022 | 0.009 | 0.065 | 0.118 | 0.33 | - | 1.04 | - | - |
| 436 | 625 | Fu | 0.016 | 0.103 | 0.034 | 0.128 | 0.35 | 0.33 | 0.85 | 1.12 | - |
| 437 | 625 | Fu | 0.004 | 0.030 | 0.075 | 0.139 | 0.31 | 0.27 | 1.14 | 1.08 | 1.63 |
| 438 | 650 | Wa | 0.015 | 0.020 | 0.119 | 0.116 | 0.33 | 0.29 | 1.10 | 1.69 | - |
| 439 | 650 | Wa | 0.014 | 0.083 | 0.073 | 0.156 | 0.35 | 0.31 | 1.17 | 1.62 | 1.85 |
| 440 | 650 | Fu | 0.012 | 0.028 | 0.107 | 0.273 | 0.28 | 0.29 | 1.33 | 1.30 | - |
| 441 | 650 | Fu | 0 | 0.022 | 0.060 | 0.180 | 0.31 | 0.26 | 0.90 | 1.02 | - |
| 442 | 675 | Wa | 0.018 | 0.025 | 0.090 | 0.185 | 0.32 | 0.32 | 0.97 | - | 1.85 |
| 443 | 675 | Wa | 0.016 | 0.020 | 0.069 | 0.139 | 0.39 | 0.29 | 0.79 | 1.52 | 1.22 |
| 444 | 675 | Fu | 0.012 | 0.020 | 0.070 | 0.150 | 0.39 | 0.29 | 1.12 | - | 1.24 |
| 445 | 675 | Fu | 0.015 | 0.088 | 0.081 | 0.112 | 0.33 | 0.27 | 1.02 | 1.75 | 1.43 |
| 446 | 700 | Wa | 0.026 | 0.071 | 0.097 | 0.237 | 0.31 | 0.46 | 0.92 | - | - |
| 447 | 700 | Wa | 0.026 | 0.037 | 0.081 | 0.243 | 0.31 | 0.26 | 1.14 | 1.42 | - |
| 448 | 700 | Fu | 0.022 | 0.039 | 0.081 | 0.120 | - | 0.29 | 1.00 | 1.64 | - |
| 449 | 700 | Fu | 0.026 | 0.046 | 0.119 | 0.168 | 0.34 | 0.31 | 1.26 | 1.69 | 1.66 |
| 450 | 725 | Wa | 0.101 | 0.020 | 0.088 | 0.174 | 0.34 | 0.24 | 0.90 | 1.12 | 1.56 |
| 451 | 725 | Wa | 0.034 | 0.040 | 0.136 | 0.280 | 0.32 | 0.63 | 1.19 | 1.54 | - |
| 452 | 725 | Fu | 0.020 | 0.028 | 0.084 | 0.146 | 0.33 | 0.34 | 1.10 | 1.87 | - |
| 453 | - | - | 0.026 | 0.090 | 0.101 | 0.130 | - | 0.31 | 1.47 | 1.83 | - |

*Tempering temperature in degrees Centigrade
**Quenching method: Wa = Water, Fu = Furnace

TABLE XI

VELOCITY v VERSUS FREQUENCY f

TEMPERED BLOCKS

Longitudinal Waves

| f, mcps | | | 18 | 54 |
|---|---|---|---|---|
| Error | | | 0.0023 | 0.0048 |
| Block | Temp.* | Quench** | | |
| 406 | 450 | Wa | 0.2319 | 0.2315 |
| 408 | 450 | Fu | 0.2320 | 0.2308 |
| 426 | 575 | Wa | 0.2322 | 0.2334 |
| 428 | 575 | Fu | 0.2326 | 0.2346 |
| 446 | 700 | Wa | 0.2331 | 0.2292 |
| 448 | 700 | Fu | 0.2334 | 0.2354 |

Velocity is given in inches per microsecond.

*Tempering temperature in degrees Centigrade

**Quenching method: Wa = Water, Fu = Furnace

TABLE XII

VELOCITY v VERSUS FREQUENCY f

TEMPERED BLOCKS

Transverse Waves

| f, mcps | | | 7 | 18 | 21 | 54 |
|---|---|---|---|---|---|---|
| Error | | | 0.0009 | 0.0008 | 0.0012 | 0.0038 |
| Block | Temp.* | Quench** | | | | |
| 406 | 450 | Wa | 0.1263 | 0.1260 | 0.1256 | 0.1273 |
| 408 | 450 | Fu | 0.1264 | 0.1265 | 0.1261 | 0.1264 |
| 426 | 575 | Wa | 0.1265 | 0.1270 | 0.1258 | - |
| 428 | 575 | Fu | 0.1270 | 0.1275 | 0.1270 | - |
| 446 | 700 | Wa | 0.1273 | 0.1276 | 0.1271 | 0.1271 |
| 448 | 700 | Fu | 0.1275 | 0.1276 | 0.1269 | 0.1270 |

Velocity is given in inches per microsecond.

*Tempering temperature in degrees Centigrade

**Quenching method: Wa = Water, Fu = Furnace

## TABLE XIII

## TRANSVERSE WAVE INTERFERENCE PARAMETERS

## TEMPERED BLOCKS

j = First, second ... interference  $M_j$ = echo at which it occurs

| f. mops | Block | Temp.* | Quench** | j = 1 | 2 | 3 | 4 | 5 | 6 | 7 | $\frac{\Delta v}{v} \times 10^4$ *** |
|---|---|---|---|---|---|---|---|---|---|---|---|
| 7 | 401 | | | $M_j$ = 8 | 25 | 30 | 43 | | | | 10.17 |
| 10 | 404 | 425 | Fu | 9.5 | - | - | - | - | - | - | 4.94 |
| | 405 | 425 | Fu | 7 | - | - | - | - | - | - | 6.70 |
| | 406 | 450 | Wa | 7 | 23 | - | - | - | - | - | 6.31 |
| | 407 | 450 | Wa | 9.5 | - | - | - | - | - | - | 4.84 |
| | 411 | 475 | Wa | 6 | 17 | - | - | - | - | - | 8.13 |
| | 412 | 475 | Fu | 5.5 | 16 | - | - | - | - | - | 8.71 |
| | 416 | 500 | Fu | 8 | - | - | - | - | - | - | 5.86 |
| 18 | 401 | - | - | 2 | 7 | 10 | - | - | - | - | 12.43 |
| | 402 | 425 | Wa | 10 | - | - | - | - | - | - | 2.61 |
| | 406 | 450 | Wa | 4 | 12 | 21 | 29 | 37 | - | - | 6.34 |
| | 407 | 450 | Wa | 4 | 11 | 18 | 25 | 32 | 40 | 45 | 7.29 |
| | 408 | 450 | Fu | 5 | 14 | 23 | 33 | 44 | - | - | 5.48 |
| | 410 | 475 | Wa | 6 | 17 | - | - | - | - | - | 4.52 |
| | 413 | 475 | Fu | 6 | 16 | 27 | 38 | 48 | 59 | 69 | 4.86 |
| | 415 | 500 | Wa | 8 | 24 | 38 | 50 | - | - | - | 3.47 |
| | 416 | 500 | Fu | 5 | 15 | 26 | 36 | 46 | - | - | 6.27 |
| | 418 | 525 | Wa | 5 | 13 | 28 | - | - | - | - | 5.21 |
| | 421 | 550 | Fu | 4 | 12 | 20 | 28 | 35 | 42 | 49 | 6.69 |
| | 430 | 600 | Wa | 6 | 17 | 27 | 35 | 45 | - | - | 5.00 |
| | 438 | 650 | Wa | 14 | 40 | - | - | - | - | - | 1.93 |
| | 440 | 650 | Fu | 12 | - | - | - | - | - | - | 2.18 |
| | 449 | 700 | Fu | 16 | - | - | - | - | - | - | 1.63 |
| 21 | 402 | 425 | Wa | 6 | 18 | 30 | - | - | - | - | 3.72 |
| | 404 | 425 | Fu | 6 | 22 | - | - | - | - | - | 3.27 |
| | 408 | 450 | Fu | 5 | 13 | 22 | - | - | - | - | 5.00 |
| | 409 | 450 | Fu | 6 | 18 | - | - | - | - | - | 3.72 |
| | 421 | 525 | Fu | 5 | 13 | 22 | 31 | - | - | - | 5.01 |
| | 447 | 700 | Wa | 5 | 8 | 15 | 17 | 24 | - | - | 8.14 |
| | 451 | 725 | Wa | 9 | - | - | - | - | - | - | 2.48 |
| 30 | 404 | 425 | Fu | 3 | 10 | - | - | - | - | - | 4.88 |
| | 405 | 425 | Fu | 2 | 7 | 11 | - | - | - | - | 7.08 |
| | 406 | 450 | Wa | 2 | 8 | - | - | - | - | - | 6.50 |
| | 407 | 450 | Wa | 3 | 8 | 14 | - | - | - | - | 5.64 |
| | 411 | 475 | Wa | 2 | 6 | 11 | 15 | - | - | - | 7.38 |
| | 412 | 475 | Fu | 2 | 6 | 9 | 13 | - | - | - | 8.30 |
| | 447 | 700 | Wa | 3 | 5 | 10 | - | - | - | - | 7.89 |
| 35 | 405 | 425 | Fu | 2 | 6 | - | - | - | - | - | 6.70 |
| | 408 | 450 | Fu | 3 | - | - | - | - | - | - | 4.47 |
| | 409 | 450 | Fu | 2 | - | - | - | - | - | - | 4.47 |
| | 411 | 475 | Wa | 2 | - | - | - | - | - | - | 6.70 |
| | 421 | 525 | Fu | 3 | 8 | - | - | - | - | - | 4.84 |
| | 427 | 575 | Wa | 3 | 9 | - | - | - | - | - | 4.47 |
| | 440 | 650 | Fu | 6 | 9 | - | - | - | - | - | 3.73 |
| | 447 | 700 | Wa | 4 | 10 | - | - | - | - | - | 3.80 |
| | 450 | 725 | Wa | 7 | - | - | - | - | - | - | 1.91 |
| | 451 | 725 | Wa | 6 | - | - | - | - | - | - | 2.24 |

*Tempering temperature in degrees Centigrade

**Quenching method: Wa = Water, Fu = Furnace

***Average value of all modes weighted by j.

## TABLE XIV

## ROCKWELL C HARDNESS

## TEMPERED BLOCKS

## AVERAGE OF FOUR POINTS

| Block | Temp.* | Quench** | Hardness | Block | Temp.* | Quench** | Hardness | Block | Temp.* | Quench** | Hardness |
|---|---|---|---|---|---|---|---|---|---|---|---|
| 401 | - | - | 62.2 | 421 | 525 | Fu | 37.8 | 441 | 650 | Fu | 29.2 |
| 402 | 425 | Wa | 48.2 | 422 | 550 | Wa | 39.0 | 442 | 675 | Wa | 31.0 |
| 403 | 425 | Wa | 47.8 | 423 | 550 | Wa | 39.2 | 443 | 675 | Wa | 31.0 |
| 404 | 425 | Fu | 46.2 | 424 | 550 | Fu | 35.9 | 444 | 675 | Fu | 23.4 |
| 405 | 425 | Fu | 46.2 | 425 | 550 | Fu | 36.3 | 445 | 675 | Fu | 23.0 |
| 406 | 450 | Wa | 46.3 | 426 | 575 | Wa | 37.3 | 446 | 700 | Wa | 27.8 |
| 407 | 450 | Wa | 45.7 | 427 | 575 | Wa | 37.2 | 447 | 700 | Wa | 27.0 |
| 408 | 450 | Fu | 45.4 | 428 | 575 | Fu | 34.5 | 448 | 700 | Fu | 19.0 |
| 409 | 450 | Fu | 46.2 | 429 | 575 | Fu | 34.7 | 449 | 700 | Fu | 20.6 |
| 410 | 475 | Wa | 45.0 | 430 | 600 | Wa | 35.6 | 450 | 725 | Wa | 25.3 |
| 411 | 475 | Wa | 44.3 | 431 | 600 | Wa | 35.2 | 451 | 725 | Wa | 25.3 |
| 412 | 475 | Fu | 43.2 | 432 | 600 | Fu | 32.5 | 452 | 725 | Fu | 16.3 |
| 413 | 475 | Fu | 43.4 | 433 | 600 | Fu | 32.4 | 453 | - | - | 17.8 |
| 414 | 500 | Wa | 42.6 | 434 | 625 | Wa | 34.2 | | | | |
| 415 | 500 | Wa | 42.5 | 435 | 625 | Wa | 34.0 | | | | |
| 416 | 500 | Fu | 41.7 | 436 | 625 | Fu | 30.3 | | | | |
| 417 | 500 | Fu | 40.9 | 437 | 625 | Fu | 31.2 | | | | |
| 418 | 525 | Wa | 41.6 | 438 | 650 | Wa | 33.0 | | | | |
| 419 | 525 | Wa | 41.3 | 439 | 650 | Wa | 32.5 | | | | |
| 420 | 525 | Fu | 37.8 | 440 | 650 | Fu | 28.3 | | | | |

*Tempering temperature in degrees Centigrade

**Quenching method: Wa = Water, Fu = Furnace

## TABLE XV

## CHARPY BAR IMPACT DATA

## TEMPERED BLOCKS

| | | | Breaking Energy | | | | | Breaking Energy | | | | | Breaking Energy | |
|---|---|---|---|---|---|---|---|---|---|---|---|---|---|---|
| Block | Temp.* | Quench** | Room Temp. | -60 F | Block | Temp.* | Quench** | Room Temp. | -60 F | Block | Temp.* | Quench** | Room Temp. | -60 F |
| 401 | - | - | - | - | 421 | 525 | Fu | 45.3 | 10.6 | 441 | 650 | Fu | 152.7 | 44.0 |
| 402 | 425 | Wa | 10.0 | 5.7 | 422 | 550 | Wa | 47.0 | 17.8 | 442 | 675 | Wa | 92.2 | 97.1 |
| 403 | 425 | Wa | 11.2 | 6.2 | 423 | 550 | Wa | 67.9 | 18.8 | 443 | 675 | Wa | 146.8 | 123.9 |
| 404 | 425 | Fu | - | - | 424 | 550 | Fu | 43.6 | 13.0 | 444 | 675 | Fu | - | 99.6 |
| 405 | 425 | Fu | 10.6 | 7.0 | 425 | 550 | Fu | 39.8 | 13.3 | 445 | 675 | Fu | 146.8 | 127.8 |
| 406 | 450 | Wa | 11.5 | 8.4 | 426 | 575 | Wa | 43.6 | 26.5 | 446 | 700 | Wa | - | 161.8 |
| 407 | 450 | Wa | 12.7 | 10.6 | 427 | 575 | Wa | 57.2 | 23.6 | 447 | 700 | Wa | 47.2 | 74.1 |
| 408 | 450 | Fu | 10.9 | 7.5 | 428 | 575 | Fu | 52.7 | 14.2 | 448 | 700 | Fu | - | 159.7 |
| 409 | 450 | Fu | 10.9 | 8.6 | 429 | 575 | Fu | 56.7 | 23.3 | 449 | 700 | Fu | - | 177.5 |
| 410 | 475 | Wa | 18.8 | 9.5 | 430 | 600 | Wa | 76.5 | 74.1 | 450 | 725 | Wa | 66.0 | 101.1 |
| 411 | 475 | Wa | 25.4 | 11.5 | 431 | 600 | Wa | 58.2 | 58.6 | 451 | 725 | Wa | - | - |
| 412 | 475 | Fu | 16.5 | 9.5 | 432 | 600 | Fu | 88.7 | 45.3 | 452 | 725 | Fu | - | 166.8 |
| 413 | 475 | Fu | 17.8 | 9.5 | 433 | 600 | Fu | 63.7 | 26.5 | 453 | - | - | - | 117.0 |
| 414 | 500 | Wa | 27.2 | 11.8 | 434 | 625 | Wa | 89.2 | 57.7 | | | | | |
| 415 | 500 | Wa | 27.6 | 12.7 | 435 | 625 | Wa | 124.8 | 106.6 | | | | | |
| 416 | 500 | Fu | 29.5 | 9.7 | 436 | 625 | Fu | 106.6 | 50.1 | | | | | |
| 417 | 500 | Fu | 28.7 | 12.4 | 437 | 625 | Fu | 81.8 | 34.5 | | | | | |
| 418 | 525 | Wa | 36.1 | 13.9 | 438 | 650 | Wa | 132.2 | 71.3 | | | | | |
| 419 | 525 | Wa | 29.5 | 6.2 | 439 | 650 | Wa | 117.5 | 61.4 | | | | | |
| 420 | 525 | Fu | 36.1 | 11.8 | 440 | 650 | Fu | 152.2 | 67.5 | | | | | |

*Tempering temperature in degrees Centigrade

**Quenching method: Wa = Water, Fu = Furnace

TABLE XVI

METALLOGRAPHIC DATA

TEMPERED BLOCKS

| Block | Temp.* | Quench** | Grain Size ASTM*** | | Tempered Martensite Character | Grain Boundary Segregation**** |
|---|---|---|---|---|---|---|
| | | | Transverse | Longitudinal | | |
| 402 | 425 | Wa | 8-9 | 8-9 | fine acicular | trace |
| 403 | 425 | Wa | 8-9 | 8-9 | fine acicular | trace |
| 404 | 425 | Fu | - | - | fine acicular | noticeable |
| 405 | 425 | Fu | - | - | fine acicular | noticeable |
| 406 | 450 | Wa | 8-9 | 8-9 | fine acicular | small amount |
| 408 | 450 | Fu | 8-9 | 8-9 | - | - |
| 412 | 475 | Fu | 8-9 | 8-9 | fine acicular | small amount |
| 414 | 500 | Wa | 7-9 | 8-9 | - | - |
| 418 | 525 | Wa | 7-9 | 7-9 | fine acicular | some evident |
| 419 | 525 | Wa | - | - | fine acicular | small amount |
| 420 | 525 | Fu | 8-9 | 7-10 | fine acicular | noticeable |
| 421 | 525 | Fu | - | - | fine acicular | noticeable |
| 422 | 550 | Wa | 8-9 | 8-9 | - | - |
| 424 | 550 | Fu | 8-9 | 8-9 | - | - |
| 426 | 575 | Wa | 8-9 | 7-9 | - | - |
| 428 | 575 | Fu | 8-9 | 8-9 | - | - |
| 430 | 600 | Wa | 7-9 | 7-9 | - | - |
| 432 | 600 | Fu | 8-9 | 8-9 | - | - |
| 434 | 625 | Wa | 8-9 | 8-9 | fine acicular | small amount |
| 435 | 625 | Wa | - | - | fine acicular | small amount |
| 436 | 625 | Fu | 8-9 | 8-9 | fine acicular | noticeable |
| 437 | 625 | Fu | - | - | fine acicular | noticeable |
| 438 | 650 | Wa | 8-9 | 8-9 | - | - |
| 439 | 650 | Wa | 7-9 | 8-9 | - | - |
| 440 | 650 | Fu | 7-9 | 7-9 | - | - |
| 442 | 675 | Wa | 8-9 | 7-9 | - | - |
| 444 | 675 | Fu | 7-9 | 7-9 | - | - |
| 446 | 700 | Wa | 8-9 | 9 | - | - |
| 448 | 700 | Fu | 8-9 | 8-9 | - | - |
| 450 | 725 | Wa | 7-9 | 8-9 | carbides resolved | small amount |
| 451 | 725 | Wa | - | - | carbides resolved | small amount |
| 452 | 725 | Fu | 7-9 | 7-9 | carbides resolved | noticeable |
| 453 | - | - | - | - | carbides resolved | noticeable |

*Tempering temperature in degrees Centigrade

**Quenching method: Wa = Water, Fu = Furnace

***Measurements taken on a surface perpendicular to the rolling direction (transverse) and on a surface parallel to the rolling direction (longitudinal).

****Etch of Cohen, Hurlich, and Jacobson.

## TABLE XVII

## REPORT OF SPECTROGRAPHIC ANALYSIS

| Block | Elements | | | | |
|---|---|---|---|---|---|
| | Mn | Si | Cr | Mo | Al |
| 401 | .83 | .26 | 1.20 | .09 | .02 |
| 402 | .99 | .30 | 1.08 | .09 | .02 |
| 403 | 1.11 | .32 | 1.10 | .07 | .01 |
| 404 | .98 | .37 | 1.15 | .07 | .01 |
| 405 | 1.05 | .36 | 1.24 | .07 | .01 |
| 406 | 1.00 | .31 | 1.38 | .08 | .01 |
| 407 | .97 | .28 | 1.25 | .08 | .01 |
| 408 | .98 | .27 | 1.19 | .09 | .02 |
| 409 | .79 | .29 | 1.44 | .06 | .02 |
| 410 | 1.08 | .32 | 1.30 | .08 | .01 |
| 411 | 1.00 | .32 | 1.30 | .08 | .01 |
| 412 | .97 | .30 | 1.35 | .08 | .02 |
| 413 | 1.10 | .30 | 1.17 | .08 | .01 |
| 414 | 1.09 | .33 | 1.29 | .08 | .01 |
| 415 | 1.00 | .30 | 1.24 | .08 | .02 |
| 416 | .92 | .30 | 1.15 | .07 | .04 |
| 417 | 1.03 | .35 | 1.04 | .05 | .01 |
| 418 | 1.01 | .32 | 1.13 | .05 | .01 |
| 419 | .89 | .30 | 1.14 | .06 | .02 |
| 420 | 1.08 | .33 | 1.17 | .05 | .02 |
| 421 | .94 | .30 | 1.21 | .06 | .01 |
| 422 | 1.05 | .35 | 1.18 | .05 | .01 |
| 423 | .92 | .31 | 1.15 | .05 | .01 |
| 424 | .87 | .32 | 1.11 | .06 | .02 |
| 425 | 1.04 | .34 | 1.16 | .06 | .01 |
| 426 | 1.00 | .38 | 1.28 | .06 | .03 |
| 427 | .79 | .25 | 1.18 | .07 | .03 |
| 428 | .96 | .27 | 1.17 | .06 | .02 |
| 429 | .94 | .30 | 1.07 | .06 | .02 |
| 430 | 1.00 | .31 | 1.23 | .06 | .03 |
| 431 | 1.04 | .33 | 1.17 | .05 | .02 |
| 432 | .96 | .29 | 1.19 | .06 | .02 |
| 433 | .84 | .25 | 1.17 | .05 | .02 |
| 434 | 1.01 | .30 | 1.14 | .05 | .01 |
| 435 | 1.00 | .28 | 1.17 | .06 | .02 |
| 436 | .91 | .30 | 1.15 | .05 | .02 |
| 437 | 1.02 | .30 | 1.17 | .05 | .02 |
| 438 | 1.04 | .32 | 1.15 | .05 | .02 |
| 439 | 1.03 | .26 | 1.10 | .05 | .01 |
| 440 | .93 | .27 | 1.18 | .06 | .01 |
| 441 | 1.07 | .26 | 1.11 | .04 | .01 |
| 442 | 1.08 | .28 | 1.05 | .04 | .01 |
| 443 | .90 | .21 | 1.14 | .06 | .03 |
| 444 | .94 | .26 | 1.28 | .05 | .02 |
| 445 | .98 | .28 | 1.29 | .06 | .03 |
| 446 | .83 | .26 | 1.12 | .05 | .03 |
| 447 | .83 | .22 | 1.01 | .03 | .02 |
| 448 | .88 | .19 | 1.17 | .06 | .03 |
| 449 | .89 | .25 | 1.24 | .06 | .02 |
| 450 | 1.00 | .23 | 1.23 | .04 | .01 |
| 451 | .94 | .21 | 1.23 | .06 | .02 |
| 452 | .89 | .20 | 1.23 | .06 | .02 |
| 453 | .96 | .19 | 1.27 | .05 | .03 |
| 454 | 1.00 | .31 | 1.19 | .05 | .02 |
| 455 | 1.02 | .22 | 1.12 | .04 | .02 |
| Special | 1.00 | .22 | 1.16 | .04 | .03 |

## TABLE XVIII

## COEFFICIENTS IN SERIES EXPANSION OF ATTENUATION

| | | | Hot-Rolled Longitudinal | | Austenitized and Quenched Longitudinal | | Tempered | | | |
|---|---|---|---|---|---|---|---|---|---|---|
| | | | | | | | Longitudinal | | Transverse | |
| | Coeff. Mult. by | | $a_1$ $10^{-2}$ | $a_4$ $10^{-5}$ | $a_1$ $10^{-3}$ | $a_4$ $10^{-8}$ | $a_1$ $10^{-3}$ | $a_4$ $10^{-8}$ | $a_1$ $10^{-3}$ | $a_4$ $10^{-8}$ |
| Block | Temp.* | Quench** | | | | | | | | |
| 401 | - | - | 2.38 | 3.26 | 5.10 | 5.77 | - | - | - | - |
| 402 | 425 | Wa | 2.46 | 3.32 | 6.66 | 6.80 | 5.23 | 2.33 | - | - |
| 403 | 425 | Wa | 2.05 | 3.12 | 4.96 | 6.83 | 3.80 | 2.28 | - | - |
| 404 | 425 | Fu | 2.06 | 2.96 | 5.22 | 6.05 | 4.21 | 1.91 | - | - |
| 405 | 425 | Fu | 2.13 | 2.99 | 4.87 | 6.22 | 3.73 | 2.04 | 3.37 | 9.27 |
| 406 | 450 | Wa | 1.96 | 2.93 | 5.68 | 6.78 | 4.13 | 2.24 | - | - |
| 407 | 450 | Wa | 1.80 | 3.34 | 5.18 | 7.65 | 4.70 | 1.97 | 2.33 | 8.90 |
| 408 | 450 | Fu | 1.99 | 3.02 | 4.89 | 6.98 | 4.97 | 1.88 | 4.09 | 8.42 |
| 409 | 450 | Fu | 1.88 | 3.06 | 4.85 | 7.28 | 2.89 | 2.45 | 6.91 | 6.37 |
| 410 | 475 | Wa | 2.00 | 3.61 | 6.51 | 7.80 | 4.04 | 2.50 | - | - |
| 411 | 475 | Wa | 1.96 | 2.97 | 4.65 | 6.42 | 3.77 | 1.98 | - | - |
| 412 | 475 | Fu | 2.25 | 3.24 | 5.59 | 7.32 | 3.96 | 1.91 | 8.81 | 8.48 |
| 413 | 475 | Fu | 1.90 | 3.12 | 4.36 | 7.27 | 3.59 | 2.26 | 7.66 | 8.80 |
| 414 | 500 | Wa | 2.09 | 3.46 | 7.25 | 7.45 | 4.77 | 2.31 | 11.07 | 1.84 |
| 415 | 500 | Wa | 2.36 | 2.94 | 5.47 | 7.28 | 4.50 | 1.82 | 10.76 | 7.21 |
| 416 | 500 | Fu | 1.94 | 2.94 | 4.96 | 6.55 | 3.04 | 2.12 | 8.35 | 5.57 |
| 417 | 500 | Fu | 1.96 | 3.03 | 5.01 | 6.56 | 4.16 | 1.94 | 8.81 | 4.67 |
| 418 | 525 | Wa | 1.80 | 3.13 | 6.56 | 6.02 | 5.70 | 1.60 | 9.97 | 0.71 |
| 419 | 525 | Wa | 2.29 | 3.24 | 5.59 | 6.86 | 3.71 | 2.02 | 4.10 | 8.77 |
| 420 | 525 | Fu | 2.33 | 3.29 | 6.04 | 7.07 | 4.05 | 2.07 | 6.78 | 9.7[illegible] |
| 421 | 525 | Fu | 2.10 | 3.01 | 4.82 | 6.13 | 2.94 | 1.93 | 4.66 | 5.[illegible] |
| 422 | 550 | Wa | 2.28 | 3.02 | 4.23 | 6.62 | 2.71 | 2.00 | 5.39 | 8.75 |
| 423 | 550 | Wa | 1.93 | 3.00 | 4.20 | 6.10 | 3.02 | 1.90 | 6.52 | 8.07 |
| 424 | 550 | Fu | 1.87 | 2.97 | 3.72 | 6.52 | 3.22 | 1.92 | 7.36 | 7.15 |
| 425 | 550 | Fu | 1.96 | 2.94 | 3.81 | 6.34 | 2.59 | 1.66 | - | - |
| 426 | 575 | Wa | 2.14 | 3.65 | 5.29 | 6.34 | 3.29 | 1.92 | 5.40 | 8.01 |
| 427 | 575 | Wa | 2.13 | 3.12 | 4.72 | 6.26 | 4.17 | 1.57 | 5.84 | 6.06 |
| 428 | 575 | Fu | 2.28 | 2.97 | 4.42 | 6.32 | 3.44 | 1.92 | 8.37 | 8.53 |
| 429 | 575 | Fu | 1.94 | 2.95 | 5.28 | 6.55 | 3.60 | 1.85 | 4.17 | 10.07 |
| 430 | 600 | Wa | 1.94 | 2.89 | 4.20 | 6.43 | 3.79 | 1.75 | - | - |
| 431 | 600 | Wa | 1.81 | 3.33 | 4.54 | 6.14 | 2.16 | 1.98 | - | - |
| 432 | 600 | Fu | 1.87 | 3.32 | 4.49 | 6.91 | 4.03 | 1.83 | - | - |
| 433 | 600 | Fu | - | - | 4.06 | 6.80 | 2.80 | 1.85 | 6.47 | 6.86 |
| 434 | 625 | Wa | 1.89 | 3.29 | 4.35 | 6.67 | 4.24 | 1.76 | 8.76 | 7.11 |
| 435 | 625 | Wa | 1.77 | 3.10 | 4.91 | 6.86 | 3.25 | 1.90 | - | - |
| 436 | 625 | Fu | 1.98 | 3.04 | 6.89 | 7.16 | 2.37 | 2.09 | 8.19 | 4.16 |
| 437 | 625 | Fu | 2.00 | 3.09 | 4.21 | 6.95 | 3.34 | 1.83 | 8.68 | 4.35 |
| 438 | 650 | Wa | 2.10 | 3.58 | 7.48 | 7.33 | 3.80 | 2.02 | 8.28 | 8.37 |
| 439 | 650 | Wa | 2.10 | 3.51 | 7.10 | 7.51 | 3.88 | 2.00 | 7.80 | 7.61 |
| 440 | 650 | Fu | 1.98 | 3.67 | 4.72 | 6.87 | 3.41 | 1.93 | 9.84 | 5.38 |
| 441 | 650 | Fu | 2.04 | 3.66 | 6.92 | 7.10 | 3.25 | 2.11 | 7.78 | 3.96 |
| 442 | 675 | Wa | 1.88 | 3.08 | 5.06 | 5.98 | 2.32 | 2.15 | - | - |
| 443 | 675 | Wa | 1.65 | 3.39 | 4.80 | 5.82 | 3.19 | 1.85 | 5.88 | 6.94 |
| 444 | 675 | Fu | 1.87 | 3.47 | 5.94 | 7.33 | 4.07 | 1.85 | - | - |
| 445 | 675 | Fu | 2.18 | 3.40 | 4.94 | 6.66 | 3.50 | 1.96 | 8.37 | 8.88 |
| 446 | 700 | Wa | 1.94 | 3.45 | 3.98 | 6.66 | 3.34 | 1.91 | - | - |
| 447 | 700 | Wa | 1.65 | 3.31 | 5.14 | 6.18 | 4.82 | 1.91 | 7.98 | 6.34 |
| 448 | 700 | Fu | 1.70 | 3.23 | 4.69 | 6.57 | 3.09 | 1.96 | - | - |
| 449 | 700 | Fu | 1.81 | 3.08 | 4.56 | 6.08 | 3.84 | 1.88 | 7.94 | 8.82 |
| 450 | 725 | Wa | 1.75 | 3.42 | 5.16 | 6.82 | 4.65 | 1.94 | 7.82 | 4.32 |
| 451 | 725 | Wa | 1.69 | 3.42 | 4.18 | 6.24 | 5.70 | 2.11 | 12.40 | 5.15 |
| 452 | 725 | Fu | 2.13 | 3.13 | 4.49 | 6.24 | 3.93 | 2.39 | 5.61 | 10.08 |
| 453 | - | - | 1.89 | 3.24 | 8.16 | 7.17 | 3.43 | 2.19 | - | - |
| 454 | - | - | 1.93 | 3.45 | - | - | - | - | - | - |
| 455 | - | - | 1.92 | 2.96 | - | - | - | - | - | - |

*Tempering temperature in degrees Centigrade

**Quenching method: Wa = Water, Fu = Furnace

## TABLE XIX

## RATIO OF TRANSVERSE TO LONGITUDINAL RAYLEIGH SCATTERING COEFFICIENTS

### TEMPERED BLOCKS

| Block | Temp.* | Quench** | $\alpha_{4t}/\alpha_{4\ell}$ | Block | Temp.* | Quench** | $\alpha_{4t}/\alpha_{4\ell}$ | Block | Temp.* | Quench** | $\alpha_{4t}/\alpha_{4\ell}$ |
|---|---|---|---|---|---|---|---|---|---|---|---|
| 405 | 425 | Fu | 4.54 | 420 | 525 | Fu | 4.70 | 437 | 625 | Fu | 2.38 |
| 407 | 450 | Wa | 4.51 | 421 | 525 | Fu | 3.07 | 438 | 650 | Wa | 4.15 |
| 408 | 450 | Fu | 4.48 | 422 | 550 | Wa | 4.38 | 439 | 650 | Wa | 3.81 |
| 409 | 450 | Fu | 2.60 | 423 | 550 | Wa | 3.20 | 440 | 650 | Fu | 2.79 |
| 412 | 475 | Fu | 3.39 | 424 | 550 | Fu | 3.72 | 441 | 650 | Fu | 1.83 |
| 413 | 475 | Fu | 2.92 | 426 | 575 | Wa | 4.69 | 443 | 675 | Wa | 3.56 |
| 414 | 500 | Wa | 0.80 | 427 | 575 | Wa | 3.86 | 445 | 675 | Fu | 4.53 |
| 415 | 500 | Wa | 3.96 | 428 | 575 | Fu | 3.40 | 447 | 700 | Wa | 3.32 |
| 416 | 500 | Fu | 2.63 | 429 | 575 | Fu | 5.44 | 449 | 700 | Fu | 4.26 |
| 417 | 500 | Fu | 2.41 | 433 | 600 | Fu | 3.71 | 450 | 725 | Wa | 2.22 |
| 418 | 525 | Wa | 0.44 | 434 | 625 | Wa | 4.00 | 451 | 725 | Wa | 2.44 |
| 419 | 525 | Wa | 4.34 | 436 | 625 | Fu | 1.99 | 452 | 725 | Fu | 4.22 |

*Tempering temperature in degrees Centigrade

**Quenching method: Wa = Water, Fu = Furnace

## TABLE XX

### FRACTIONAL VELOCITY CHANGES

| Block | Temp.* | Quench** | f, mcps | $\Delta v/v \times 10^4$ | | | | |
|---|---|---|---|---|---|---|---|---|
| | | | | n = 0 | n = 1 | n = 2 | n = 3 | n = 4 |
| 402 | 425 | Wa | 18<br>21 | 2.61<br>3.72 | 49.6<br>40.9 | 54.8<br>48.4 | 101.8<br>51.3 | 107.0<br>58.0 |
| 404 | 425 | Fu | 10<br>21<br>30 | 4.94<br>3.27<br>4.88 | 88.5<br>40.7<br>26.0 | 98.8<br>48.4<br>36.4 | 183.0<br>85.5<br>57.2 | 192.0<br>92.9<br>67.6 |
| 405 | 425 | Fu | 10<br>30<br>35 | 6.70<br>7.08<br>6.70 | 86.8<br>24.0<br>20.0 | 100.0<br>36.3<br>33.4 | 181.0<br>54.6<br>46.9 | 194.0<br>70.2<br>60.3 |
| 406 | 450 | Wa | 10<br>18<br>30 | 6.31<br>6.34<br>6.50 | 87.0<br>45.5<br>24.4 | 100.0<br>58.4<br>39.0 | 180.0<br>97.5<br>54.6 | 193.0<br>110.0<br>70.2 |
| 408 | 450 | Fu | 10<br>21<br>35 | 5.48<br>5.90<br>4.47 | 46.7<br>39.4<br>22.4 | 57.4<br>49.1<br>31.2 | 99.2<br>84.8<br>49.2 | 110.0<br>93.7<br>58.1 |

*Tempering temperature in degrees Centigrade

**Quenching method: Wa = Water, Fu = Furnace

APPENDIX B

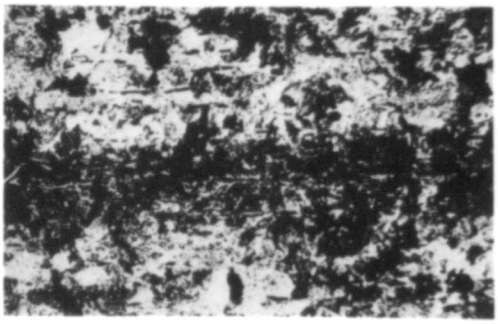

100X

BANDING

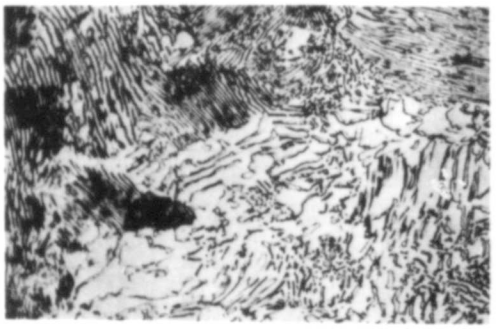

1000X

PEARLITE

HOT-ROLLED

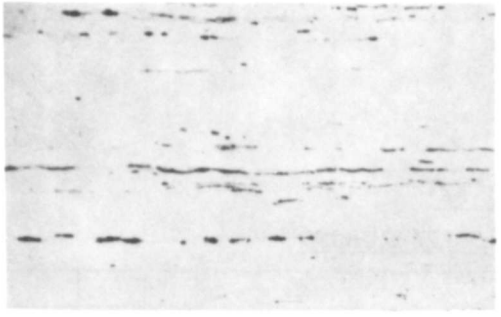

100X

STRINGERS
HOT-ROLLED

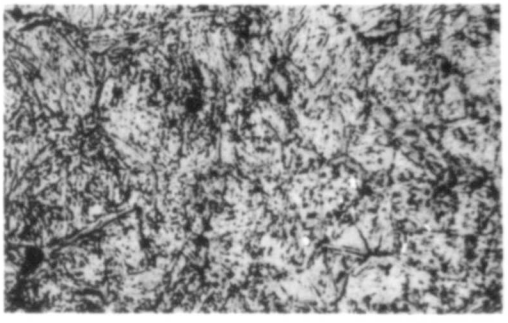

1000X

MARTENSITE
AUSTENITIZED & QUENCHED

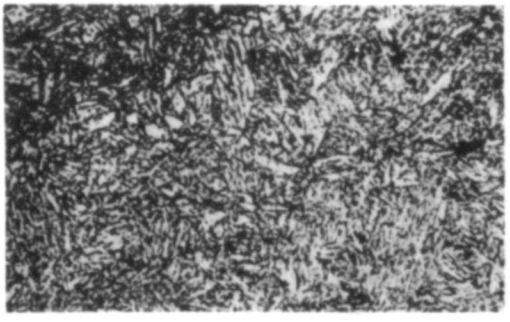

1000X

MARTENSITE

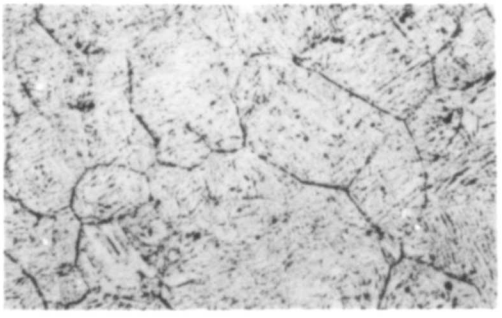

1000X

GRAIN BOUNDARY SEGREGATION

TEMPERED

MICROSTRUCTURES



FIGURE 1

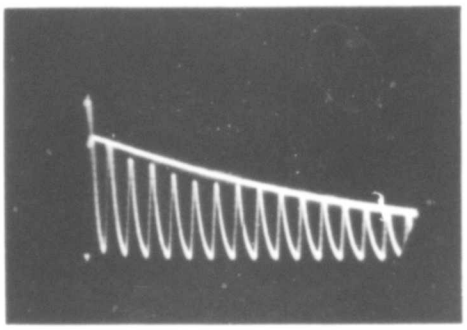

412 @ 18 mc

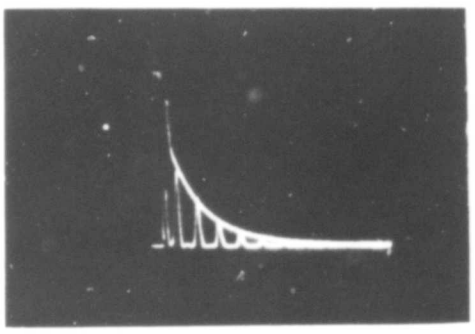

406 @ 54 mc

LONGITUDINAL WAVES

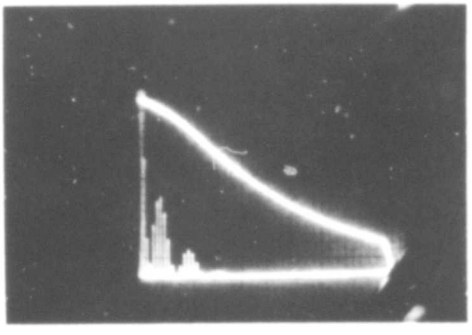

407 @ 18 mc

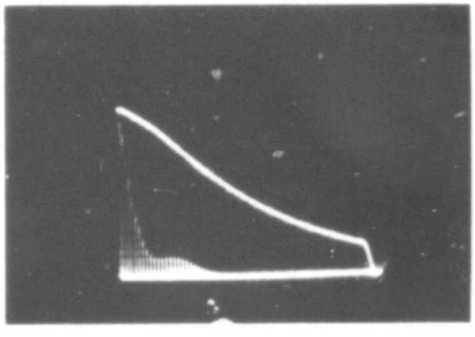

440 @ 18 mc

TRANSVERSE WAVES

OSCILLOSCOPE PICTURES



FIGURE 2

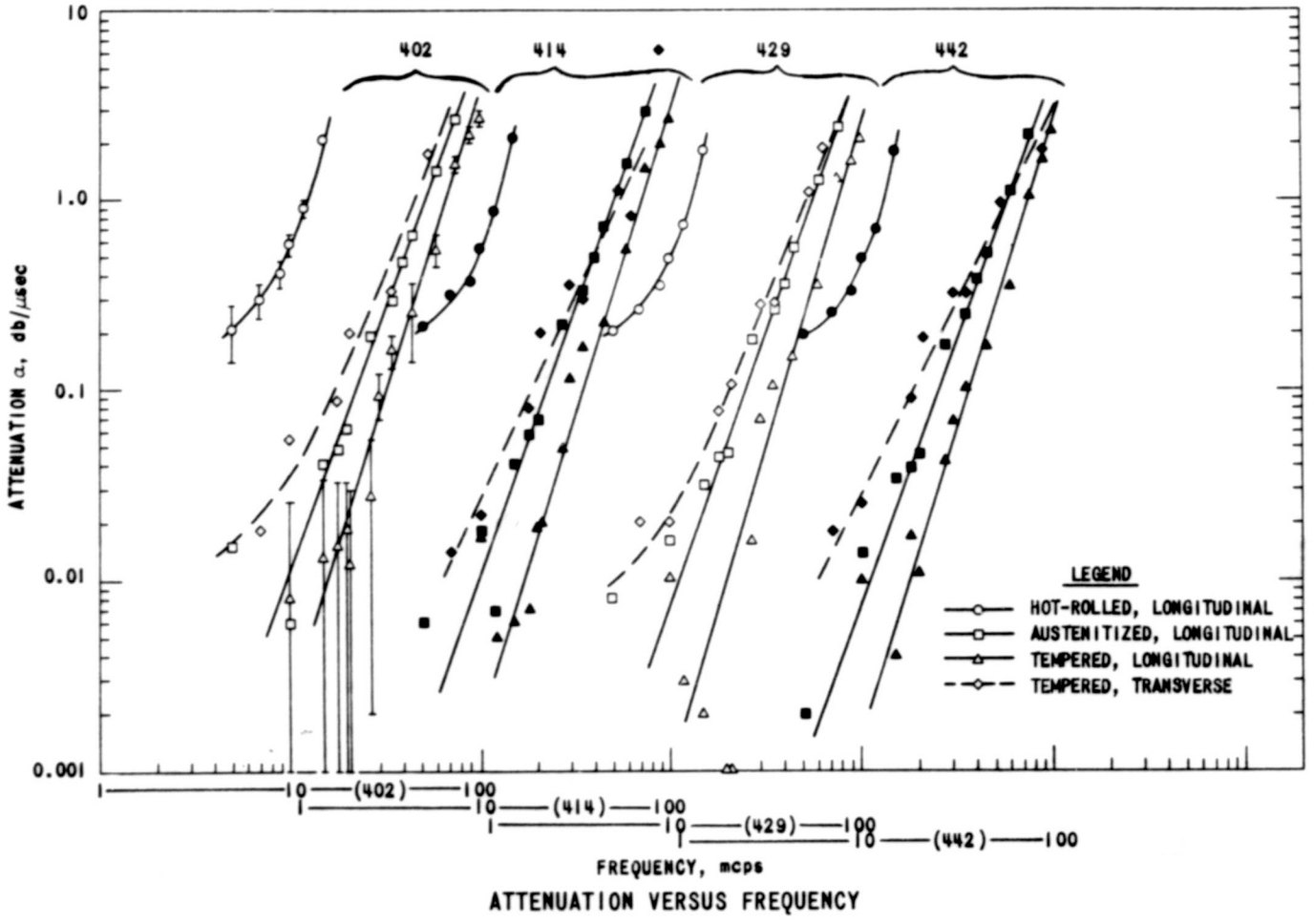


FIGURE 3

ATTENUATION VERSUS FREQUENCY

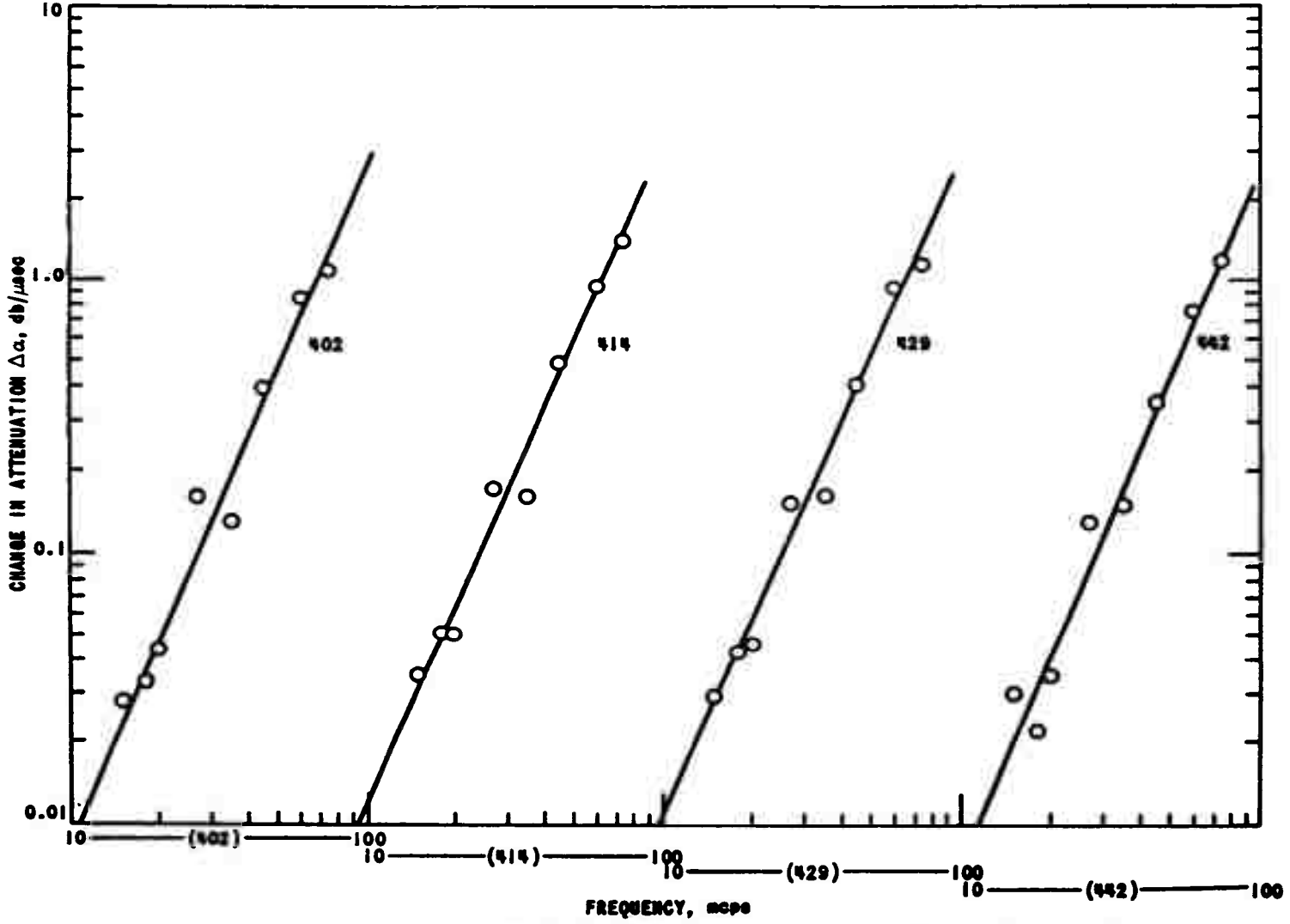


FIGURE 4

ATTENUATION LOST ON TEMPERING VERSUS FREQUENCY FOR LONGITUDINAL WAVES

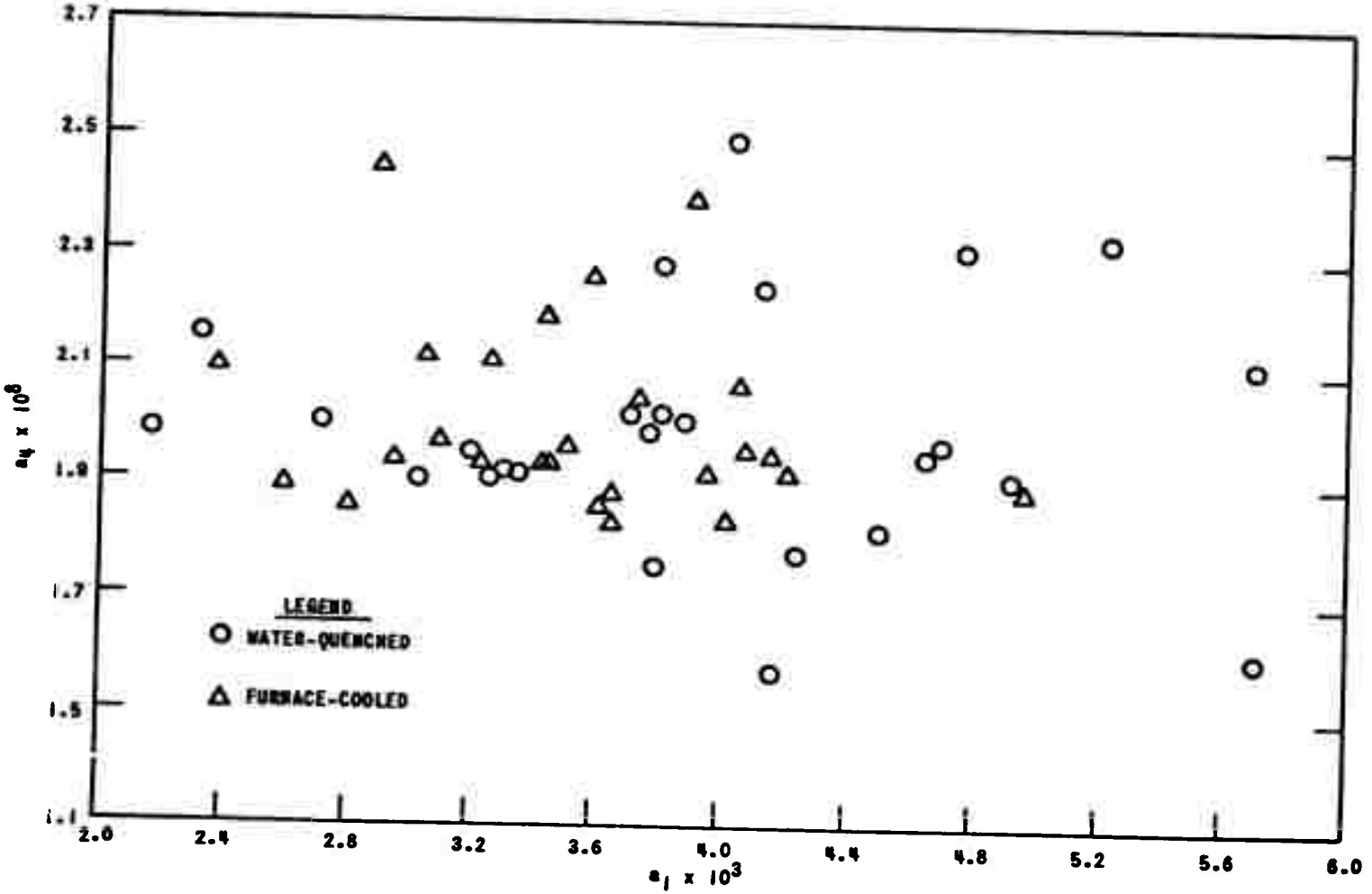


$a_q$ VERSUS $a_l$ FOR LONGITUDINAL WAVES IN TEMPERED BLOCKS

FIGURE 9

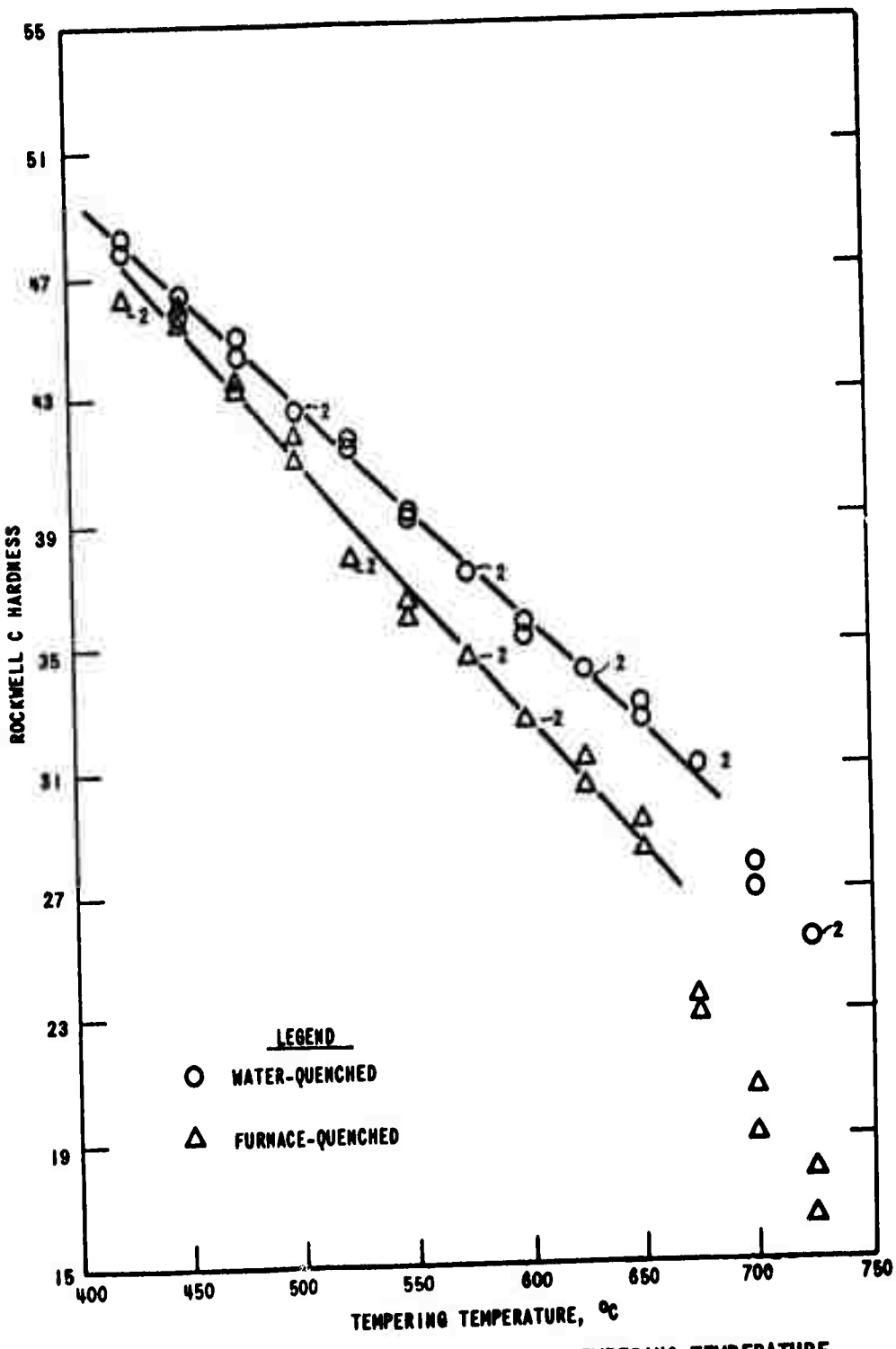


ROCKWELL C HARDNESS VERSUS TEMPERING TEMPERATURE

FIGURE 6

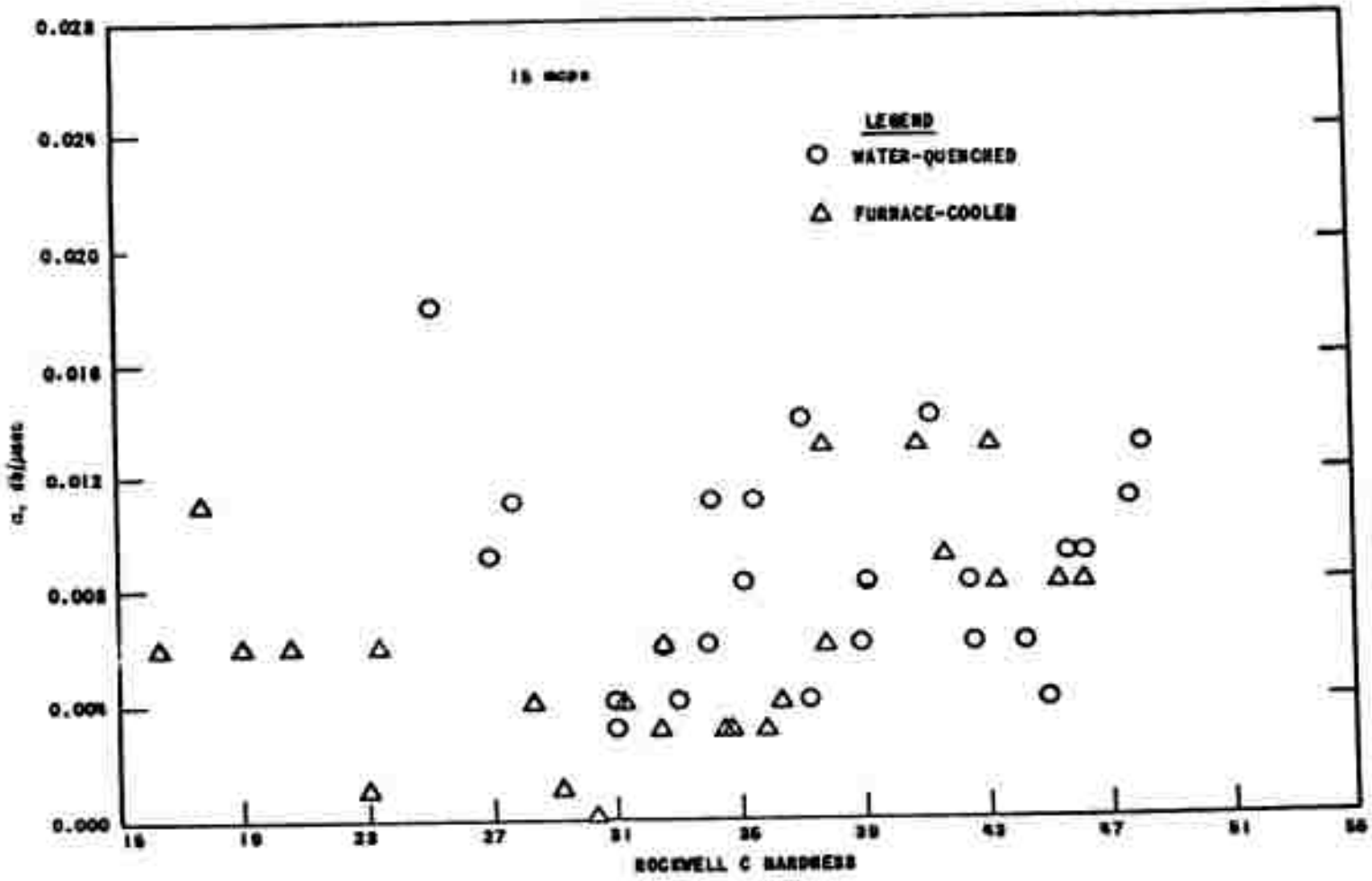


ATTENUATION VERSUS HARDNESS, LONGITUDINAL WAVES IN TEMPERED BLOCKS

FIGURE 7A

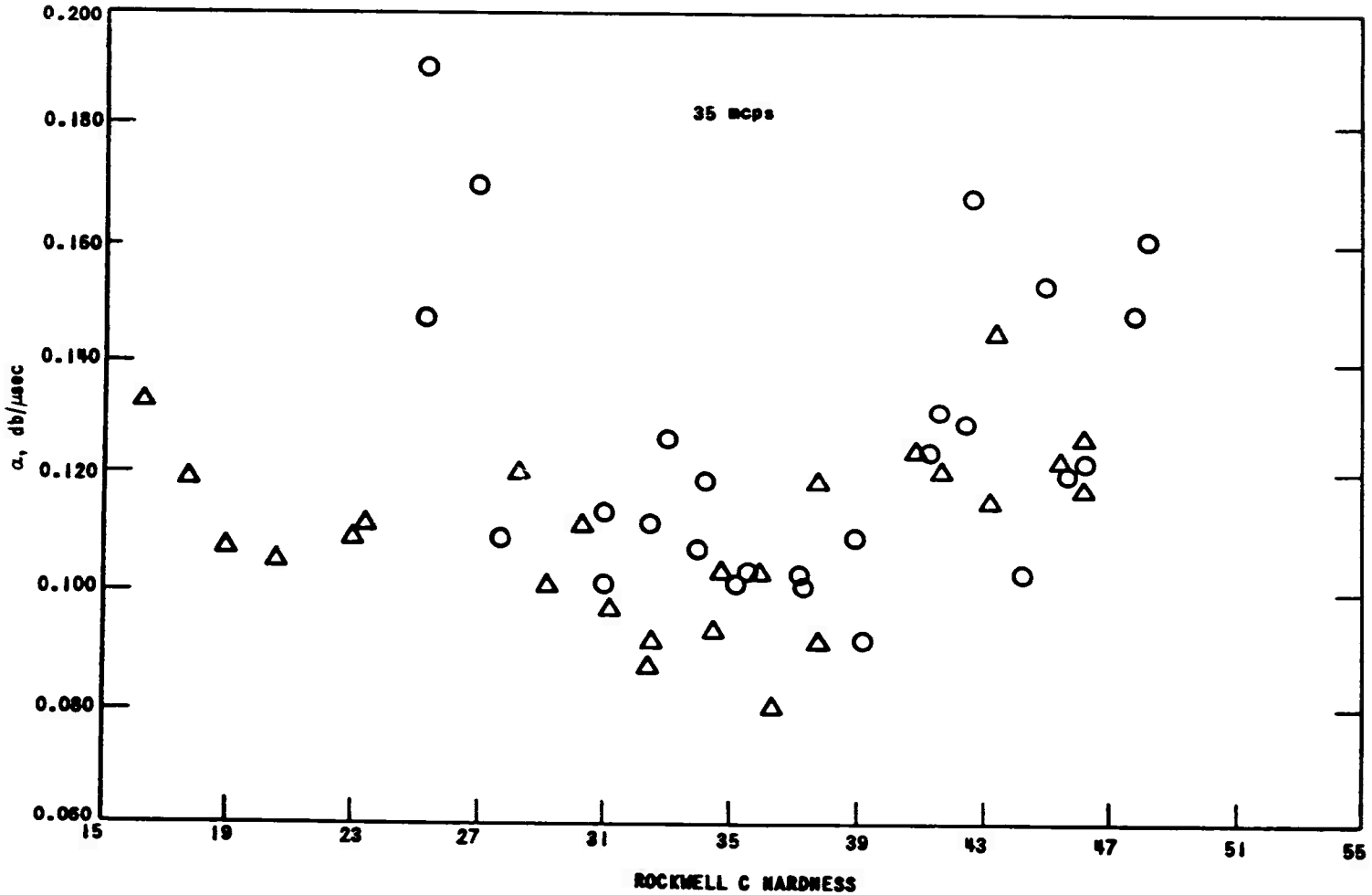


FIGURE 7B

ATTENUATION VERSUS HARDNESS, LONGITUDINAL WAVES IN TEMPERED BLOCKS

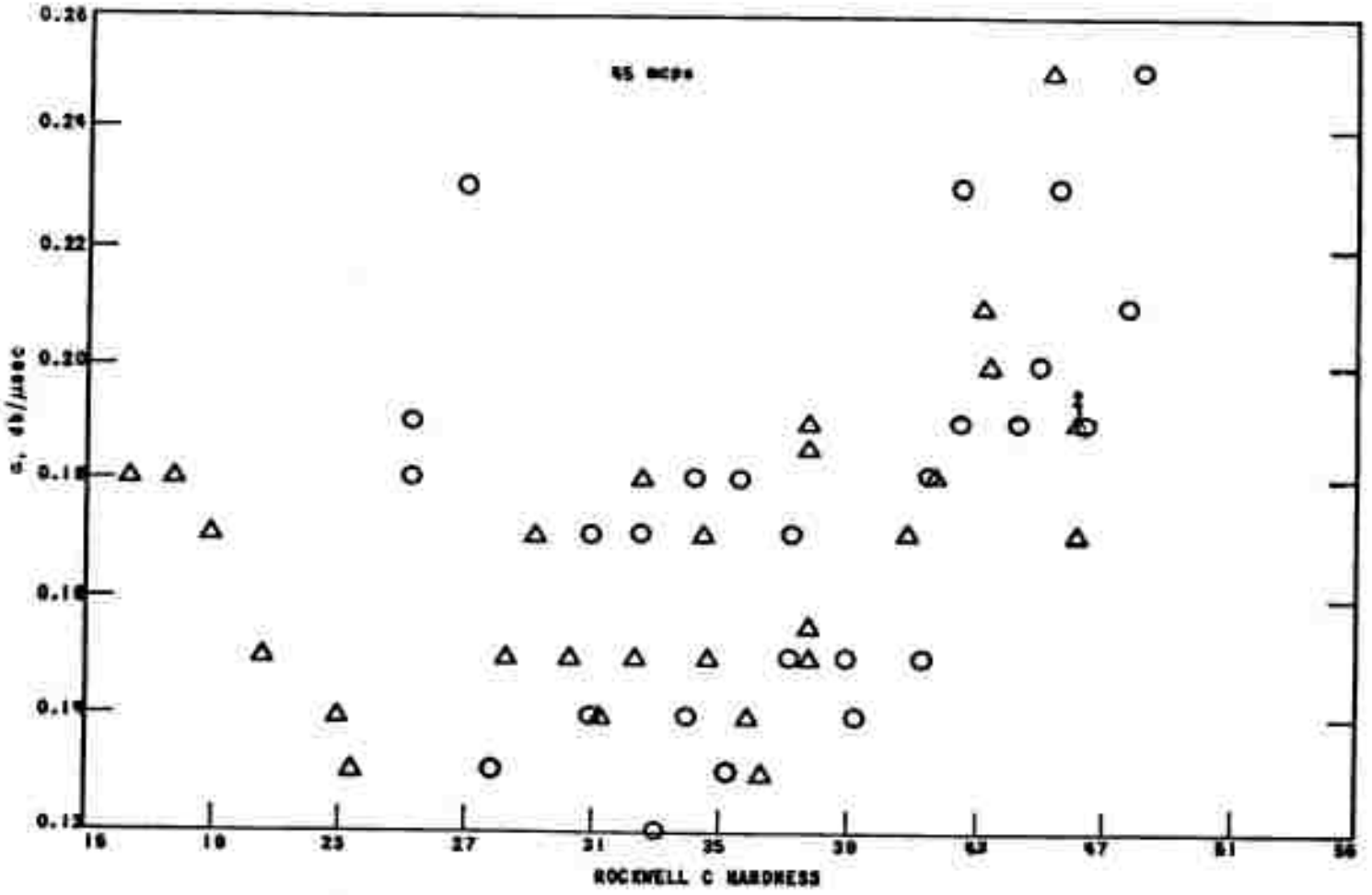


ATTENUATION VERSUS HARDNESS, LONGITUDINAL WAVES IN TEMPERED BLOCKS

FIGURE 7C

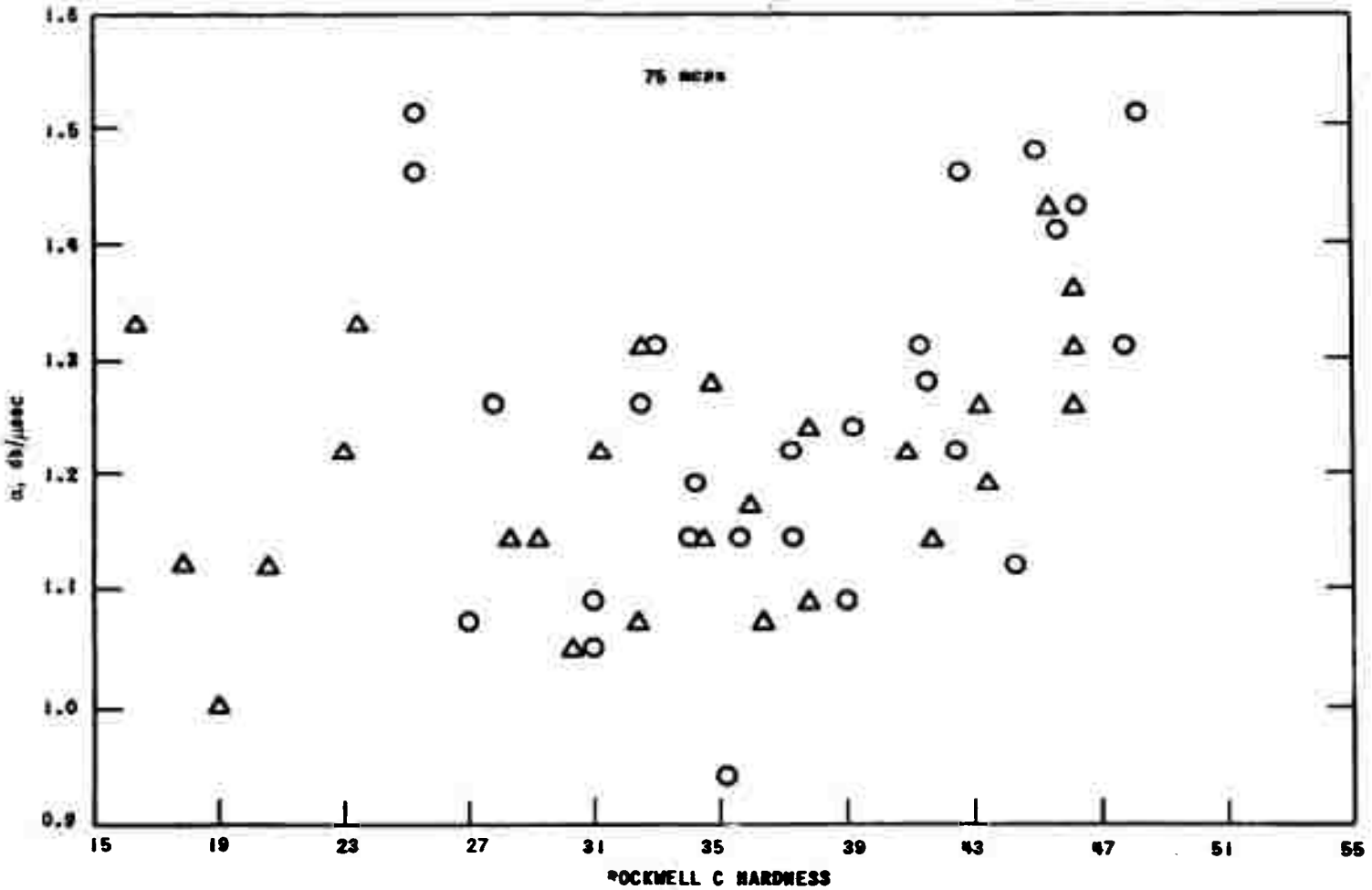


FIGURE 70

ATTENUATION VERSUS HARDNESS, LONGITUDINAL WAVES IN TEMPERED BLOCKS

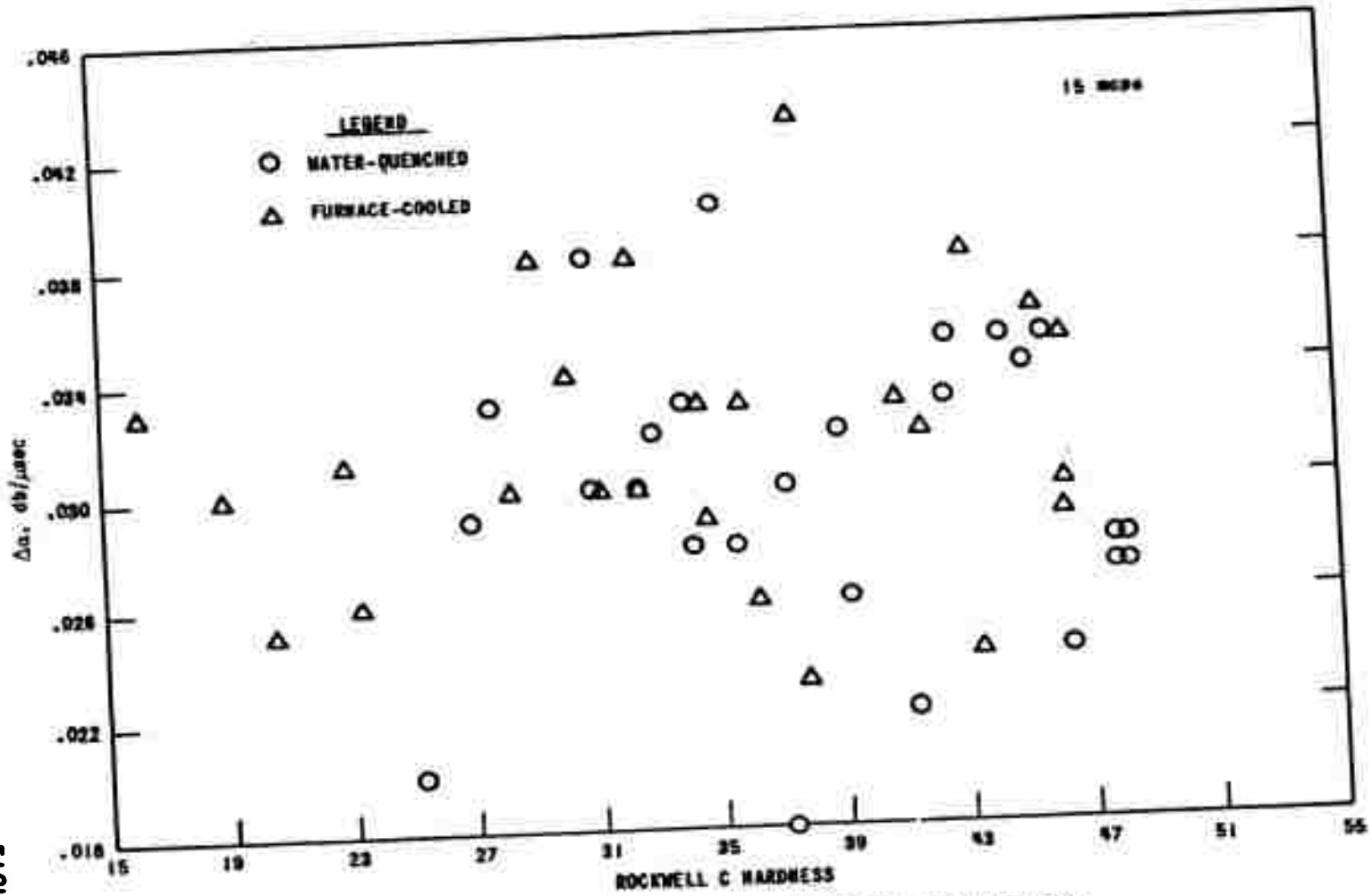


FIGURE 8A

ATTENUATION LOST ON TEMPERING VERSUS HARDNESS

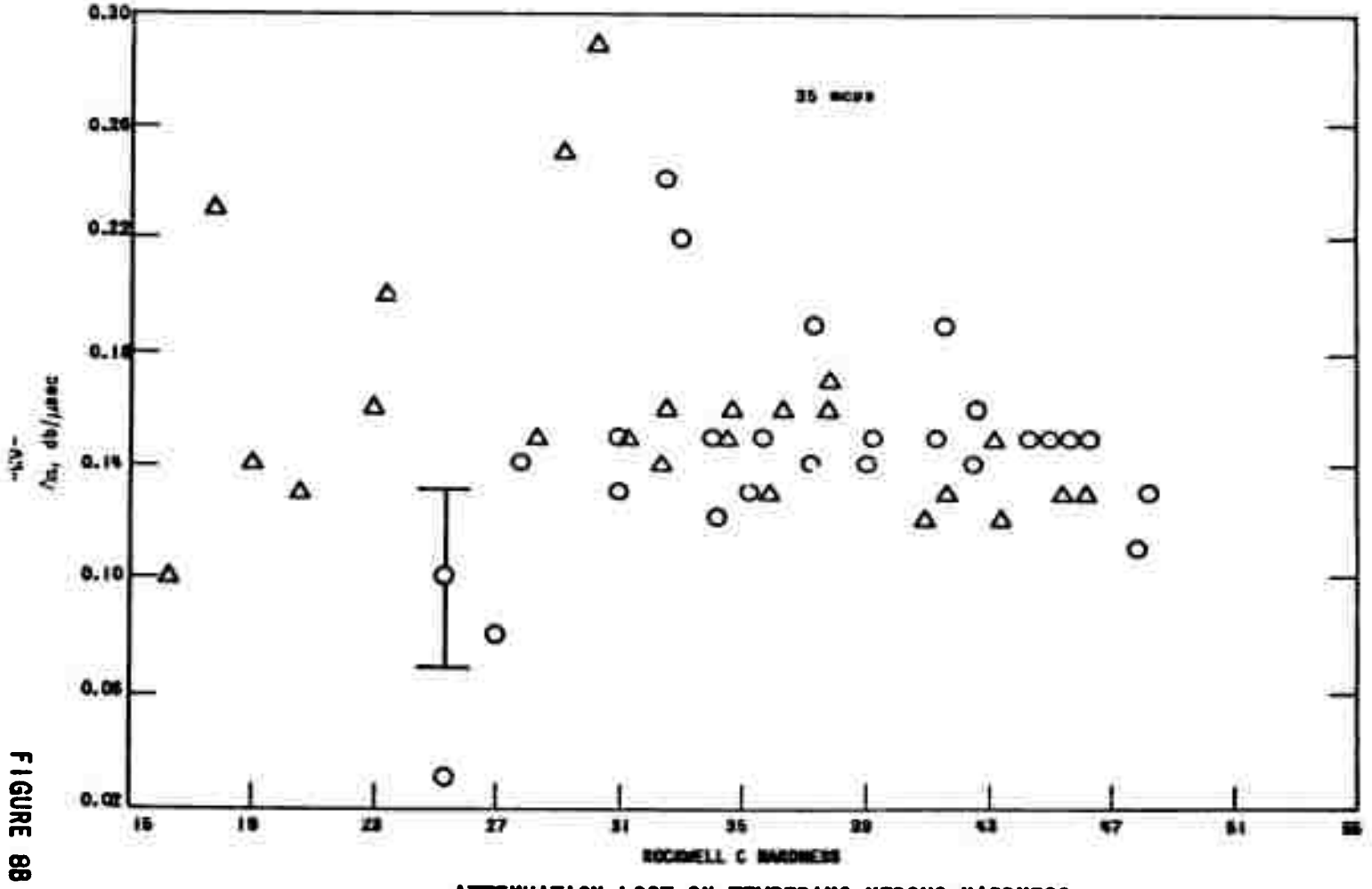


FIGURE 88

ATTENUATION LOST ON TEMPERING VERSUS HARDNESS

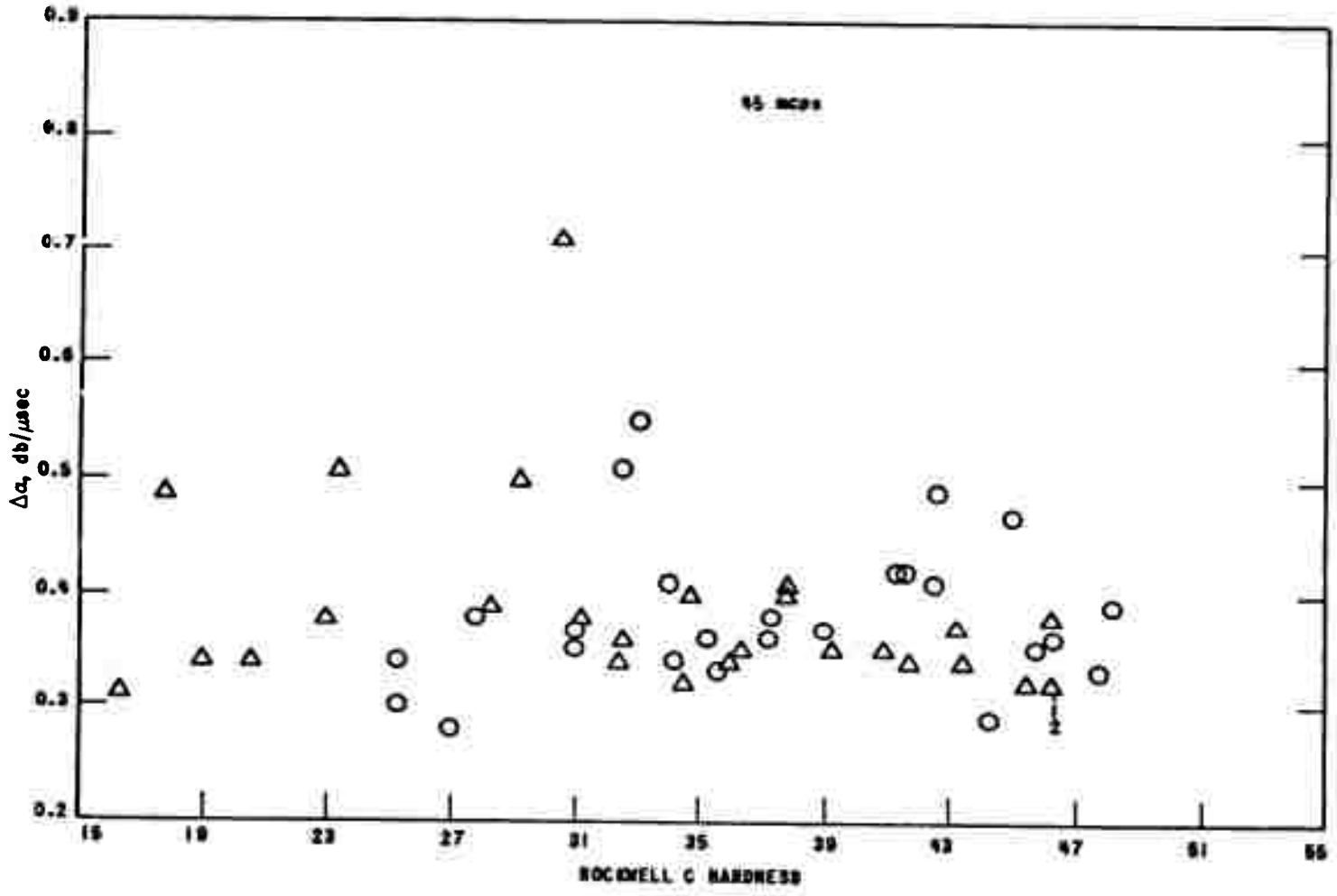


FIGURE 8C

ATTENUATION LOST ON TEMPERING VERSUS HARDNESS

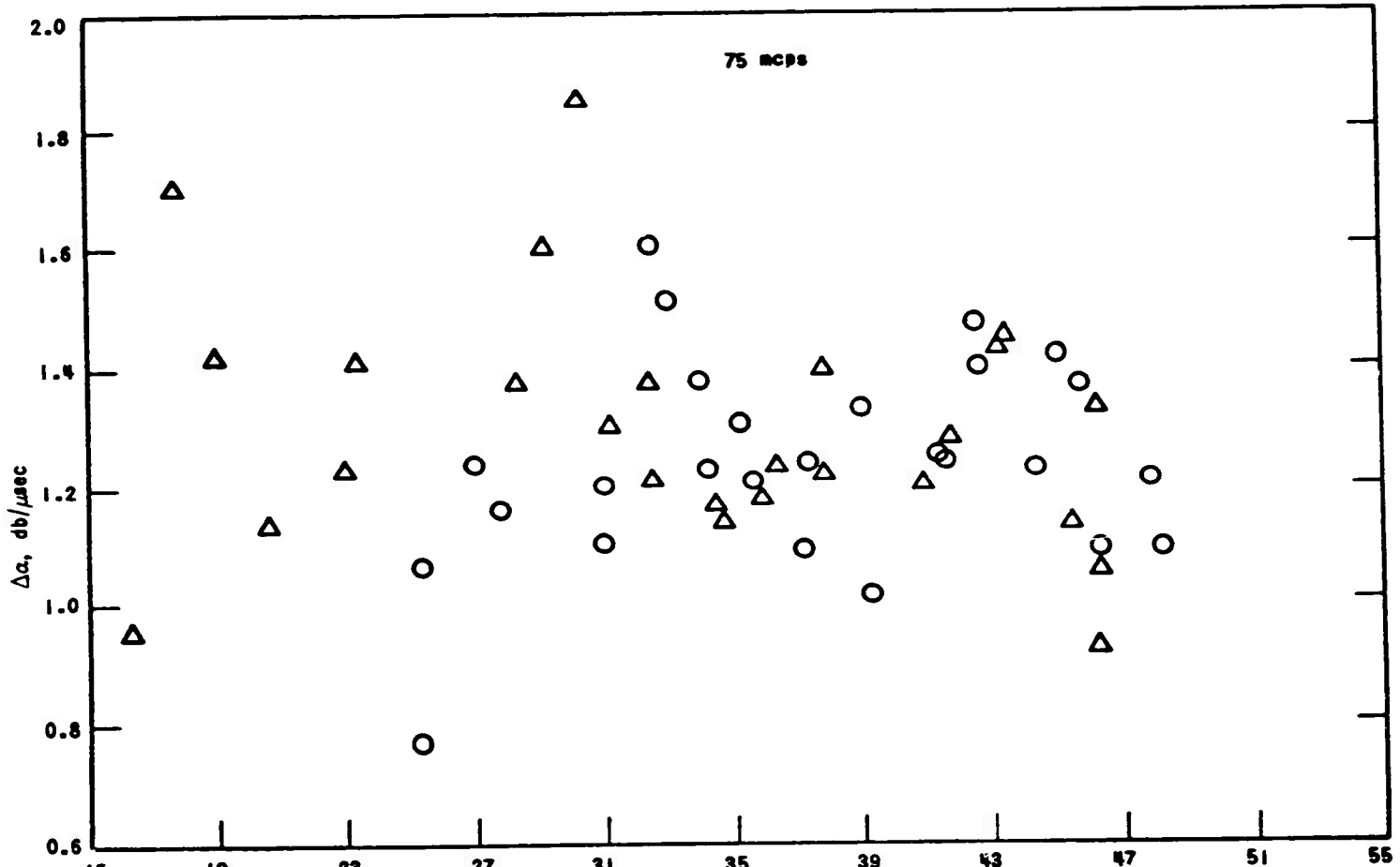


FIGURE 80

ATTENUATION LOST ON TEMPERING VERSUS HARDNESS

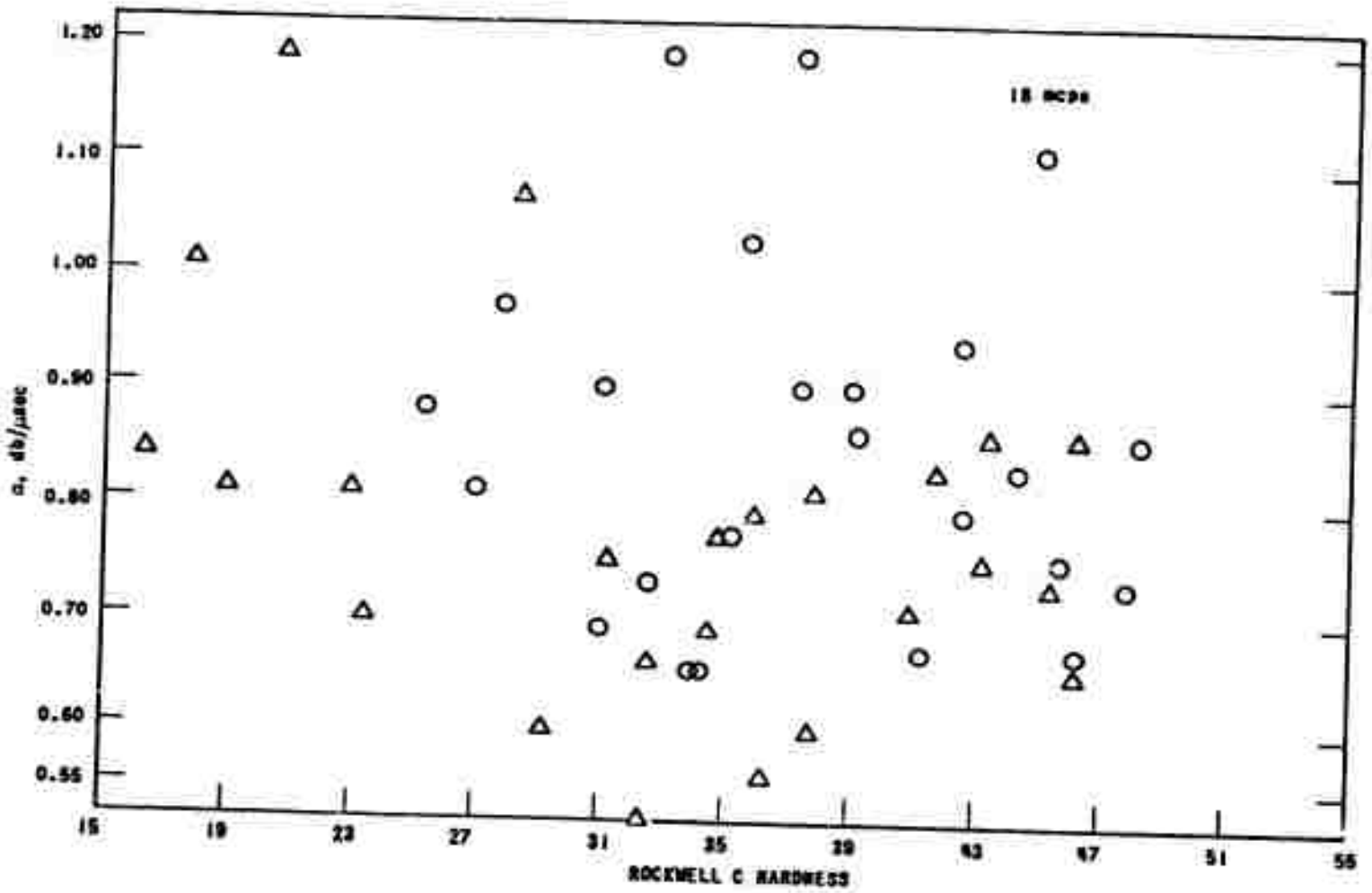


FIGURE 9A

ATTENUATION VERSUS HARDNESS, TRANSVERSE WAVES

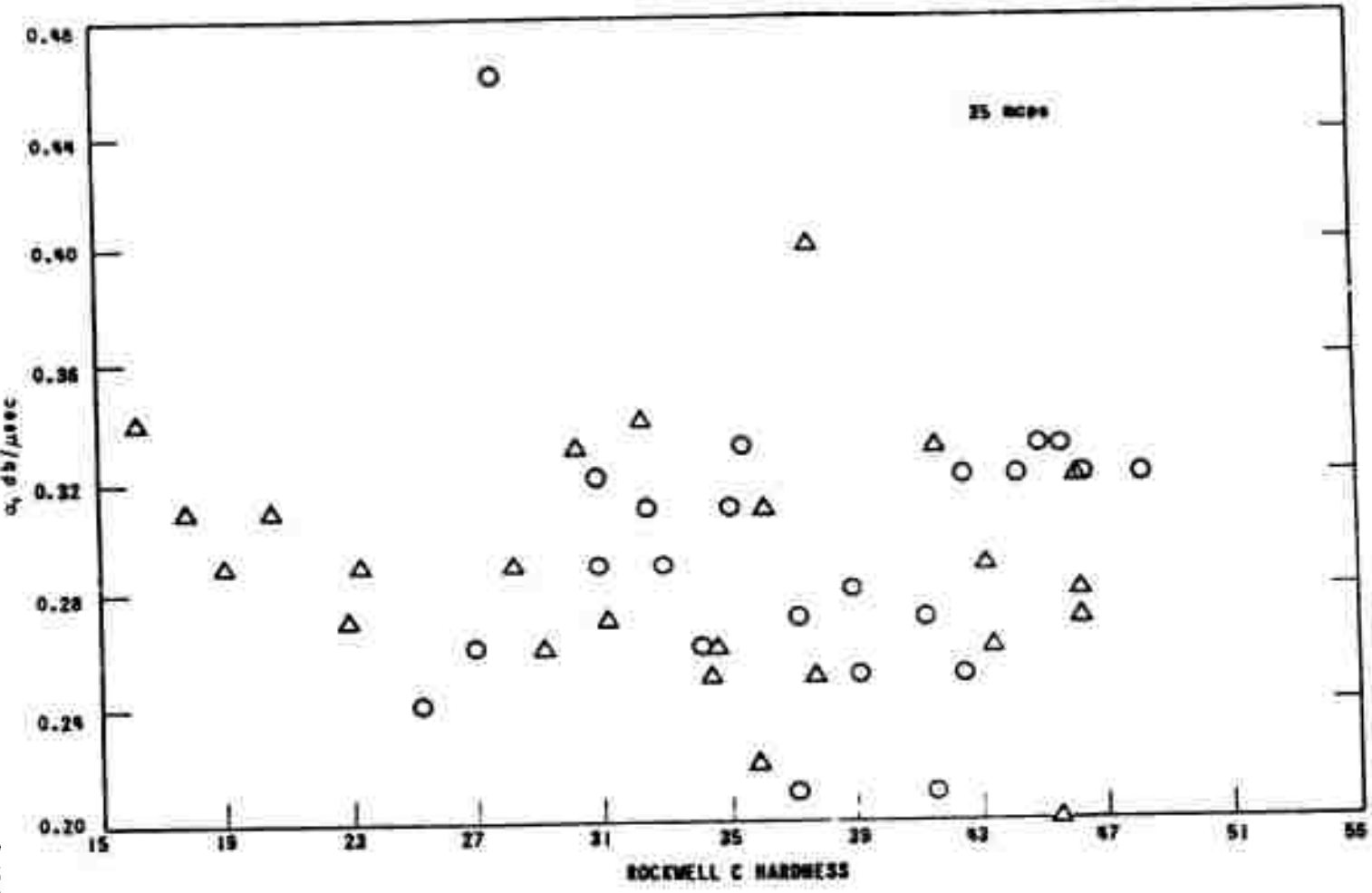


FIGURE 9B

ATTENUATION VERSUS HARDNESS, TRANSVERSE WAVES

ELASTIC HYSTERESIS COEFFICIENT e1 VERSUS HARDNESS, LONGITUDINAL WAVES, TEMPERED BLOCKS
ROCKWELL C HARDNESS
e1 x 10³

FIGURE 10

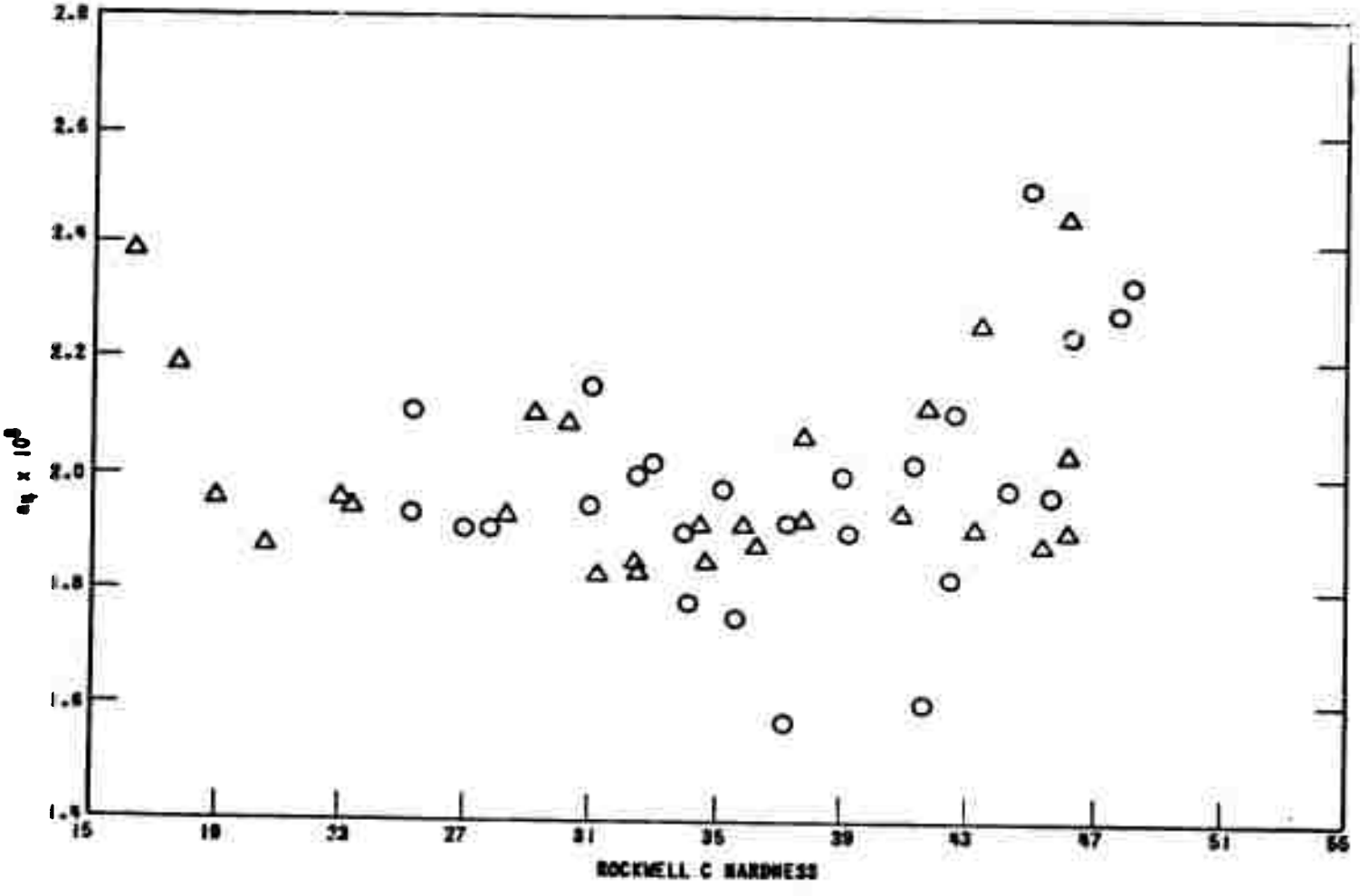


FIGURE 11

RAYLEIGH SCATTERING COEFFICIENT $a_R$ VERSUS HARDNESS

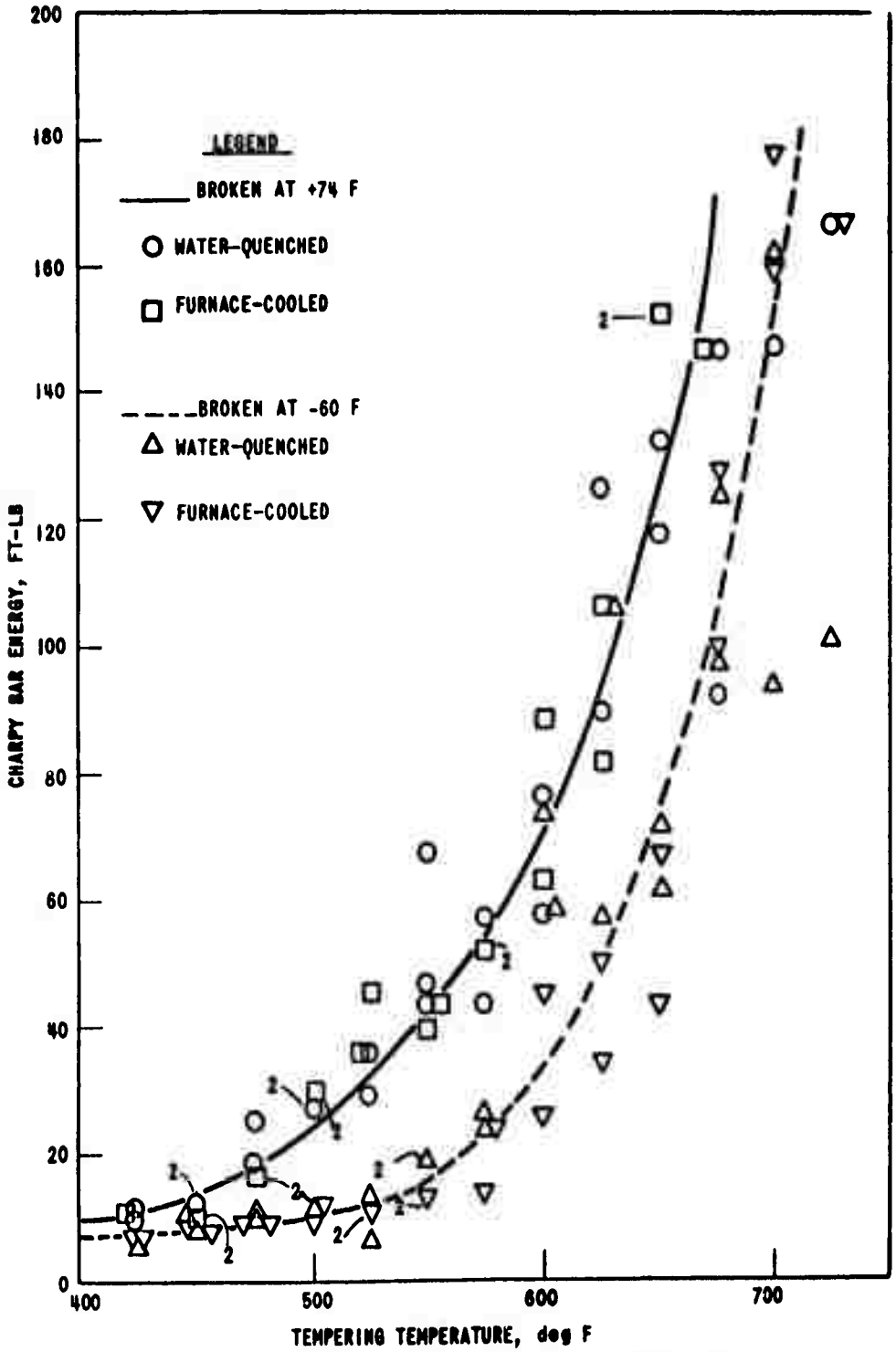


BREAKING ENERGY VERSUS TEMPERING TEMPERATURE

FIGURE 12

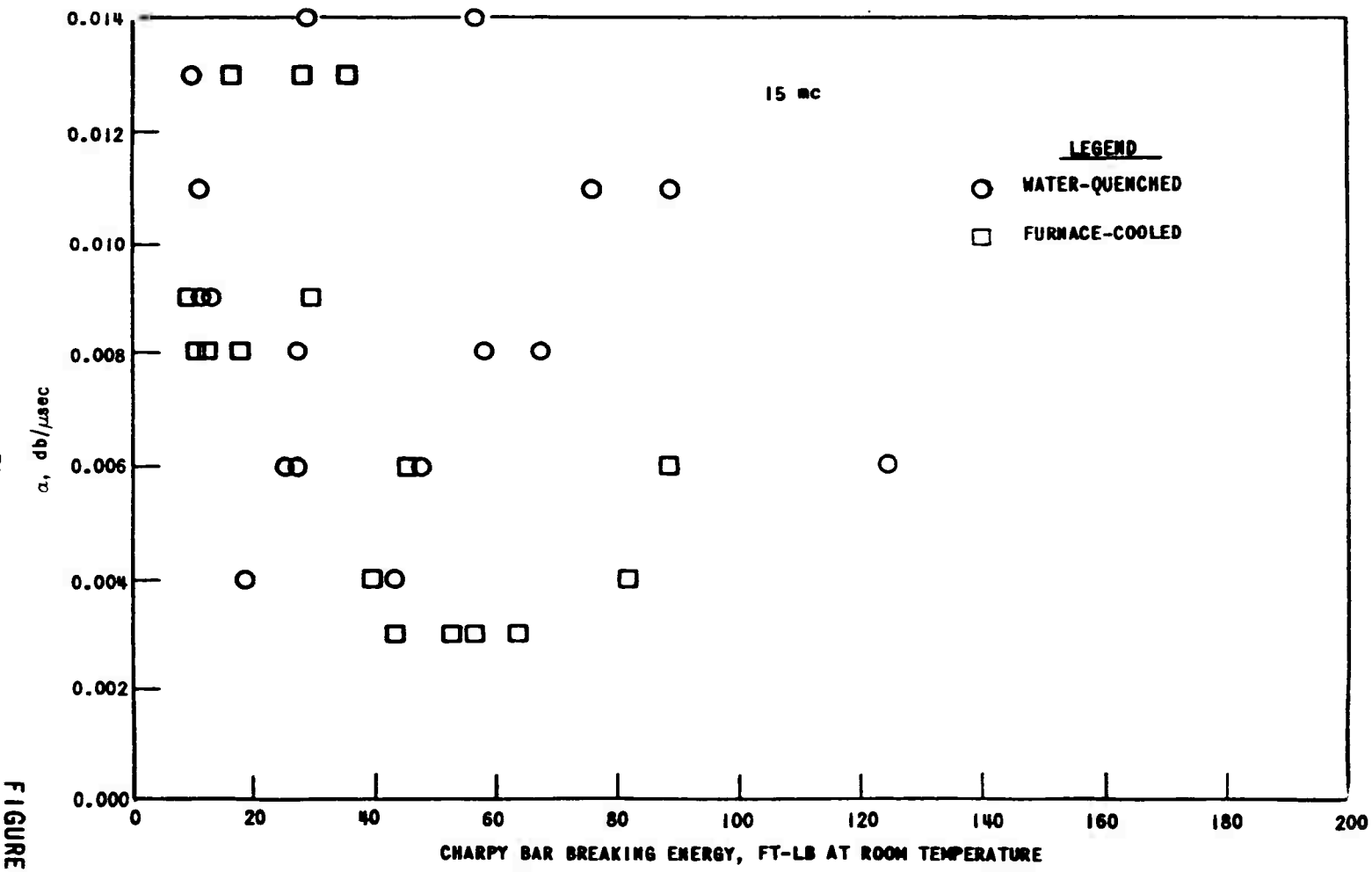


FIGURE 13A

ATTENUATION VERSUS BREAKING ENERGY, LONGITUDINAL WAVES, TEMPERED BLOCKS

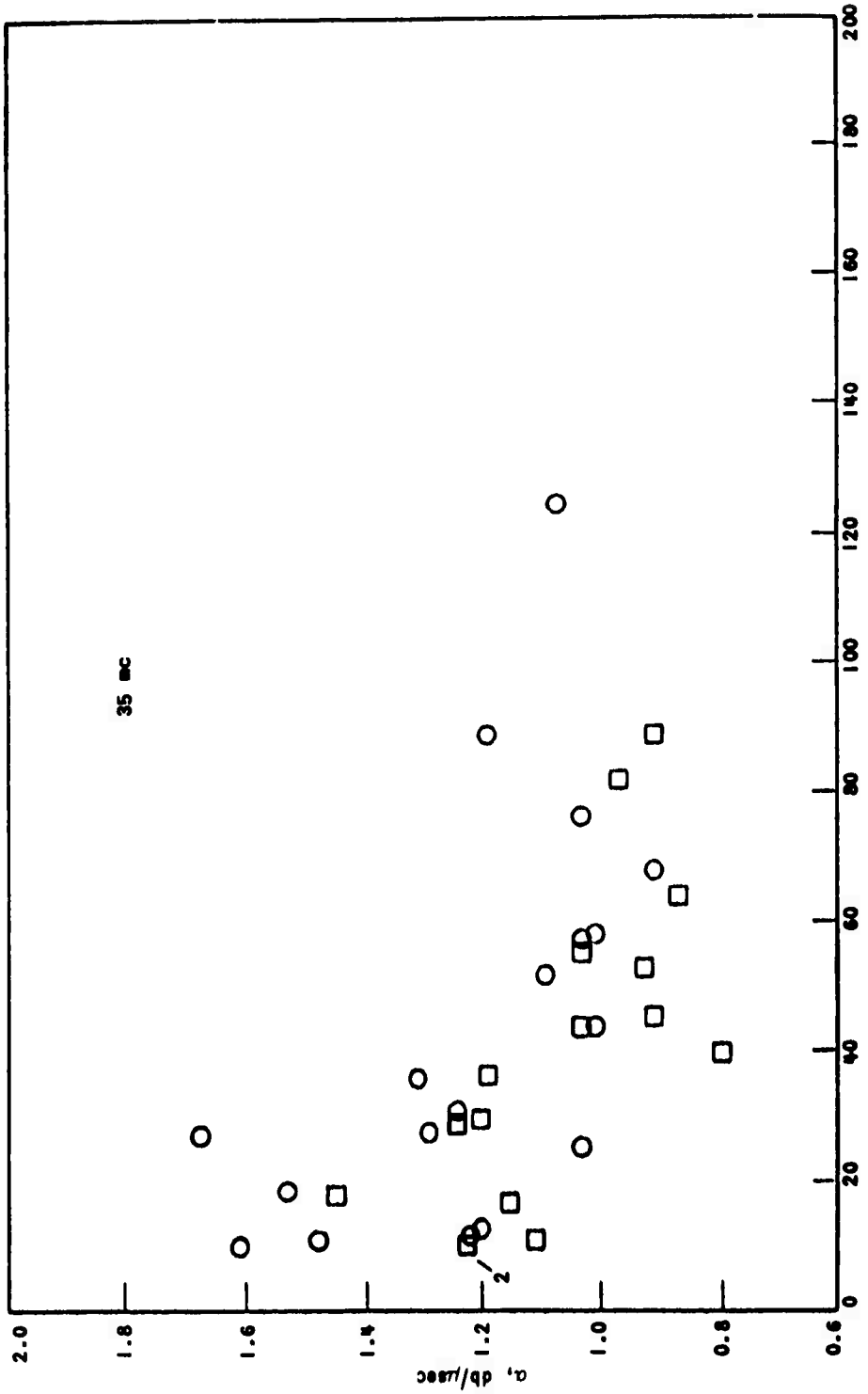
ATTENUATION VERSUS BREAKING ENERGY, LONGITUDINAL WAVES, TEMPERED BLOCKS
CHARPY BAR BREAKING ENERGY, FT-LB AT ROOM TEMPERATURE
α, db/μsec
35 mc
2.0
1.8
1.6
1.4
1.2
1.0
0.8
0.6
0
20
40
60
80
100
120
140
160
180
200



FIGURE 13B

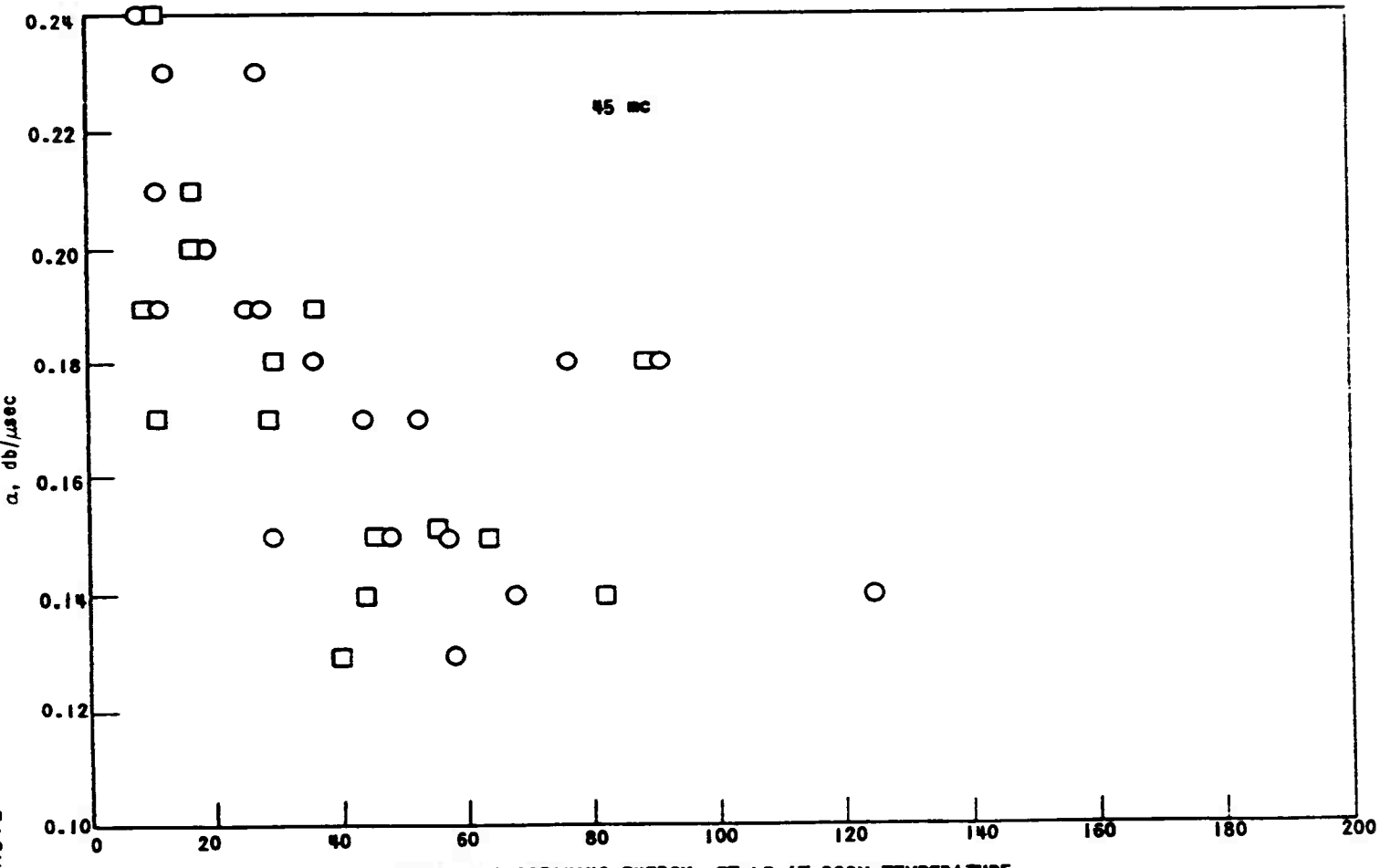


FIGURE 13C

ATTENUATION VERSUS BREAKING ENERGY, LONGITUDINAL WAVES, TEMPERED BLOCKS

ATTENUATION VERSUS BREAKING ENERGY, LONGITUDINAL WAVES, TEMPERED BLOCKS



FIGURE 13D

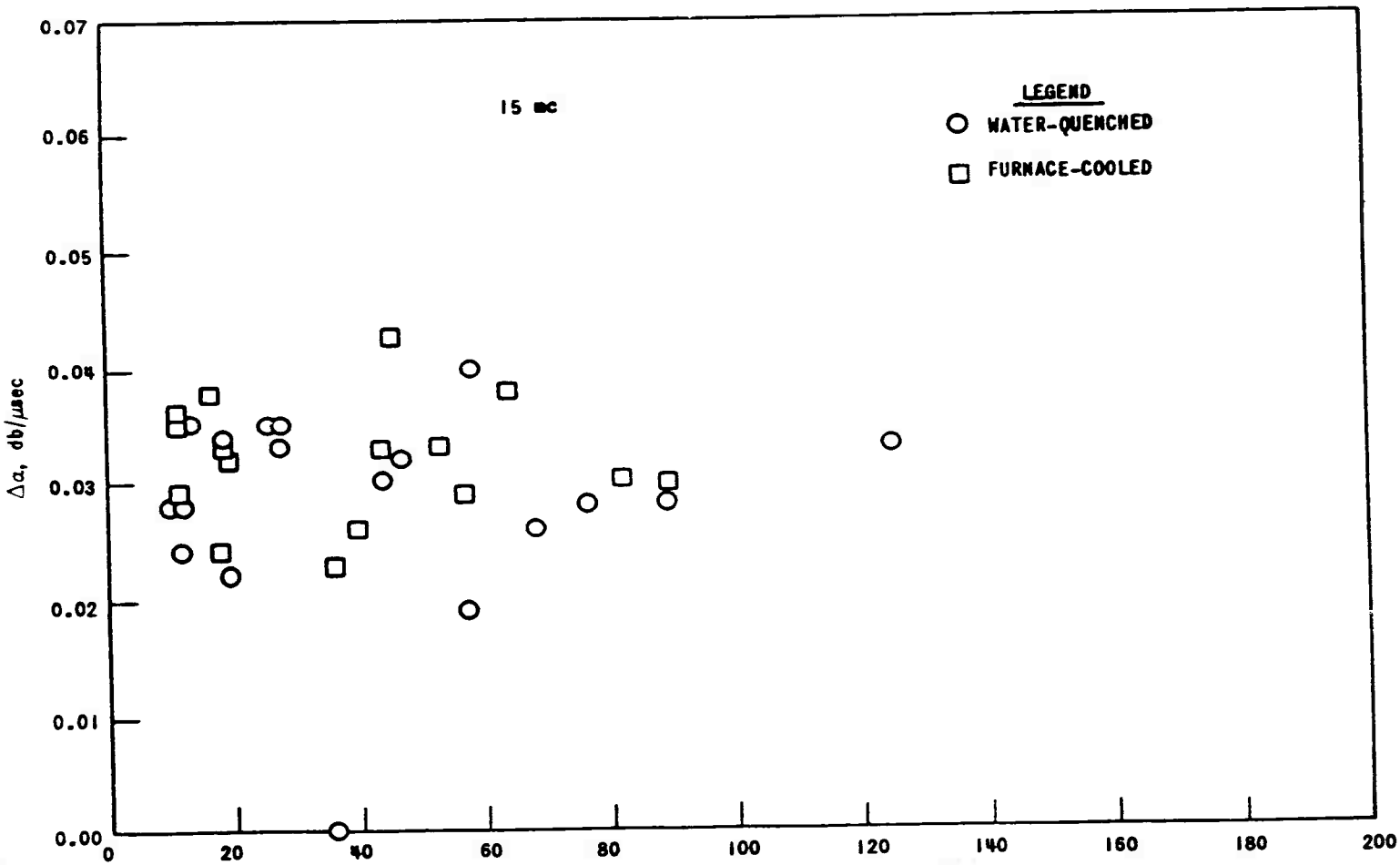


FIGURE 14A

ATTENUATION LOST ON TEMPERING VERSUS BREAKING ENERGY, LONGITUDINAL WAVES

35 ac
0.0
0.1
0.2
0.3
Δα, db/μsec
0
20
40
60
80
100
120
140
160
180
200
CHARPY BAR BREAKING ENERGY, FT-LB AT ROOM TEMPERATURE
ATTENUATION LOST ON TEMPERING VERSUS BREAKING ENERGY, LONGITUDINAL WAVES

FIGURE 14B

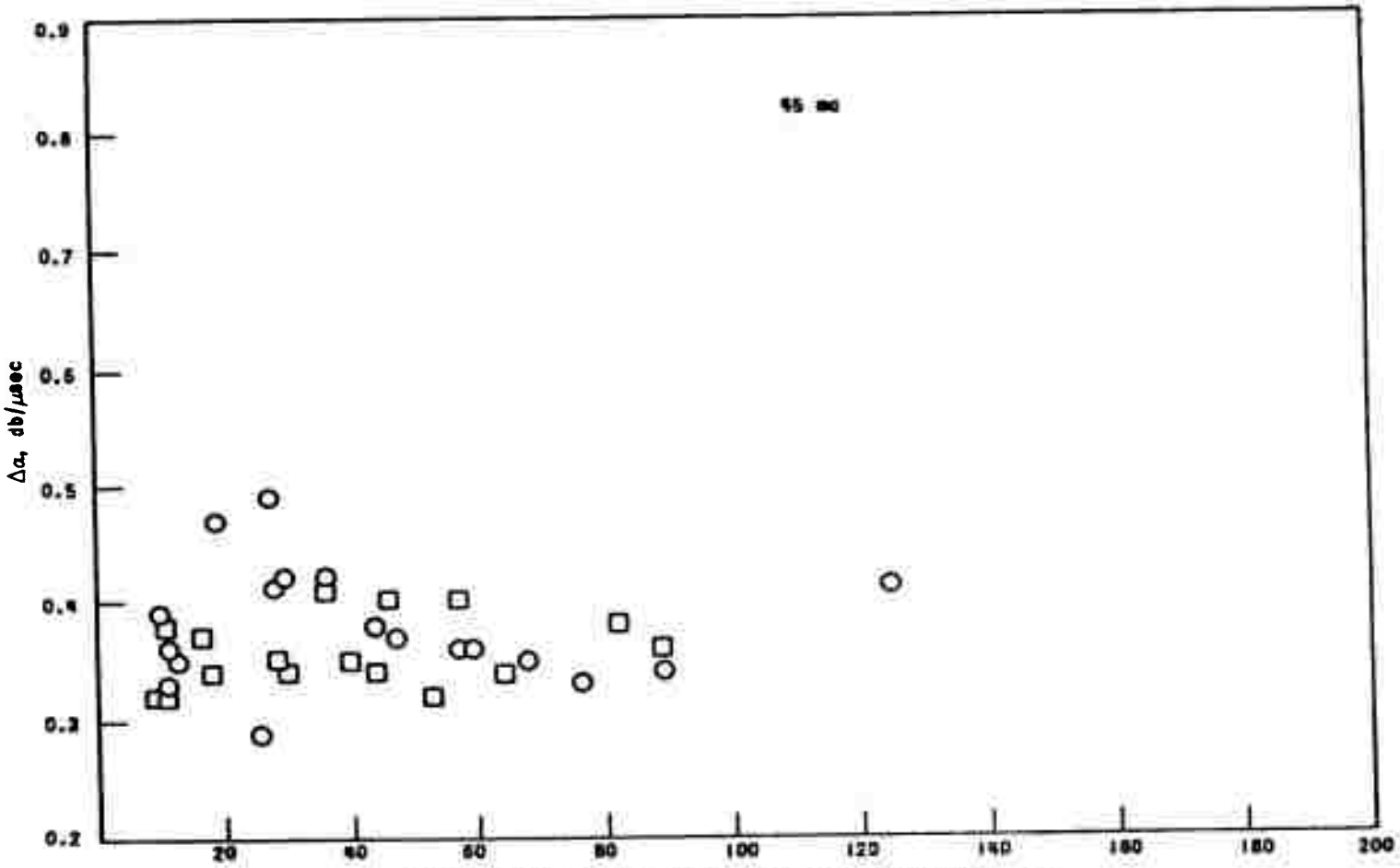


ATTENUATION LOST ON TEMPERING VERSUS BREAKING ENERGY, LONGITUDINAL WAVES

FIGURE 14C

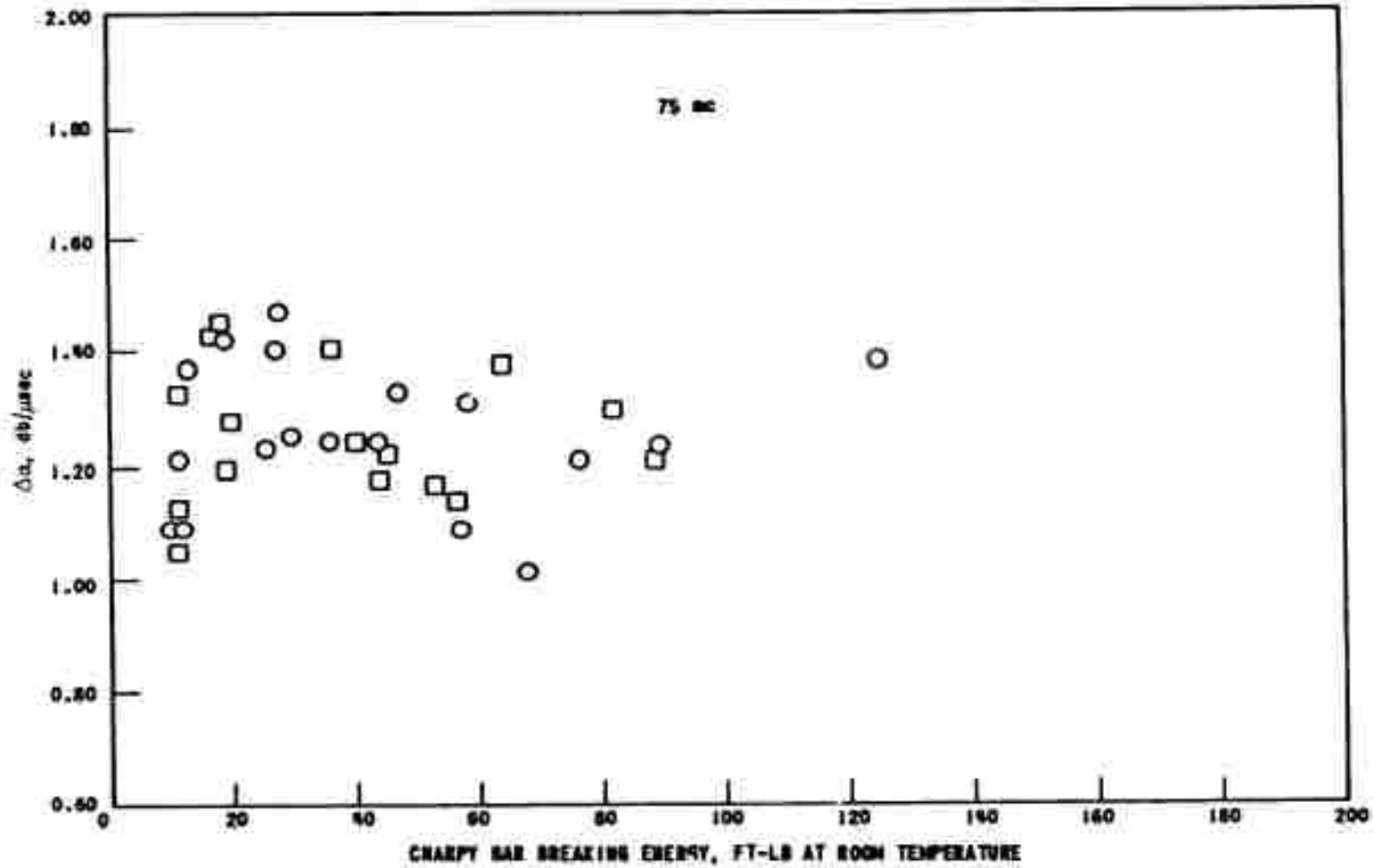


FIGURE 140

ATTENUATION LOST ON TEMPERING VERSUS BREAKING ENERGY, LONGITUDINAL WAVES

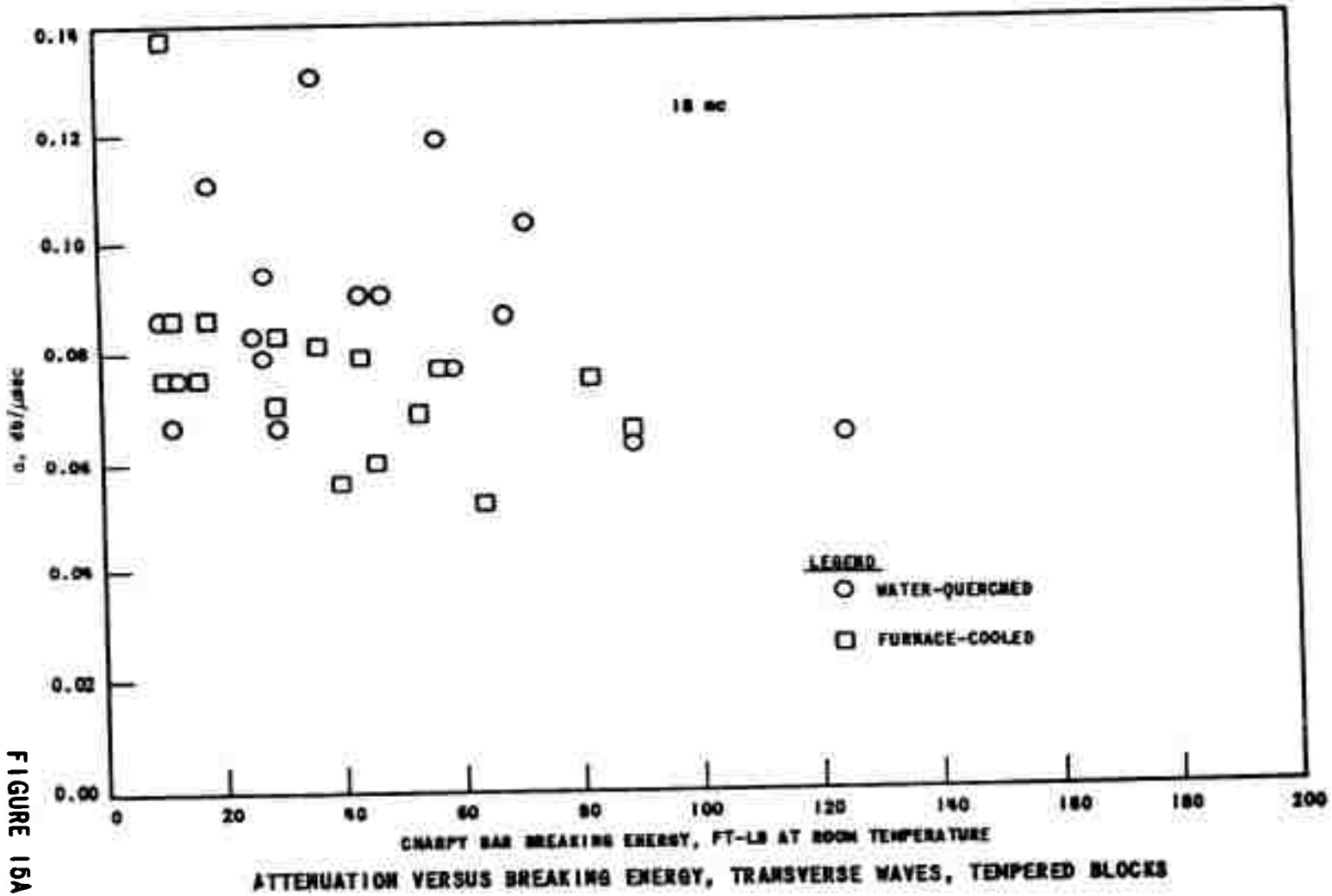


FIGURE 16A

ATTENUATION VERSUS BREAKING ENERGY, TRANSVERSE WAVES, TEMPERED BLOCKS

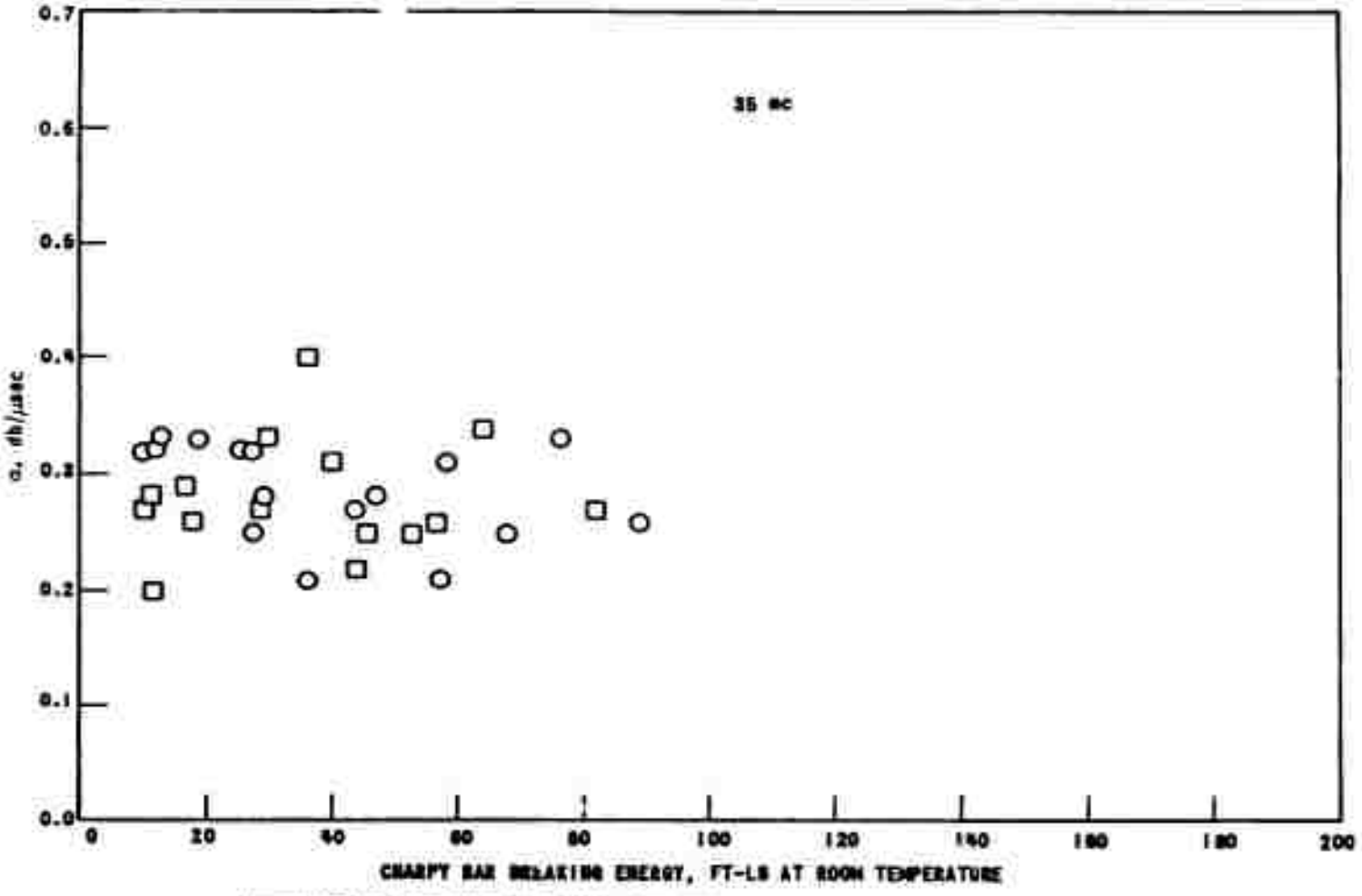


FIGURE 16B

ATTENUATION VERSUS BREAKING ENERGY, TRANSVERSE WAVES, TEMPERED BLOCKS

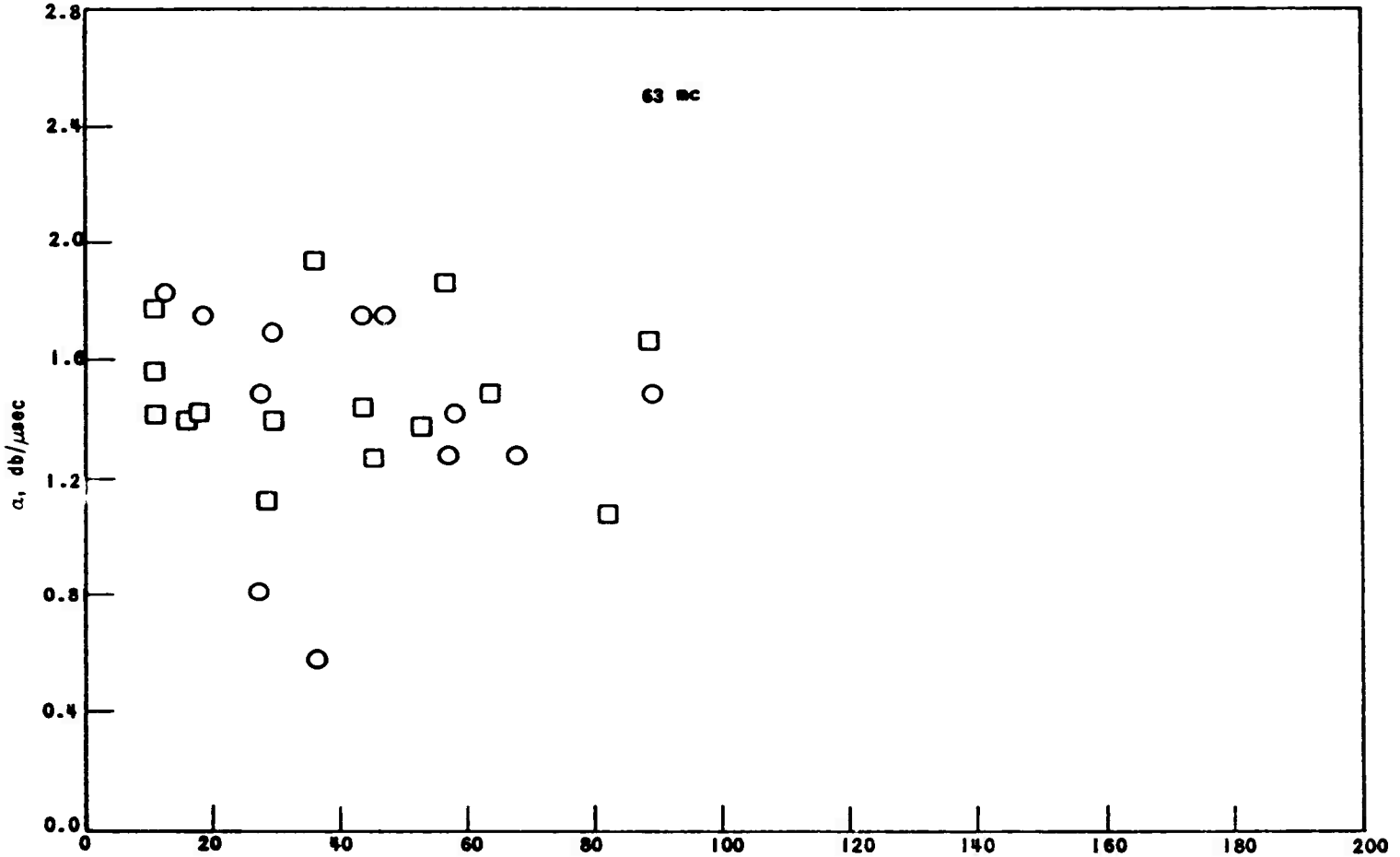


ATTENUATION VERSUS BREAKING ENERGY, TRANSVERSE WAVES, TEMPERED BLOCKS

FIGURE 15C

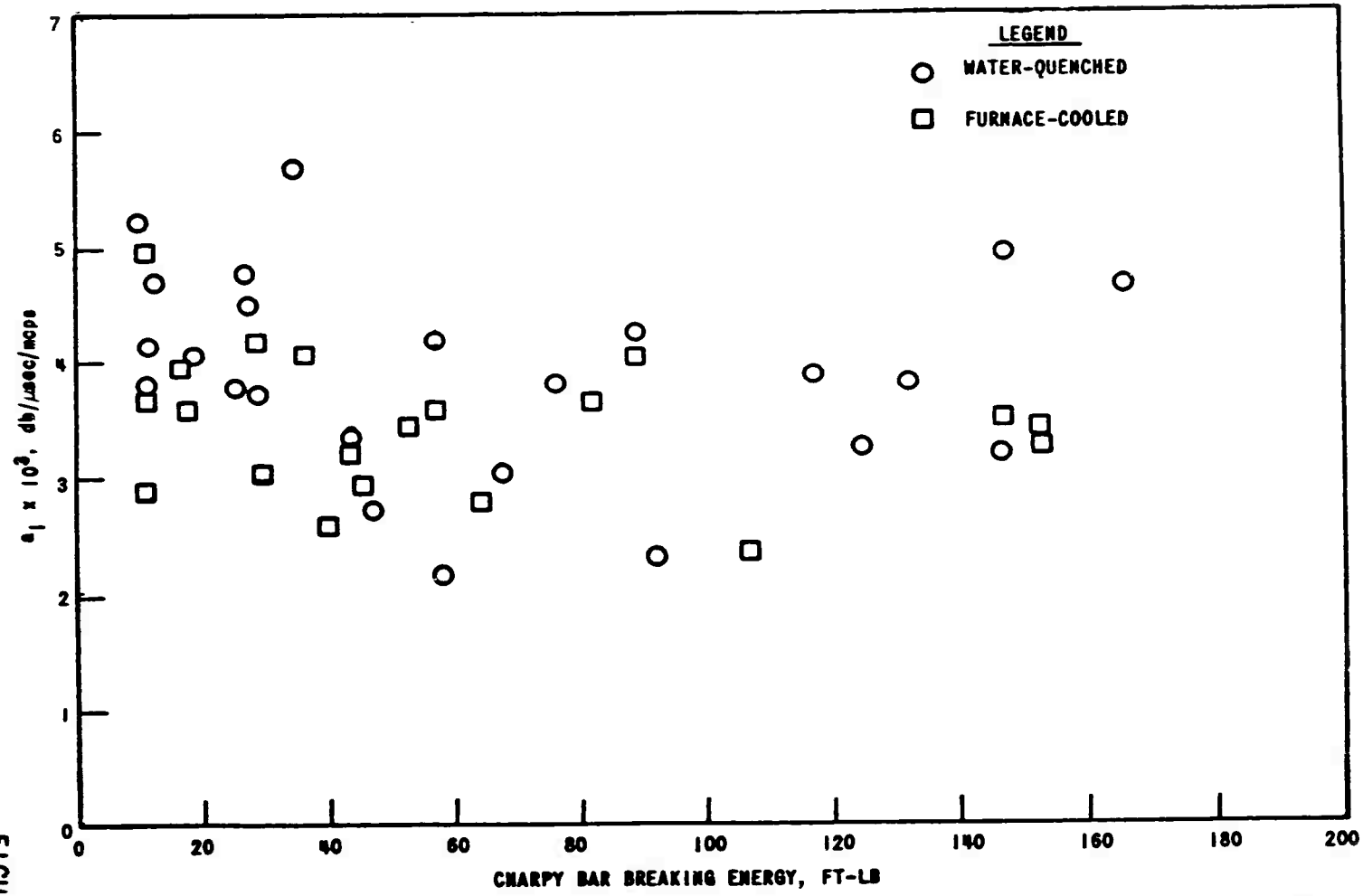


FIGURE 10

ELASTIC HYSTERESIS COEFFICIENT $a_i$ VERSUS BREAKING ENERGY, LONGITUDINAL WAVES, TEMPERED BLOCKS

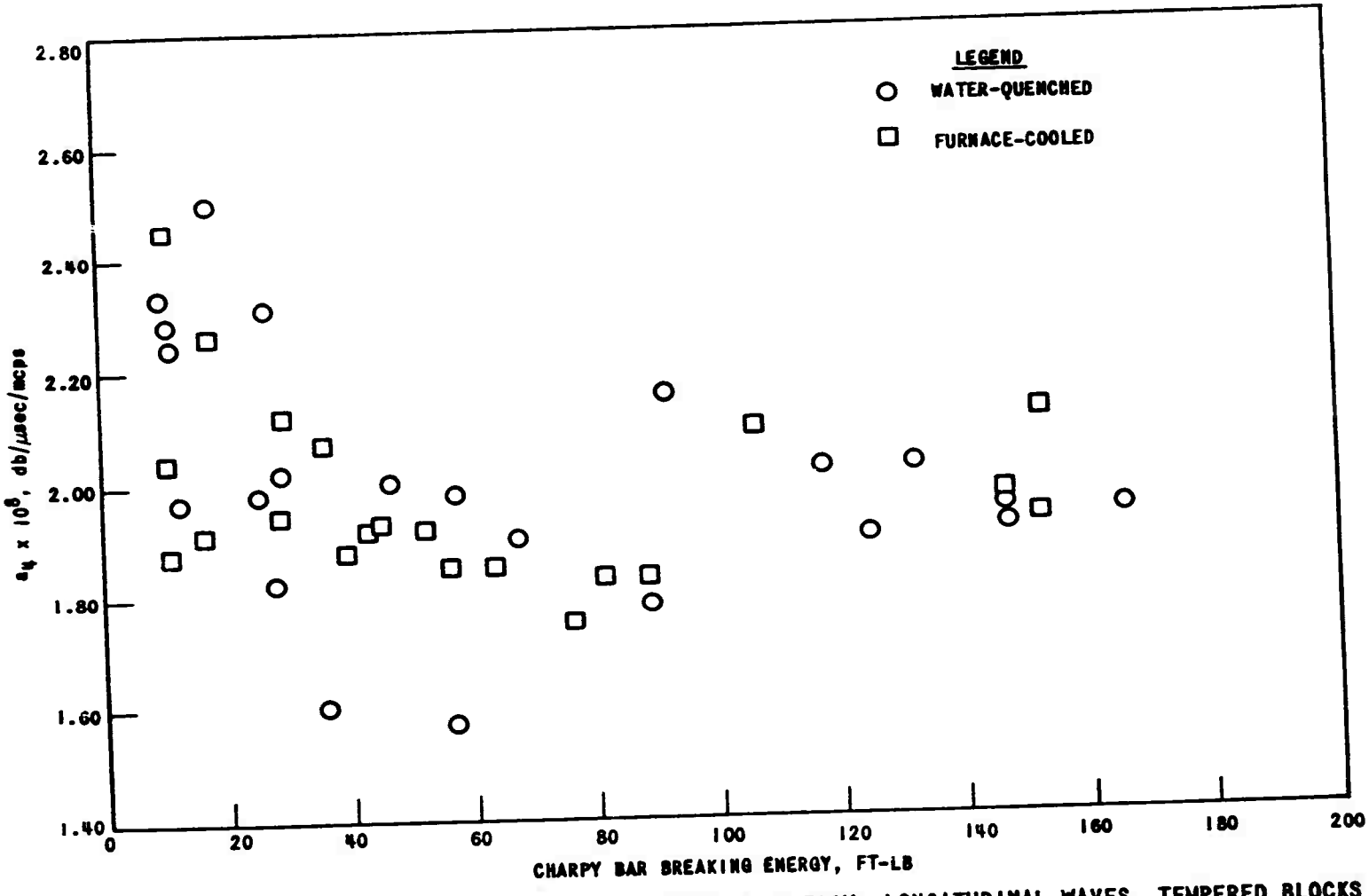


FIGURE 17 RAYLEIGH SCATTERING COEFFICIENT $a_4$ VERSUS BREAKING ENERGY, LONGITUDINAL WAVES, TEMPERED BLOCKS

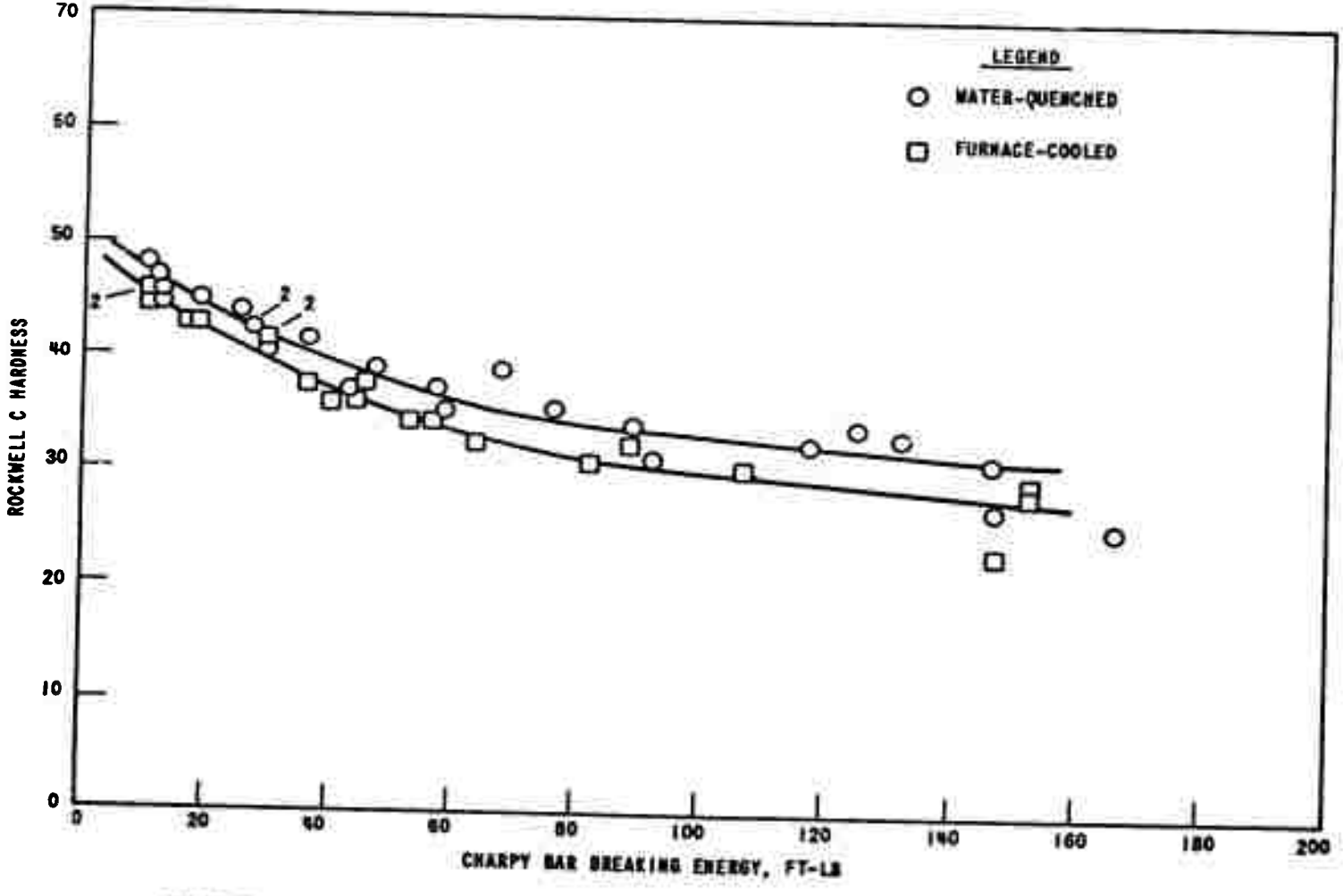


FIGURE 18

ROCKWELL C HARDNESS VERSUS CHARPY BAR BREAKING ENERGY, TEMPERED SPECIMENS

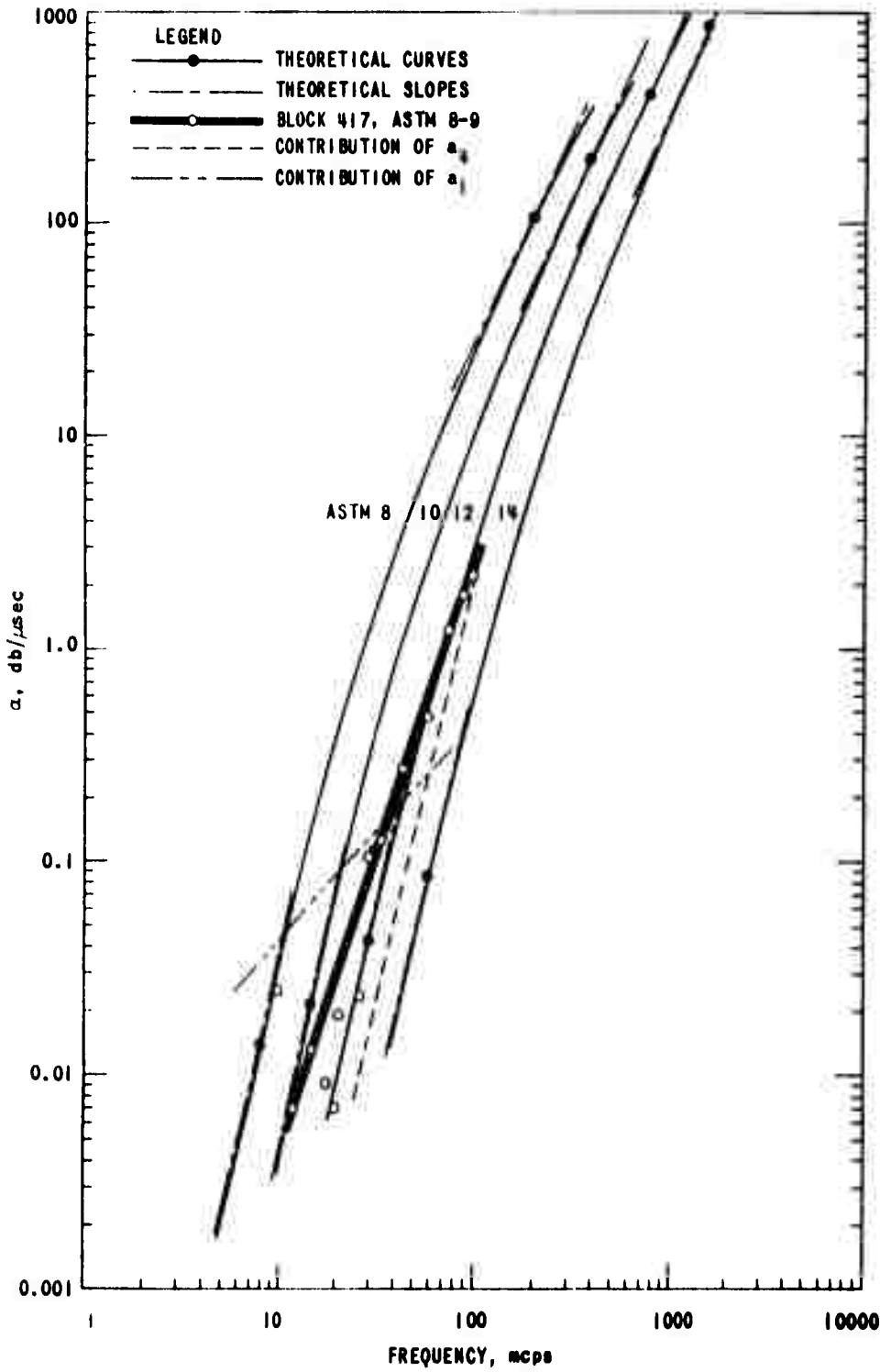


ATTENUATION COMPARED WITH THEORY, LONGITUDINAL WAVES



FIGURE 19

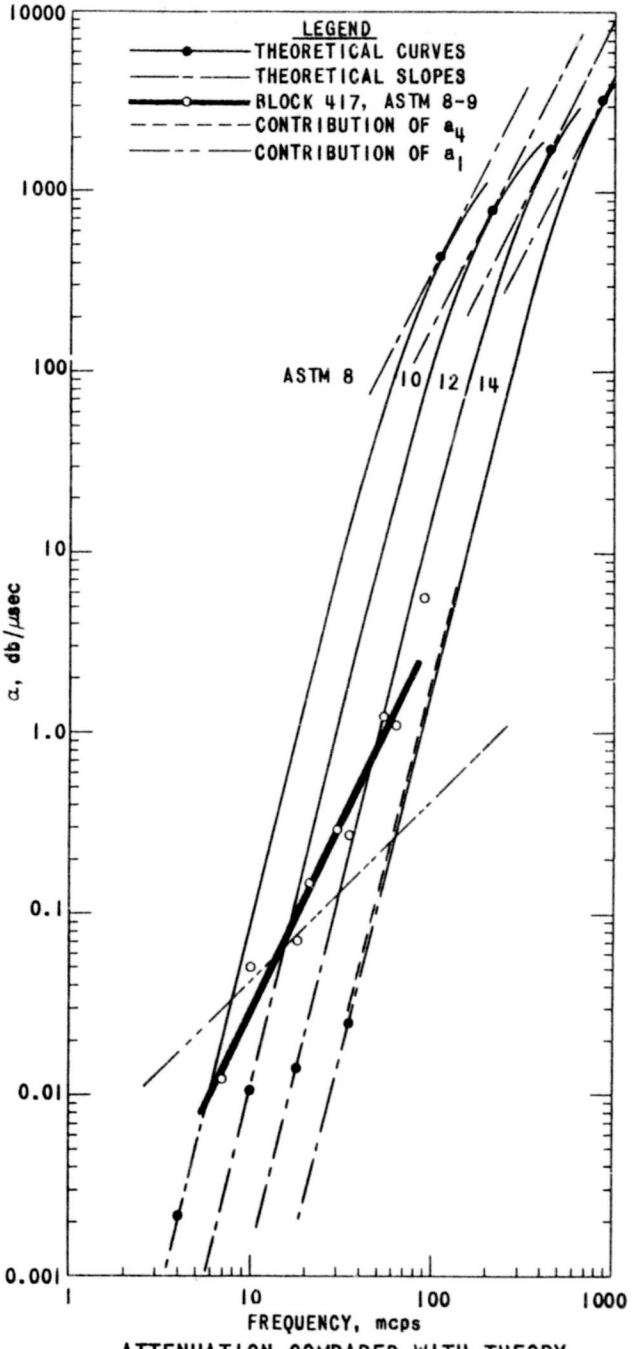


ATTENUATION COMPARED WITH THEORY,
TRANSVERSE WAVES



FIGURE 20

## REFERENCES


1. EVANS, D. H., and TRUELL, R., Ultrasonic Attenuation in a Temper-Embrittled Steel, Watertown Arsenal Laboratories, WAL TR 143/14-33, February 1953.

2. PAPADAKIS, E. P., Ultrasonic Attenuation in SAE 3140 and 4150 Steel, Watertown Arsenal Laboratories, WAL TR 143/31, April 1959.

3. WEGEL, R. L., and WALTHER, H., Internal Dissipation in Solids for Small Cyclic Strains, Physics, v. 6, 1935, p. 141-157.

4. KAMIGAKI, K., Ultrasonic Attenuation in Steel and Cast Iron, Sci. Rep. RITU, Tohoku University, Sendai, Japan, A, v. 9, 1957, p. 48-77.

5. MERKULOV, L. G., The Use of Ultrasonic Waves in Investigating the Structure of Steel, Sov. Phys. - Tech. Phys., v. 2, 1957, p. 1282, from J. Tech. Phys., (USSR), v. 27, no. 5, 1957.

6. RAYLEIGH, J. W. S., Theory of Sound, The Macmillan Company, New York, v. 2, 1929, p. 152.

7. ROTH, W., Scattering of Ultrasonic Radiation in Polycrystalline Metals, J. Appl. Phys., v. 19, 1948, p. 901-910.

8. MASON, W. P., and McSKIMIN, H. J., Energy Losses of Sound Waves in Metals Due to Scattering and Diffusion, J. Appl. Phys., v. 19, 1948, p. 940-946.

9. MERKULOV, L. G., Investigation of Ultrasonic Scattering in Metals, Sov. Phys. - Tech. Phys., v. 1, 1957, p. 59-69, from J. Tech. Phys., (USSR), v. 26, 1956.

10. MORSE, P. M., Vibration and Sound, 2d Ed., McGraw-Hill, New York, 1948, p. 354.

11. HUNTINGTON, H. B., On Ultrasonic Scattering by Polycrystals, J. Acoust. Soc. Am., v. 22, 1950, p. 362-364.

12. LIFSHITS, I. M., and PARKHOMOVSKII, G. D., Record of Kharkov State University, v. 27, 1948, p. 25.

13. LIFSHITS, I. M., and PARKHOMOVSKII, G. D., J. Exptl - Theoret. Phys., (USSR), v. 20, 1950, p. 175.

14. MASON, W. P., and McSKIMIN, H. J., Attenuation and Scattering of High Frequency Sound Waves in Metals and Glasses, J. Acoust. Soc. Am., v. 19, 1947, p. 464-473.

15. BHATIA, A. B., Scattering of High Frequency Sound Waves in Polycrystalline Materials, J. Acoust. Soc. Am., v. 31, 1959, p. 16-23.

16. BHATIA, A. B., and MOORE, R. A., Scattering of High Frequency Sound Waves in Polycrystalline Materials II, J. Acoust. Soc. Am., v. 31, 1959, p. 1140-1141.

17. PAPADAKIS, E. P., Influence of Grain Structure on Ultrasonic Attenuation in Steel, J. Appl. Phys., v. 30, 1959, p. 1463.

18. RODERICK, R. L., and TRUELL, R., The Measurement of Ultrasonic Attenuation in Solids by the Pulse Technique and Some Results in Steel, J. Appl. Phys., v. 23, 1952, p. 267-279.

19. CHICK, B., ANDERSON, G., and TRUELL, R., Ultrasonic Attenuation Unit and Its Use in Measuring Attenuation in Alkali Halides, J. Acoust. Soc. Am., v. 32, 1960, p. 186-193.

20. SEKI, H., GRANATO, A., and TRUELL, R., Diffraction Effects in the Ultrasonic Field of a Piston Source and Their Importance in the Accurate Measurement of Attenuation, J. Acoust. Soc. Am., v. 28, 1956, p. 230-238.

21. PAPADAKIS, E. P., Correction for Diffraction Losses in the Ultrasonic Field of a Piston Source, J. Acoust. Soc. Am., v. 31, 1959, p. 150-151.

22. BENNETT, C. A., and FRANKLIN, N. L., Statistical Analysis in Chemistry and the Chemical Industry, John Wiley and Sons, Inc., New York, 1954, p. 81, 95-96.

23. HILDEBRAND, FRANCIS B., Introduction to Numerical Analysis, McGraw-Hill, New York, 1956.

24. WATERMAN, P. C., and TEUTONICO, L. J., Ultrasonic Double Refraction in Single Crystals, J. Appl. Phys., v. 28, 1957, p. 266-270.

25. TRUELL, R., TEUTONICO, L. J., and LEVY, P. W., Detection of Directional Neutron Damage in Silicon by Means of Ultrasonic Double Refraction Measurements, Phys. Rev., v. 105, 1957, p. 1723-1729.

26. STEIN, F., EINSPRUCH, G., and TRUELL, R., Temperature Dependence of Fractional Velocity Changes in a Silicon Single Crystal, J. Appl. Phys., v. 30, 1959, p. 820-825.

WATERTOWN ARSENAL
WATERTOWN 72, MASS.

TECHNICAL REPORT DISTRIBUTION

| Report No.: | WAL TR 143/37<br>December 1961 | Title: | Ultrasonic Attenuation and Velocity in SAE 4150 Steel |
|---|---|---|---|

Distribution List approved by Ordnance Materials Research Office, 1 December 1960

| No. of Copies | TO |
|---|---|
| | Commander, Armed Services Technical Information Agency, Arlington Hall Station, Arlington 12, Virginia |
| 10 | ATTN: TIPDR |
| 1 | Director, Army Research Office, Department of the Army, Washington 25, D. C. |
| | U. S. Army Research Office (Durham), Box CM, Duke Station, Durham, North Carolina |
| 1 | ATTN: Technical Library |
| | Chief of Ordnance, Department of the Army, Washington 25, D. C. |
| 1 | ATTN: ORDTB, Materials |
| | Commanding General, Aberdeen Proving Ground, Maryland |
| 1 | ATTN: Ballistic Research Lab. |
| 3 | ORDBE-LM, Technical Library, Bldg. 313 |
| | Commanding General, Army Ballistic Missile Agency, Redstone Arsenal, Alabama |
| 1 | ATTN: Dr. G. H. Reisig |
| | Commanding General, Ordnance Tank-Automotive Command, Detroit Arsenal, Center Line, Michigan |
| 1 | ATTN: ORDMC-RM.1, Mr. Charles Salter |
| | Commanding General, Ordnance Weapons Command, Rock Island, Ill. |
| 1 | ATTN: ORDOW-IX |
| 2 | ORDOW-TX |
| 1 | Commanding General, U. S. Army Ordnance Special Weapons Ammunition Command, Dover, New Jersey |
| | Commanding General, U. S. Army Rocket & Guided Missile Agency, Redstone Arsenal, Alabama |
| 1 | ATTN: ORDAB-DV |
| 5 | ORDXR-RGA, Mr R. L. Wetherington |
| 1 | ORDXR-RMO, Lt. E. J. Wilson |

Issue date: 1/22/62

| No. of Copies | TO |
|---|---|
| | Commanding Officer, Detroit Arsenal, Center Line, Michigan |
| 1 | ATTN: ORDMX-BMW |
| 1 | ORDMX-AL |
| | Commanding Officer, Diamond Ordnance Fuze Laboratories, Washington 25, D. C. |
| 1 | ATTN: ORDTL .012, Technical Reference Branch |
| | Commanding Officer, Frankford Arsenal, Philadelphia 37, Pa. |
| 2 | ATTN: Pitman-Dunn Labs. |
| | Commanding Officer, Ordnance Materials Research Office, Watertown Arsenal, Watertown 72, Massachusetts |
| 1 | ATTN: RPD |
| | Commanding Officer, Picatinny Arsenal, Dover, New Jersey |
| 1 | ATTN: Feltman Research Labs. |
| | Commanding Officer, Rock Island Arsenal, Rock Island, Illinois |
| 1 | ATTN: Laboratory |
| | Commanding Officer, Springfield Armory, Springfield 1, Mass. |
| 1 | ATTN: ORDBD-TX |
| | Commanding Officer, Watervliet Arsenal, Watervliet, New York |
| 1 | ATTN: ORDBF-RT |
| | Commanding General, Chemical Warfare Laboratories, Army Chemical Center, Maryland |
| 2 | ATTN: Technical Library |
| | Commanding General, Corps of Engineers, Fort Belvoir, Virginia |
| 2 | ATTN: R&E Labs. |
| | The Quartermaster General, Department of the Army, Washington 25, D. C. |
| 2 | ATTN: R&D Division |
| | Chief, Bureau of Naval Weapons, Department of the Navy, Room 2225, Munitions Bldg., Washington 25, D. C. |
| 1 | ATTN: RMMP |
| | Chief, Bureau of Ships, Department of the Navy, Washington 25, D. C. |
| 1 | ATTN: Code 341 |
| | Chief, Office of Naval Research, Department of the Navy, Washington 25, D. C. |
| 1 | ATTN: Code 423 |

| No. of Copies | TO |
|---|---|
| 1 | Chief, Naval Engineering Experimental Station, Department of the Navy, Annapolis, Maryland |
| 2 | Commander, Naval Ordnance Laboratory, White Oak, Silver Spring, Maryland<br>ATTN: Code WM |
| 1 | Commander, Naval Ordnance Test Station, China Lake, California<br>ATTN: Code 5557 |
| 1 | Director, Naval Research Laboratory, Anacostia Station, Washington, D. C.<br>ATTN: Technical Information Officer |
| 1 | Commander, Naval Weapons Laboratory, Dahlgren, Virginia<br>ATTN: A & P Lab. |
| 1 | Commander, Boston Naval Shipyard, Boston, Massachusetts<br>ATTN: Code 375 |
| 1 | Commander, New York Naval Shipyard, Brooklyn, New York<br>ATTN: Code 982 |
| 1 | Commander, Norfolk Naval Shipyard, Norfolk, Virginia<br>ATTN: Code 380 |
| 3 | Commander, Philadelphia Naval Shipyard, Philadelphia, Pa. |
| 2 | Commander, Portsmouth Naval Shipyard, Portsmouth, N. H.<br>ATTN: Mat. Test Lab., Code 375 |
| 5 | Commander, Wright Air Development Division, Wright-Patterson Air Force Base, Ohio<br>ATTN: WWRCEE |
| 1 | Director, Boston Air Procurement District, Boston Army Base, Boston, Massachusetts<br>ATTN: Quality Control Division |
| 15 | U. S. Atomic Energy Commission, Office of Technical Information Extension, P. O. Box 62, Oak Ridge, Tennessee |
| 1 | Army Reactor Branch, Division of Research Development, Atomic Energy Commission, Washington 25, D. C. |
| 1 | National Aeronautics and Space Administration, 1520 H Street, N. W., Washington 25, D. C. |

| No. of Copies | TO |
|---|---|
| | The Director, Jet Propulsion Laboratory, California Institute of Technology, Pasadena 3, California |
| 1 | ATTN: Dr. L. Jaffe |
| | Dr. W. R. Lucas, George C. Marshall Space Flight Center, Huntsville, Alabama |
| 5 | ATTN: M-S&M-M |
| | Mr. W. A. Wilson, George C. Marshall Space Flight Center, Huntsville, Alabama |
| 1 | ATTN: M-F&AE-M, Bldg. 4720 |
| 1 | Defense Metals Information Center, Battelle Memorial Institute, Columbus, Ohio |
| 1 | Perkin-Elmer Corporation, Norwalk, Connecticut |
| | Canadian Army Staff, 2450 Massachusetts Ave., Washington 8, D. C. |
| 2 | ATTN: GSO-I, A&R Section |
| 2 | United Kingdom Scientific Information & Liaison, Washington 25, D. C. |
| | Commanding Officer, Watertown Arsenal, Watertown 72, Mass. |
| 5 | ATTN: ORDBE-LXM, Tech. Info. Sec. |
| 3 | Authors |

107 -- TOTAL COPIES DISTRIBUTED

31 -- Extra copies to Branch

1 -- OE

139 -- Total Copies Printed

cy #4 to Dr. R. G. H. Siu, Army Mat. Command 9/62